FERNANDO MONTEZANO FERNANDES

GENETIC VARIABILITY AND HOST SPECIALIZATION AMONG BRAZILIAN POPULATIONS OF *Ceratocystis fimbriata* s.l.

Thesis submitted to the Plant Pathology Graduate Program of the Universidade Federal de Viçosa, in partial fulfillment of the requirements for the degree of *Doctor Scientiae*.

Advisor: Acelino Couto Alfenas

VIÇOSA - MINAS GERAIS
2021

Ficha catalográfica elaborada pela Biblioteca Central da Universidade Federal de Viçosa - Campus Viçosa

T
F363g
2021

Fernandes, Fernando Montezano, 1993-
Genetic variability and host specialization among brazilian populations *Ceratocystis fimbriata* s.l. / Fernando Montezano Fernandes. – Viçosa, MG, 2021.
1 tese eletrônica (129 f.): il. (algumas color.).

Texto em inglês.
Inclui anexos.
Orientador: Acelino Couto Alfenas.
Tese (doutorado) - Universidade Federal de Viçosa, Departamento de Fitopatologia, 2021.
Inclui bibliografia.
DOI: https://doi.org/10.47328/ufvbbt.2021.200
Modo de acesso: World Wide Web.

1. *Ceratocystis fimbriata. 2.* Mapeamento cromossômico. 3. Eletroforese em gel campo pulsado. 4. Genômica. 5. Variação genética. I. Alfenas, Acelino Couto, 1950-. II. Universidade Federal de Viçosa. Departamento de Fitopatologia. Programa de Pós-Graduação em Fitopatologia. III. Título.

CDD 22. ed. 579.135

Bibliotecário(a) responsável: Alice Regina Pinto CRB6 2523

FERNANDO MONTEZANO FERNANDES

GENETIC VARIABILITY AND HOST SPECIALIZATION AMONG BRAZILIAN POPULATIONS OF *Ceratocystis fimbriata* s.l.

Thesis submitted to the Plant Pathology Graduate Program of the Universidade Federal de Viçosa, in partial fulfillment of the requirements for the degree of *Doctor Scientiae*.

APPROVED: August 31, 2021.

Assent:

Fernando Montezano Fernandes
Author

Acelino Couto Alfenas
Advisor

To my mom, Maria Ramona,
for my grandma Izabel,
for all love, and support,
I dedicate.

ACKNOWLEDGMENTS

I thank GOD, our Heavenly Father, for all the blessings received so far in my life and all those around me.

To my whole family, especially to my mom, Maria Ramona, and sisters, Alinne e Arianne for the example of strength, work, and honesty, and the unconditional love encouragement, and support.

To the Universidade Federal de Viçosa, especially the Plant Pathology Graduate Program for the opportunity of getting a Ph.D. in a postgraduate program of such excellence and inexhaustible source of knowledge.

To the Coordenação de Aperfeiçoamento de Pessoal de Nível Superior (Capes) for the Ph.D. fellowship.

I wish to express my eternal gratitude to Prof. Acelino Couto Alfenas for every chance he has provided me, for teaching me everything about Forest Pathology and Science, and for being an example of a professor, researcher, and professional. Thank you for your confidence, encouragement, patience, and inspiration. Every lesson will be carried with me. I'm hoping to be able to pass on what I have learned.

I am grateful to Dr. Lúcio Mauro S. Guimarães for always be willing to help, for the unconditional support, for dedication and attention to the work done, as well as the friendship.

I am also especially grateful to Prof. Marisa Vieira de Queiroz who introduced me to the molecular biology world and has helped me in all stages during my whole Ph.D., always very solicitous. I am so grateful for all training, support, and friendship during this journey. Likewise, I would like to thank Dr. Leandro Lopes and Dra. Patrícia Fontes who were always available to discuss methodologies, ideas, and results.

I am also grateful to Prof. Jorge Luis Badel Pacheco for offering excellent contributions in writing and discussions of the work of karyotyping.

I wish to thanks Prof. Rafael Ferreira Alfenas for intellectual contribution in this study and for always being solicitous.

To Márcia Brandão *"madre de todos"* who was so lovely and kind to me. Thank you for all support and help with bureaucratic.

To the Laboratories of Coffee Biotechnology, Molecular Genetics of Microorganisms, Molecular Genetics of Prokaryotes and Virus Laboratory, for the support and loans of important equipment for the development of the research.

To Clonar Resistência a Doenças Florestais and all its staff for the support offered for growing all plants used in my experiments. A special thanks to Felipe Bastos, Solange, Andinho, Eduardo and Jean for take care of my plants so well.

I also wish to express thanks to the Brazilian companies, Silvestrin, Proteca, and Instituto Sucupira for kindly sending the seeds and seedlings used in this study.

Many thanks to the team of the Forest Pathology Laboratory (Patomol) for the friendship and for the good and pleasant times over the years. A special thanks to Dra. Daiana Azevedo who, in addition to the great friendship, helped and supported me in all the experiments. I also thank the staff Paulo Sinei, Elenice Martins, and Mara Souza for their excellent work and for always being ready to help.

I thank to all my friends and Ph.D. colleagues, especially Jhonatan Barro, Thaisa Nóbrega and Clemen de Oliveira whom I have revealed all of my troubles, concerns, and fears throughout the course of two years of discipline.

A special thanks to Maíra Duffeck and Jhonatan Barro for their incredible years of learning and great times together during their student representation at the Department of Plant Pathology.

I am grateful to Bernardo Melo for our friendship, fraternity, and great living together in Viçosa throughout the years.

I would want to thank all of the researchers, scientists, and professionals who have been and continue to be involved in the fight against the SARS-CoV-2 virus, also known as the Novo Coronavirus.

Finally, I thank everyone who contributed directly or indirectly to the realization of my doctoral project that I forgot to mention, but they are certainly important to me.

Thank you everyone!

"If I have seen further,
it is by standing upon the shoulders of giants"
(Sir Isaac Newton)

ABSTRACT

FERNANDES, Fernando Montezano, D.Sc., Universidade Federal de Viçosa, August, 2021. **Genetic variability and host specialization among brazilian populations of *Ceratocystis fimbriata* s.l.** Adviser: Acelino Couto Alfenas.

Ceratocystis fimbriata is one of the most important woody plant pathogens worldwide. The fungi colonize the vascular tissue, causing stains on the wood and death of branches or whole plants. Due the wide range of hosts, it is possible that adapted populations of *C. fimbriata* have been selected to specific hosts and that there is high genetic and physiological variability within the pathogen population. The knowledge of physiological factors that determine host range and host specificity are important aspects for disease management. Therefore, the aims of this study were: (i) determine the specializing for their hosts of 11 isolates on eight hosts; (ii) to investigate the karyotype of isolates of the *C. fimbriata* species complex from different host plants and geographical origins in Brazil and; (iii) assessed the variability genetic of karyotyped isolates using retrotransposon-microsatellite amplified polymorphism (REMAP). In addition, the identity of the isolates was confirmed conducting multilocus phylogeny using DNA sequences of mating type genes, TEF-1α, and β-tubulin. The analysis based on the *C. fimbriat*a microsatellite (SSR) profiles showed a separation of isolates according to the host. Based on the results of inoculation of 11 isolates on eight hosts, a wide variation in aggressiveness was found. The isolates that were used in this study were more aggressive in their respective hosts. Some hosts, however, were susceptible to isolates from other hosts. Considering the length of xylem lesion caused by *C. fimbriata* isolates, *F. carica* was the most susceptible to the isolates tested, followed by *M. indica*. Only *T. cacao* and *C. guianensis* isolates proved to be specialized by their hosts. Polymorphism in chromosome number and size was found, indicating the existence of genomic differences among isolates and occurrence of chromosomal rearrangements in the species complex. The number of chromosomes varied from six to eight and the estimated minimum chromosome sizes were estimated to be between 2.7 to 6.0 Mbp. Small polymorphic chromosomes were observed in all isolates, raising the hypothesis that they could be supernumerary chromosomes. Because chromosomal variation can be caused by transposable elements (TEs), we also assessed the variability of the same isolates using retrotransposon-microsatellite amplified polymorphism (REMAP) molecular marker. REMAP analysis of karyotyped isolates revealed genetic variability and isolates from the same host tend to group in a same cluster.

Keywords: Chromosomal rearrangements. Genomic architecture. PFGE. *Ceratocystis* wilt. Cross-inoculations. Physiological variability.

RESUMO

FERNANDES, Fernando Montezano, D.Sc., Universidade Federal de Viçosa, agosto de 2021. **Variabilidade genética e especialização pelo hospedeiro entre as populações brasileiras de *Ceratocystis fimbriata* s.l.** Orientador: Acelino Couto Alfenas.

Ceratocystis fimbriata é um dos mais importantes patógenos de plantas lenhosas em todo o mundo. Os fungos colonizam o tecido vascular, causando manchas na madeira e morte de galhos ou plantas inteiras. Devido à grande variedade de hospedeiros, é possível que populações adaptadas de *C. fimbriata* tenham sido selecionadas para hospedeiros específicos e que haja alta variabilidade genética e fisiológica dentro da população do patógeno. O conhecimento dos fatores fisiológicos que determinam a gama de hospedeiros e a especificidade do hospedeiro são aspectos importantes para o manejo da doença. Portanto, os objetivos deste estudo foram: (i) determinar a especialização fisiológica de 11 isolados em oito hospesdeiros; (ii) investigar o cariótipo de isolados do complexo de espécies de *C. fimbriata* de diferentes plantas hospedeiras e origens geográficas no Brasil e; (iii) avaliar a variabilidade genética de isolados cariotipados utilizando o marcador molecular retrotransposon-microssatélite amplificado polimorfismo (REMAP). Além disso, a identidade dos isolados foi confirmada por meio de filogenia multilocus usando sequências de DNA de genes de *mating type*, TEF-1α e β-tubulina. Com base nos resultados da inoculação de 11 isolados em oito hospedeiros, foi encontrada uma grande variação na agressividade. Os isolados utilizados neste estudo foram mais agressivos em seus respectivos hospedeiros. Alguns hospedeiros, entretanto, eram suscetíveis a isolados de outros hospedeiros. Considerando o comprimento da lesão do xilema causada pelos isolados de *C. fimbriata*, as plantas de *F. carica* foram as mais suscetíveis aos isolados testados, seguido por *M. indica*. Apenas os isolados de *T. cacao* e *C. guianensis* se mostraram especializados por seus hospedeiros. Foi encontrado polimorfismo no número e tamanho dos cromossomos, indicando a existência de diferenças genômicas entre os isolados e a ocorrência de rearranjos cromossômicos no complexo de espécies. O número de cromossomos variou de seis a oito e os tamanhos mínimos estimados dos cromossomos foram estimados entre 2,7 e 6,0 Mbp. Pequenos cromossomos polimórficos foram observados em todos os isolados, levantando a hipótese de que eles poderiam ser cromossomos supranumerários. Como a variação cromossômica pode ser causada por elementos transponíveis (TEs), também avaliamos a variabilidade dos mesmos isolados usando o marcador molecular retrotransposon-microssatélite amplificado polimorfismo (REMAP). A análise REMAP dos isolados cariotipados revelou variabilidade genética e isolados do mesmo hospedeiro tendem a se agrupar em um mesmo *cluster*. A análise baseada nos perfis de microssatélites (SSR) de *C. fimbriata* mostrou uma separação dos isolados de acordo com o hospedeiro.

Palavras-chave: Rearranjos cromossômicos. Arquitetura genômica. PFGE. Murcha de Ceratocystis. Inoculações cruzadas. Variabilidade fisiológica.

SUMÁRIO

GENERAL INTRODUCTION

Ceratocystis fimbriata Ellis & Halst is one of the most important plant pathogens worldwide, due to the systemic nature of the infections, the damage caused and the ability of the fungus to cause disease on several woody plants. These characteristics of the pathogen make difficult to control the disease. The fungi was first described as the causal agent of black rot of sweet potato [*Ipomoea batatas* (L.) Lam] in New Jersey, United States of America (Halsted, 1890). Since then, the fungus has been reported worldwide, and more than 80 species of plants have been confirmed as hosts of this pathogen (Farr & Rossman, 2021). In Brazil, *C. fimbriata* was originally described in the state of São Paulo on *Crotalaria juncea* L. (Costa & Krug, 1935). Later, the disease has been reported in several species of plants, such as *Mangifera indica* L. (Carvalho, 1938), *Hevea brasiliensis* L. (rubber tree) (Albuquerque *et al.*, 1972), *Gmelina arborea* Roxb. Ex Sm. (gmelina) (Muchovej *et al.*, 1978), *Ficus carica* L. (edible fig), (Valarini & Tokeshi, 1980), *Eucalyptus* spp. (eucalyptus) (Ferreira *et al.*, 1999), *Theobroma cacao* L. (cacao) (Baker *et al.*, 2003), *Annona squamosa* L. (sugar-apple) (Silveira *et al.*, 2006), *Carapa guianensis* Aubl. (andiroba) (Halfeld-Vieira *et al.*, 2012; Valdetaro *et al.*, 2019), *Tectona grandi*s L. f. (teak) (Firmino *et al.*, 2012), *Actinidia deliciosa* (A. Chev) CF Lianget & AR Ferguson (kiwifruit) (Piveta *et al.*, 2013) and *Caryocar brasiliense* Cambess. (pequi) (Silva *et al.*, 2017). Furthermore, the pathogen can infection and cause the rot storage roots or corms of *Colocasia esculenta* (taro or inhame) (Harrington *et al.*, 2005) and *Ipomoea batatas* (sweet potato) (Halsted, 1890).

The fungus can infect the host through wounds present on the roots and move through sapwood tissue or through openings in the branches and trunk that are normally caused by tools and equipment used during cultural practices (Giraldo, 1957; Viégas, 1960; Rossetto & Ribeiro, 1990). In addition, *C. fimbriata* produce fruity-smelling volatiles, which attract insects such as nitidulid (Coleoptera: Nitidulidae) and ambrosia beetles (Coleoptera: Curculionidae: Scolytinae and Platypodinae) that perforate diseased trees and disperse the fungus through excrement and/or spores adhereded to their bodies (Iton & Conway, 1961; Baker *et al.*, 2003; Engelbrecht *et al.*, 2007). The pathogen, which is often responsible for wilt symptoms, primarily infects the parenchyma, phloem, and xylem vessels, causing discoloration in the radial direction of the wood (Ferreira *et al.*, 2006; Silva *et al.*, 2020).

Ceratocystis fimbriata comprises a complex of cryptic species, being the pathogen that causes black rot in sweet potatoes is consider as *C. fimbriata sensu stricto* (*s.s.*), while those isolated from other hosts are treated as *C. fimbriata sensu lato* (*s.l.*) (de Beer *et al.*, 2014). Four well-supported phylogenetic clades linked to geographic regions were established for *C. fimbrata*: Latin American clade (LAC), North American clade (NAC), Asian-Australian clade (AAC), and African clade (AFC) (Harrington *et al.*, 2011; Fourie *et al.*, 2015; Liu *et al.*, 2018).

Within the *C. fimbriata* complex, there is significant genetic variation, with some of this variation occurring among clades and lineages linked with certain specific geographic regions or hosts. Extensive researches have been carried out with the aim of better characterize the *C. fimbriata* isolates based on multilocus phylogeny, morphology, physiological characteristics, and microsatellite markers (Baker *et al.*, 2003; Thorpe *et al.*, 2005; Ferreira *et al.*, 2010; Harrington *et al.*, 2011). In LAC the isolates that cause wilt in *T. cacao* and *Platanus ocidentalis* L. are described as distinct species, *C. cacaofunesta* Engelbr. & T.C. Harr. and *C. platani* (Walter) Engelbrecht & Harrington respectively (Baker *et al.*, 2003; Harrington *et al.*, 2011). Additionally, inoculation studies indicated that the andiroba isolates are host-specialized on andiroba, supporting the proposition of the special form *C. fimbriata* f. sp. *carapa* (Valdetaro *et al.*, 2019). Due to the wide host range, it is probable that more adapted populations of *C. fimbriata* have been selected, and that there is a significant degree of diversity in pathogenicity and aggressiveness within the pathogen population.

Despite advances in genomic research and whole-genome sequencing for the *C. fimriata*, the karyotype of this fungus remains uncertain. Recently, the number of *C. fimbriata* chromosomes was indicated based on a linkage map that resulted in nine linkage groups (Fourie *et al.*, 2019). However, because of the significant genetic diversity found in *C. fimbriata*, it is probable that karyotype variants occur. Pulsed-field gel electrophoresis (PFGE) has been widely utilized for fungal karyotyping, especially to its ability to see small chromosomes and independence from meiosis (Zolan, 1995). Many fungal pathogen genomes have estimated their chromosome number and sizes using PFGE (Rincones *et al.*, 2006; Mehrabi *et al.*, 2007; Zhong & Steffenson, 2007; Sasaki *et al.*, 2014; Ayukawa *et al.*, 2018). The PFGE has been used to determine not only the chromosome number (CN), but also the amount of chromosomal DNA (chDNA) and the presence of chromosomal polymorphism (Mehrabi *et al.*, 2017). The characterization of the chromosomal set of plant pathogenic fungus is important for giving information on the genome of organisms and to offer evidence for the pathogenicity factors and genomic structure.

The present Thesis consists of two chapters. The first chapter, entitled Genetic variability and host specialization of the *Ceratocystis fimbriata* species complex in Brazil, aimed to: i) determine the host-specialization of *C. fimbriata* isolates through cross inoculations in different host species; ii) cccess the population diversity of *C. fimbriata* in Brazil using SSR markers. The second chapter, entitled Chromosomal polymorphism of the *Ceratocystis fimbriata* species complex in Brazil, aimed to: i) determine the karyotype of isolates of the *C. fimbriata* species complex from different host plants and geographic origins in Brazil using PFGE; ii) evaluate the chromosomal variation caused by TEs using REMAP markers; iii) Confirm the identity of the isolates by multilocus phylogeny approach.

REFERENCES

Albuquerque FC, Duarte MLR, Silva HM, 1972. Ocorrência do mofo cinzento (*Ceratocystis fimbriata*) da seringueira. *In: Seminário Nacional da Seringueira*, 125–128.

Ayukawa Y, Komatsu K, Taga M, Arie T, 2018. Cytological karyotyping of *Fusarium oxysporum* by the germ tube burst method (GTBM). *Journal of General Plant Pathology 2018 84:4* **84**, 254–261.

Baker CJ, Harrington TC, Krauss U, Alfenas AC, 2003. Genetic variability and host specialization in the Latin American Clade of *Ceratocystis fimbriata*. *Ecology and Population Biology* **93**, 1274–1284.

Carvalho MB, 1938. Sobre dois insetos nocivos à mangueira. *Bol. da Secr. da Agric. Indústria e Comércio*, 130–132.

de Beer ZW, Duong TA, Barnes I, Wingfield BD, Wingfield MJ, 2014. Redefining *Ceratocystis* and allied genera. *Studies in Mycology* **79**, 187–219.

Engelbrecht CJB, Harrington TC, Alfenas AC, Suarez C, 2007. Genetic variation in populations of the cacao wilt pathogen, *Ceratocystis cacaofunesta*. *Plant Pathology* **56**, 923–933.

Farr DF, Rossman AY, 2021. Fungal Databases. *U.S. National Fungus Collections*.

Ferreira FA, Demuner AM, Demuner NL, Pigatto S, 1999. Murcha de Ceratocystis em eucalipto no Brasil. *Fitopatologia Brasileira* **24**, 284.

Ferreira EM, Harrington TC, Thorpe DJ, Alfenas AC, 2010. Genetic diversity and interfertility among highly differentiated populations of *Ceratocystis fimbriata* in Brazil. *Plant Pathology* **59**, 721–735.

Ferreira FA, Maffia LA, Barreto RW, Demuner NL, Pigatto S, 2006. Sintomatologia da murcha de *Ceratocystis fimbriata* em eucalipto. *Revista Árvore* **30**, 155–162.

Firmino AC, Tozze Jr HJ, Furtado EL, 2012. First report of *Ceratocystis fimbriata* causing wilt in *Tectona grandis* in Brazil. *New Disease Reports* **25**.

Fourie A, van der Nest MA, de Vos L, Wingfield MJ, Wingfield BD, Barnes I, 2019. QTL mapping of mycelial growth and aggressiveness to distinct hosts in *Ceratocystis* pathogens. *Fungal Genetics and Biology* **131**.

Fourie A, Wingfield MJ, Wingfield BD, Barnes I, 2015. Molecular markers delimit cryptic species in *Ceratocystis* sensu stricto. *Mycological Progress* **14**, 1020.

Giraldo EA, 1957. La llaga macana del tronco del cacao. *Acta Agronómica* **7**, 71–103.

Halfeld-Vieira BA, Zilli JE, Nechet KL, Pereira GMD, Souza GR, 2012. First record of *Ceratocystis fimbriata* on *Carapa guianensis*. *New Disease Reports* **26**, 13.

Halsted BD, 1890. Some fungous diseases of the sweet potato. The black rot. *New Jersey Agriculture Experiment Station Bulletin* **76**, 7–14.

Harrington TC, Thorpe DJ, Alfenas AC, 2011. Genetic variation and variation in aggressiveness to native and exotic hosts among brazilian populations of *Ceratocystis fimbriata*. *Population Biology* **101**, 566.

Harrington TC, Thorpe DJ, Marinho VLA, Furtado EL, 2005. First report of black rot of Colocasia esculenta caused by Ceratocystis fimbriata in Brazil. *Fitopatologia Brasileira* **30**, 88–89.

Iton EF, Conway GE, 1961. Studies on a wilt disease of cacao at River Estate III. Some aspects of the biology and habits of Xyleborus spp. and their relation to disease transmission. In: St. Augustine, ed. *Annual Report on Cacao Research, 1959-1960.* Trinidad: Imperial College of Tropical Agriculture, 59–65.

Liu FF, Barnes I, Roux J, Wingfield MJ, Chen SF, 2018. Molecular phylogenetics and microsatellite analysis reveal a new pathogenic *Ceratocystis* species in the Asian-Australian clade. *Plant Pathology* **67**, 1097–1113.

Mehrabi R, Mirzadi Gohari A, Kema GHJ, 2017. Karyotype variability in plant-pathogenic fungi. *Annual Review of Phytopathology* **55**, 483–503.

Mehrabi R, Taga M, Kema GHJ, 2007. Electrophoretic and cytological karyotyping of the foliar wheat pathogen *Mycosphaerella graminicola* reveals many chromosomes with a large size range. *Mycologia* **99**, 868–876.

Muchovej JJ, Albuquerque FC, Ribeiro GT, 1978. *Genelina arborea* a new host of *Ceratocystis fimbriata*. *Plant Disease* **62**, 717–719.

Piveta G, Alfenas AC, Muniz M de FB, Valdebenito-Sanhueza RM, Ferreira MA, 2013. Ocorrência de Ceratocystis fimbriata em kiwi (*Actinidia deliciosa*) no Sul do Brasil. *Revista Brasileira de Fruticultura* **35**, 665–669.

Rincones J, Mazotti GD, Grifftih GW *et al.*, 2006. Genetic variability and chromosome-length polymorphisms of the witches' broom pathogen Crinipellis perniciosa from various plant hosts in South America. *Mycological Research* **110**, 821–832.

Rossetto CJ, Ribeiro I, 1990. Mango wilt. XII. Recommendations for control. *Revista de Agricultura* **65**, 173–180.

Sasaki AA, Fernandes GF, Rodrigues AM *et al.*, 2014. Chromosomal Polymorphism in the *Sporothrix schenckii* Complex. *PLOS ONE* **9**, e86819.

Silva AC, Betancourth BML, Ferreira DC, Elerati TL, Rodrigues F, Alfenas AC, 2020. Responses of resistant and susceptible hybrid clones of *Eucalyptus urophylla* × *Eucalyptus grandis* to infection by *Ceratocystis fimbriata*. *Annals of Forest Science* **77**, 1–19.

Silva AC, Cândido TS, Sales NLP, Harrington TC, Alfenas AC, 2017. First report of ceratocystis wilt caused by *Ceratocystis fimbriata* on *Caryocar brasiliense* trees in Brazil. *Plant Disease* **101**, 1822.

Silveira SF, Harrington TC, Mussi-Dias V, Engelbrecht CJB, Alfenas AC, Silva CR, 2006. *Annona squamosa*, a new host of *Ceratocystis fimbriata*. *Fitopatologia Brasileira* **31**, 394–397.

Thorpe DJ, Harrington TC, Uchida JY, 2005. Population Biology Pathogenicity, Internal Transcribed Spacer-rDNA Variation, and Human Dispersal of Ceratocystis fimbriata on the Family Araceae.

Valarini PJ, Tokeshi H, 1980. *Ceratocystis fimbriata*, causal agent of fig dieback, and its control. *Summa Phytopathologica* **6**, 102–106.

Valdetaro DCOF, Harrington TC, Oliveira LSS *et al.*, 2019. A host specialized form of *Ceratocystis fimbriata* causes seed and seedling blight on native *Carapa guianensis* (andiroba) in Amazonian rainforests. *Fungal Biology* **123**, 170–182.

Viégas AP, 1960. Seca da mangueira. *Bragantia* **19**, 162–182.

Van Wyk M, Wingfield BD, Marin M, Wingfield MJ, 2010. New *Ceratocystis* species infecting coffee, cacao, citrus and native trees in Colombia. *Fungal Diversity* **40**, 103–117.

Zhong S, Steffenson BJ, 2007. Molecular karyotyping and chromosome length polymorphism in Cochliobolus sativus. *Mycological Research* **111**, 78–86.

Zolan ME, 1995. Chromosome-length polymorphism in fungi. *MICROBIOLOGICAL REVIEWS* **59**, 686–698.

CHAPTER 1 - GENETIC VARIABILITY AND HOST SPECIALIZATION OF THE *Ceratocystis fimbriata* SPECIES COMPLEX IN BRAZIL

Fernando Montezano Fernandes[1], Daiana Maria Queiroz Azevedo[1], Lúcio Mauro da Silva Guimarães[1], Leonardo Sarno Soares Oliveira[2], Rafael Ferreira Alfenas[1], Jaime Honorato Júnior[3], Acelino C. Alfenas[1*]

[1] Departamento de Fitopatologia, Universidade Federal de Viçosa, Viçosa, MG 36570-900, Brazil.

[3] Universidade Federal do Oeste da Bahia, Centro Multidisciplinar da Barra, Barra, BA 47100-000, Brazil.

*Corresponding author: Acelino C. Alfenas, Laboratory of Forest Pathology, Department of Plant Pathology, Universidade Federal de Viçosa, Minas Gerais State, Brazil; Tel: +55 (31) 3612-2428; E-mail: aalfenas@ufv.br

To be submitted to the Plant Pathology

ABSTRACT

Ceratocystis fimbriata is an important pathogen that causes xylem lesion, wilt and death in different plant species. Considering the wide host range, it is possible that more adapted populations of *C. fimbriata* have been selected and there is high genetic and physiological variability within the pathogen populations. Genotypic analyses and inoculation studies were performed to investigate the genetic and physiological variability of isolates of *C. fimbriata* complex obtained from different host species and geographic regions in Brazil. The minimum spanning tree analysis based on the *C. fimbriata* of 14 SSR markers exhibited a clear separation of isolates according to the host, which was defined as groups of isolates that differ in at least five loci. Based on the results of inoculation of 11 isolates on eight hosts, a wide variation in aggressiveness was found. Considering the length of xylem lesion caused by *C. fimbriata* isolates, *F. carica* was the most susceptible to the isolates tested, followed by *M. indica*. Only *T. cacao* and *C. guianensis* isolates proved to be specialized by their hosts. The isolates tested were more aggressive in their respective hosts.

Keywords: Ceratocystis wilt, cross-inoculations, physiological variability

INTRODUCTION

Ceratocystis fimbriata Ellis & Halsted is a polyphagous pathogen with a wide geographic distribution that causes disease in economically important agricultural and forestry crops and natural ecosystems. The fungus was first described as the causal agent of black rot of sweet potato [*Ipomoea batatas* (L.) Lam] in New Jersey, United States of America (Halsted, 1890). In Brazil, *C. fimbriata* was originally described in the state of São Paulo on *Crotalaria juncea* L. (Costa & Krug, 1935). However, in the 1930s the disease had already been reported in the state of Pernambuco, causing disease in *Mangifera indica* L., being called "Mal do Recife" (Carvalho, 1938). Later, the disease was reported in other hosts, such as *Mangifera indica* L. (Carvalho, 1938), *Hevea brasiliensis* L. (Albuquerque *et al.*, 1972), *Gmelina arborea* Roxb. Ex Sm. (Muchovej *et al.*, 1978), *Ficus carica* L. (Valarini & Tokeshi, 1980), *Eucalyptus* spp. (Ferreira *et al.*, 1999), *Theobroma cacao* L. (Baker *et al.*, 2003), *Annona squamosa* L. (Silveira *et al.*, 2006), *Carapa guianensis* Aubl. (Halfeld-Vieira *et al.*, 2012; Valdetaro *et al.*, 2019), *Tectona grandis* L. f. (Firmino *et al.*, 2012), *Actinidia deliciosa* (A. Chev) CF Lianget

& AR Ferguson (Piveta *et al.*, 2013) and *Caryocar brasiliense* Cambess. (Silva *et al.*, 2017). Worldwide, more than 80 species of plants have been confirmed as hosts of this pathogen (Farr & Rossman, 2021). Symptoms of wilt, loss of turgidity, and brightness of the leaves that subsequently dry and fall, leading to plant death, are commonly observed on diseased plants in the field. Infection generally results from fresh wounds, often those made by infested cutting tools (Viégas, 1960) or through root infection via soilborne aleurioconidia (Ribeiro *et al.*, 1984; Rossetto & Ribeiro, 1990). The pathogen mainly infects the parenchyma, phloem, and xylem vessels, and causes discoloration in the radial direction of the wood, as well as the rot of various root crops (Ferreira *et al.*, 2006; Silva *et al*., 2020).

Because of the similarity of morphological characteristics *C. fimbriata* is known as a complex of many cryptic species. Thus, the pathogen responsible for black rot in sweet potatoes (*I. batatas*) is treated as *C. fimbriata* sensu stricto (s.s.) while those that cause the disease in other hosts are treated as *C. fimbriata* sensu lato (s.l.) (de Beer *et al.*, 2014). There is significant genetic variation within the *C. fimbriata* complex (de Beer *et al.*, 2014), much of which occurs between clades and lineages associated with specific geographic regions or hosts (Baker *et al.*, 2003; Ferreira *et al.*, 2010). Four phylogenetic clades are known in this complex, and can be separated according to geographic region: Latin American clade (LAC), North American clade (NAC), Asian-Australian clade (AAC), and African clade (AFC) that include *C. albofundus* M. J. Wingf., De Beer, & M. J. Morris, a important pathogen *of Acacia mearnsii* in Africa (Harrington *et al.*, 2011; Fourie *et al.*, 2015; Liu *et al.*, 2018). Brazilian isolates of *C. fimbriata* complex, are positioned in the LAC, along with the isolates of the pathogen from *I. batatas*, on which the species was first described. The genetic diversity of *C. fimbriata* in Brazil has been successfully evaluated in population studies using microsatellite markers (SSR) (Steimel *et al.*, 2004). In this way, it was possible to determine the genetic structure of populations of isolates associated with a particular cultivated or native host as well as geographic locations (Harrington *et al.*, 2015; Li *et al.*, 2016; Oliveira *et al.*, 2018).

Pathogenicity assays have shown that certain species of *Ceratocystis* have physiological specialization for their hosts. Within the LAC, the isolates that cause wilt in *T. cacao* and *Platanus ocidentalis* L. were described as distinct species, *C. cacaofunesta* Engelbr. & T.C. Harr. and *C. platani* (Walter) Engelbrecht & Harrington respectively (Baker *et al.*, 2003; Engelbrecht *et al.*, 2007a). In addition to physiological specialization, these species are intersterile with all other strains tested in the *C. fimbriata* complex (Engelbrecht & Harrington, 2005). In Brazil, Ceratocystis wilt has been reported in several crops and geographic regions. However, the degree of aggressiveness on exotic and native hosts varies considerably among some members of the complex (Baker *et al.*, 2003; Harrington *et al.*, 2011; Valdetaro *et al.*, 2015, 2019). Recent studies have demonstrated the physiological specialization of a population of the *C. fimbriata* complex that causes an atypical symptom, colonizing seeds and seedlings of *C. guianensis*. In this work, the authors proposed that this population could be recognized as a special form and was named *C. fimbriata* f. sp. *carapa* (Valdetaro *et al.*, 2019).

Other studies of physiological variability (Harrington *et al.*, 2011) suggest that some *C. fimbriata* genotypes are adapting to specific hosts and, therefore, in this work, it was hypothesized that some populations of *C. fimbriata* in Brazil are specializing for their hosts. To confirm our hypothesis, this study aimed to determine the physiological variability of *C. fimbriata* isolates through cross inoculations in different host species. Furthermore, the population diversity of *C. fimbriata* in Brazil was evaluated using SSR markers.

MATERIALS AND METHODS

Fungal isolates and culture conditions

Fungal isolates of the *C. fimbriata* complex used in this study belong to the Fungal Collection of the Forest Pathology Laboratory /Bioagro of the Universidade Federal de Viçosa, Minas Gerais, Brazil. The isolates analyzed were collected from 11 different symptomatic hosts and geographic origins in Brazil. Previous studies showed that these isolates are pathogenic to their corresponding hosts (Baker et al., 2003; Oliveira et al., 2015a; Oliveira et al., 2016, 2021; Silveira et al., 2006; Valdetaro et al., 2015, 2019). Information on isolates studied is summarized in Table 1. The isolate of *C. fimbriata* s.s. that causes black rot of sweet potato (*I. batatas*) was not included in this study because it is not found in Brazil. Isolates were grown on MEYA culture medium (2% malt extract, 0.2% yeast extract, and 2% agar) maintaining the plates in BOD at 25 ± 2ºC with photoperiod 12 h under 20 $\mu mol \cdot m^{-2} \cdot s^{-1}$.

Genotyping and microsatellite analysis

The DNA extraction of cultures from 15-day-old at 28°C was performed as previously described (Specht *et al.* 1982), with modifications (Teixeira *et al.*, 2011). The quantity of the total DNA was assessed using a NanoDrop 2000c spectrophotometer (Thermo Scientific). Fourteen microsatellite markers (SSR) (AAG8, AAG9, CAA9, CAA10, CAA15, CAA38, CAA900, CAT1, CAT12, CAG5, CAG15, CAG900, GACA60, and GACA6K) developed from an isolate of *C. cacaofunesta* (Steimel *et al.*, 2004) and mapped into the *C. fimbriata* genome (Simpson *et al.*, 2013) were used for isolate genotyping. Each of the primer pairs was fluorescently labeled. PCR amplifications were performed using the Veriti 96-well thermal cycler (Applied Biosystems), following the protocol previously described (Ferreira *et al.*, 2010). The amplicon size of PCR products was determined by capillary electrophoresis, for which the ABI Prism 3500-Avant Genetic Analyzer (Applied Biosystems) and GeneMapper v. 4.1 Software (Applied Biosystems) were used. Most microsatellite loci have trinucleotide repeats, except for GACA6K and GACA60 loci, which have bi- and tetranucleotide repeats, respectively. Each estimated product length was rounded to the nearest whole number, and alleles were assigned based on comparison to a large dataset of more than 1,300 isolates.

The 11 isolates of *C. fimbriata* s.l. used in this study were genotyped and the alleles were added to a preexisting dataset of this organism (Supplementary Table S1) (Ferreira *et al.*, 2010, 2017; Oliveira *et al.*, 2015b, 2021; Valdetaro *et al.*, 2015, 2019). For determining the minimum number of loci necessary to discriminate between individuals in a population, genotype accumulation curves with 1,000 bootstrap replications were created for each population. Nei's gene diversity *(H)* index (Nei, 1973) was calculated with a clone correction in order to remove the bias of over-representation of clones based on the microsatellite alleles for the populations of each host. Multilocus genotypic diversity was estimated using Stoddart and Taylor's (*G*) index (Stoddart & Taylor, 1988) with rarefaction. All analyzes were performed using the POPPR package (Kamvar *et al.*, 2014) for software RStudio.

Plant material

For the host range experiment, we performed a series of inoculation with 11 isolates from different hosts and geographic origins in Brazil (Table 1). Previous studies showed that these isolates are pathogenic to their corresponding hosts (Baker *et al.*, 2003; Silveira *et al.*, 2006; Oliveira *et al.*, 2015a, 2016, 2021; Valdetaro *et al.*, 2015, 2019). All the isolates were inoculated into *A. deliciosa* seedlings (cultivar Monty, 3-mo-old), *A. squamosa* seedlings (8-mo-old), rooted cuttings of the hybrid clone CLR1172 (=1172) of *E. urophylla* x *E. grandis* (3-mo-old), *F. carica* seedlings (6-mo-old), rooted cuttings of clone FDR5788 of *H. brasiliensis*

(6-mo-old), *M. indica* seedlings (cultivar Espada, 6-mo-old), rooted cuttings of clone C1 of *T. grandis* (5-mo-old) e *T. cacao* seedlings (10-mo-old). The plants were transplanted into 2 L pots containing the substrate Tropstrato V8® (Vida Verde) supplemented with 6 kg m^{-3} of simple superphosphate and 6 kg m^{-3} Osmocote® (15-09-12) (ICL Specialty Fertilizers). Maintenance fertilization was carried out 45 days after transplanting and when necessary, with NPK fertilizer (20-20-20).

Pathogenicity tests

For inoculation, the isolates were multiplied separately in Petri dishes (60 x 15 mm) containing MEYA culture medium and maintained in a growth room at 25 ± 2ºC with photoperiod 12 h under 20 $\mu mol \cdot m^{-2} \cdot s^{-1}$ for 10 days. Inoculation was performed by wounding (approx. 3 mm deep) the stem base of the plants with a sterile circular punch (Ø = 9 mm) followed by the deposition of a mycelium plug of equal diameter (Supplementary Figure S2). The inoculation site was wrapped with parafilm to reduce desiccation and contamination. For the control plants, a MEYA medium plug was used. A completely randomized design with five replicates per isolate was used. Plants were incubated in a greenhouse for 60 days with an average temperature of 23°C (range 8 - 45°C), depending on the time of the year. This experiment was performed twice. The two experiments were carried out between May 2020 and May 2021. The length of the xylem lesion was measured after 60 days of incubation, or when the plants exhibited wilting symptoms. The carrot baiting method (Moller and Devay, 1968) was used to re-isolate the fungus. Data were analyzed for each trial and were submitted to analysis of variance (ANOVA) and means comparison by the Tukey test ($p < .05$) using software RStudio.

RESULTS

Genetic diversity

A total of 173 multilocus genotypes were identified amongst the 589 *C. fimbriata* isolates using microsatellite markers. Of the 14 microsatellite loci tested, all but locus CAG900 were polymorphic among the isolates analyzed (Table 2). Nei's gene diversity (*H*) was calculated for each of the 11 populations of *C. fimbriata* from Brazil (Table 3). A second calculation of gene diversity was made using unique genotypes from each population (clone corrected for population). Relatively high levels of gene diversity were found for isolates from *M. indica, A. deliciosa, Eucalyptus* sp. and *H. brasiliensis*. A gene diversity value of 0.0 was found in the *G. arborea* population because they were single-genotype population. *Annona squamosa* and *C. brasiliensis* had only one isolate and therefore it was not possible to perform an analysis of gene diversity for these hosts. The highest genotypic diversity with rarefaction was found in populations of *Eucalyptus* sp. (*G* = 11.54), *M. indica* (*G* = 7.46)*, C. guianensis* (*G* = 5.56), and *A. deliciosa* (*G* = 5.06). The remaining populations had genotypic diversity values G = 1.44 to 2.88 (Table 2). The genotype accumulation curves indicated that 100% of the genotypes were detected by 13 markers (Figure 1).

The minimum spanning tree analysis based on the *C. fimbriata* SSR profiles showed seven large groups for the isolates of *A. deliciosa*, *C. guianensis*, *F. carica*, *G. arborea*, *H. brasiliensis*, *T. grandis,* and *T. cacao*, which were defined here as groups of isolates that differ by only five loci. Isolates of *Eucalyptus* sp. and *M. indica* did not form well-defined groups like those isolates from other hosts (Figure 2).

The population of *M. indica* isolates clustered in three groups according to geographic region: East of Rio de Janeiro (EastRJ), Southeast and Mato Grosso do Sul (SE+MS) and

Northeast (NE) as previously found (Oliveira *et al.*, 2015b). The EastRJ population exhibited a clonal complex with 21 isolates, while the SE+MS population formed two large clonal complexes containing 31 and 40 isolates respectively. The clonal complexes were defined here as groups of isolates that do not differ at any microsatellite loci. The NE populations showed greater genotypic diversity and there was no formation of large clonal complexes. The largest clonal complex from the SE+MS population grouped the *C. brasiliensis* isolate LPF1489, while the *A. squamosa* isolate LPF1331 differed in only one locus from the clonal complex from the EastRJ population. The *A. deliciosa* isolates, like the *M. indica* isolates, formed a large clonal complex with 42 isolates. The population of *H. brasiliensis* isolates formed two clonal complexes based on geographic location, one from the state of Acre and the other from the state of Bahia.

Pathogenicity tests

Differences in the length of xylem lesion caused by *C. fimbriata* isolates were observed among the eight hosts tested (Figure 4). Only *T. grandis*, *F. carica*, *M. indica*, and *Eucalyptus* sp. plants exhibited wilting symptoms (Figure 5). Re-isolations of the pathogen from discolored tissue of the inoculated plants yielded typical colonies of *C. fimbriata* (Supplementary Figure S2f) even in those with small lesions. This demonstrates that the fungus was alive; however, it remained restricted in a small portion of host tissue. The control plants, inoculated with MEYA culture medium, remained asymptomatic and we observed limited discoloration (wound reaction) near the wound.

The data from the two experiments were analyzed separately. In both analyses, significant variation was found among the isolates ($P \leq 0.05$) (Supplementary Table S2). In *A. deliciosa* plants, the isolates LPF1443 from *A. delciosa* and LPF1489 from *C. brasilienses* caused the biggest lesions in the two trials. However, in the first trial, lesion length values above 100cm were obtained for the *T. grandis* isolate LPF2199, which was not repeated in the second trial. Different results in both trials were also observed in *A. squamosa* plants. In the first trial, plants inoculated with LPF1331 from *A. squamosa* displayed the longest lesions. In the second trial, the LPF1912 from *Eucalyptus* sp. caused the longest lesions.

Ficus carica was the most susceptible host to all isolates tested (Figure 4g-i, 5a) and was considered an "universal susceptible host" of *C. fimbriata*, exhibiting substantial xylem discoloration and plant mortality. From the 20th day, wilt symptoms were observed in plants inoculated with the isolates LPF1156 from *M. indica* and LPF2199 from *T. grandis* in both trials. Except for the isolates LPF1560 from *C. guianensis,* LPF1489 from *C. brasiliense,* and LPF1332 from *T. cacao*, all others caused wilt and death in *F. carica*. In *Eucalyptus*, isolate LPF1912 from *Eucalyptus* spp. caused the greatest xylem lesion, wilt, and death of the evaluated plants. Isolates LPF1156 from *M. indica* and LPF1336 from *F. carica*, showed higher xylem discoloration than other isolates. However, only the isolate LPF1912 induced wilt in eucalypt plants in the first trail (Figure 4v-x, 5b).

In *H. brasiliensis* plants, the isolate LPF1394 from *H. brasiliensis* was the most aggressive. It induced extensive lesions on the bark and formed a grayish-white layer of mycelium, typical of the disease in this host. (Figure 4j-l). However, none of the inoculated plants died or wilted at the end of the experiment. The *M. indica* plants wilted before the final evaluation and developed lesions on the stem bark (Figure 4m-o, 5c). At 40 days, wilt symptoms were observed in plants inoculated with isolates LPF1156 from *M. indica*, LPF1331 from *A. squamosa,* and LPF1489 from *C. brasilienses* in the first trial. The same isolates caused wilt 25 days after inoculation in the second trial.

In *T. grandis*, wilt symptoms were observed in plants inoculated with the *T. gandis* isolate LPF2199 on the 20th day of the second trial (Figure 4p-r, 5d). This isolate caused the highest mean lesion length in the first trial. In *T. cacao*, only the isolate LPF1332 from *T. cacao* was pathogenic to cacao. The isolate LPF1560 from *C. guianenses* was also host-specific.

DISCUSSION

Microsatellite data showed that *C. fimbriata* isolates studied formed distinct populations, as previously reported (Ferreira *et al.*, 2010; Oliveira *et al.*, 2015b, 2021; Valdetaro *et al.*, 2015, 2019). The minimum spanning tree analysis was able to delimit these populations of isolates according to the host. The reproductive features of this organism are one of the elements that allow this clear separation of isolates by their respective hosts. Members of the *C. fimbriata* species complex are homothallic and therefore do not need a mating partner to complete the sexual cycle and are able to self-fertile (Harrington & McNew, 1997; Witthuhn *et al.*, 2000). Furthermore, the limited dispersal of ascospores, the ability to survive in the soil, and asexual reproduction, combined with the predominance of self-fertilization result in isolated populations of the *C. fimbriata* complex that have relatively low genetic diversity and are highly differentiated from other populations, suggesting limited gene flow (Roux *et al.*, 2001; Ferreira *et al.*, 2010, 2017). The physiological variation among isolates of *C. fimbriata* has been attributed to a wide genetic variability in the population of the pathogen, especially for the isolates of *M. indica* and *Eucalyptus* sp. (Zauza *et al.*, 2004; Ferreira *et al.*, 2010; Oliveira *et al.*, 2016).

Isolates from *M. indica* appear to be native to the coastal forest type of the Atlantic Forest in Rio de Janeiro and the Caatinga (Oliveira *et al.*, 2015b, 2018), and our findings showed a clear separation of the population of isolates of *M. indica* according to the geographic region. The population with the greatest genetic variation was found in the NE, which may be due to the sampling strategy utilized. The isolates of *C. fimbriata* were collected in several small cities in different states of Northeastern Brazil, located mainly on the gardens and street trees, and not in commercial orchards of *M. indica*, exhibiting a low gene flow among NE populations. In contrast, the populations from EastRJ and SE+MS exhibited widely shared genotypes that formed large clonal complexes. Isolates from these populations were sampled from single commercial orchards or small farms in the state of Rio de Janeiro, São Paulo, Minas Gerais, and a few diseased trees in a city in Mato Grosso do Sul (Ferreira *et al.*, 2010; Oliveira *et al.*, 2015b). The limited genotypic diversity and localized spread of genotypes are possible through the movement of the pathogen on infested tools, or by bark beetles, *Hypocryphalus mangifera* (Coleoptera: Scolytinae) (Masood & Saeed, 2012; Al Adawi *et al.*, 2013). This insect is native to southern Asia including India, Malaysia, and Indonesia (Pena & Mohyuddin, 1997) and it has been introduced to many areas in which *M. indica* is cultivated, including Brazil (Rossetto & Medeiros, 1967). The insect drills the sapwood of diseased trees and disperses the fungus propagules through excrement and/or spores adhered to their bodies.

Ceratocystis fimbriata population on *Eucalyptus* sp., exhibited the highest genotypic diversity index (*G* = 11.54). Isolates from this host are probably native to the Cerrado that infect plants through soil inoculum originating from native vegetation (Ferreira *et al.*, 2010, 2011; Oliveira *et al.*, 2015b). Furthermore, in the recent past, the production of eucalyptus rooted cuttings was based on field-collected sprouts from fresh stumps (Alfenas *et al.*, 2009), and it has been suggested that the fungus may have been introduced to new sites through symptomless rooted cuttings. Although sexual reproduction usually occurs through selfing to members of the *C. fimbriata* complex, mating events among isolates from distinct populations can also occur, which can lead to the emergence of new genotypes recombinants with unknown aggressiveness and, consequently, affect the host range. Plant pathogens are frequently spatiotemporally variable, with new genotypes emerging regularly as a result of mutation, recombination, and gene flow (Zhan *et al.*, 2015). The population of *A. deliciosa* isolates also presented high levels of gene (*H*) and genotypic (*G*) diversity. This population is restricted in the southern region of Brazil, in the states of Santa Catarina and Rio Grande do Sul (Ferreira *et al.*, 2017; Oliveira *et al.*, 2021). It has been hypothesized that the population of *A. deliciosa* isolates may have been introduced from infected plant material from the source nursery, or that the population is native and could be naturally soilborne (Ferreira *et al.*, 2017). Throughout addition to the fact that the fungus is naturally soilborne, the use of infested tools during cultural practices can also contribute to the fungus spread in the cultivated regions.

Genetic variability and variation in aggressiveness were observed among *C. fimbriata* isolates from 11 different hosts, revealing genetic and physiological differentiation among isolates. Our inoculation results were broadly consistent with those of previous experiments that employed a few of the same hosts (Baker *et al.*, 2003; Harrington *et al.*, 2011). Although isolates from a particular host tended to be the most aggressive isolates to that host, it was not possible to verify clear patterns of physiological specialization. Pathogens that are completely host-specialized are infective only to the host on which they specialize (Gudelj *et al.*, 2004). Therefore, our hypothesis of specialization of *C. fimbriata* isolates by their hosts in Brazil was not supported by the inoculation results except for *C. guianensis* and *T. cacao*, implying that *C. fimbriata* is still a host generalist pathogen. Inoculation trials showed host specialization only for *T. cacao*, being one of the few documented cases of a LAC member of Ceratocystis with host specialization to native hosts. Even in *F. carica* that was highly susceptible to the analyzed isolates, the *T. cacao* isolate LPF1332 was not able to cause xylem discoloration. Populations of *C. cacaofunesta* are thought to be native to the upper Amazon Basin (Rondônia) and are specialized to infect cacao plants and relatives (Baker *et al.*, 2003; Engelbrecht *et al.*, 2007b). The *C. guianensis* isolate LPF1560 was unable to cause xylem discoloration in the hosts used in this study even in *C. guianensis* plants (data not shown), but it infected seeds, seedlings and induced damping-off in natural ecosystem (Valdetaro *et al.*, 2019). Like the population of *T.*

cacao, the population of *C. guianensis* appears to be native to the Amazon and exclusively pathogenic in seed and seedlings. Based on host specificity, this population was recognized as a special form, *C. fimbriata* f. sp. *carapa,* and not as a new species. Additionally mating studies indicated that this population constitutes a single biological species that are interfertile with *C. fimbriata* from sweet potato, on which the species is based, as well as with Brazilian *Eucalyptus* sp, *M. indica,* and *T. grandis* isolates that are considered to be *C. fimbriata*. (Valdetaro *et al.*, 2019).

In fungal plant pathogens, pathogenicity and host specificity features may be regulated by multiple genes. Recently, unique genomic segments including several effector proteins in the genome of *C. manginecans* (CMW46461), considered a lineage within *C. fimbriata* complex (Oliveira *et al.*, 2015b), have been demonstrated (Fourie *et al.*, 2020). In this work, the authors discovered several genetic elements that could play a role in host specificity, including species-specific enzymes involved in nutrient metabolism and transformation, as well as a number of possible effector genes. Differences in nutrient processing may be a determining factor influencing host specificity in *C. fimbriata.* A higher growth rate was observed in *C. manginecans* isolates when cultivated in *A. mangium* extract agar (AEA) and slower in MEA culture medium (Fourie *et al.*, 2019). In the *C. cacaofunesta* genome a great variety of proteins with effector-like characteristics was also found, such as the allergen Asp and cyanovirin, which can elicit plant responses, and also proteins possibly involved in resistance to host-generated oxidative stress (Molano *et al.*, 2018).

The inoculated isolates showed the same pattern across the investigated hosts, despite variations between the two experiments. Wilt of *T. grandis* plants was only found in the second trial, probably due to the higher temperature from November to January when the experiment was performed. The first trial was conducted from 27 February 2020 to 27 May 2020, when the average daily minimum was 13.7°C. The optimum temperature for *C. fimbriata* ranges between

24 and 26°C (Oliveira *et al.*, 2015a). Despite not showing wilt symptoms in the first trial, the *T. grandis* isolate LPF2199 was the most aggressive. Interestingly, the other *C. fimbriata* isolates were not able to colonize into *T. grandis* even though the genetic material used (clone C1) was susceptible to this disease. It was hypothesized that the LPF2199 isolate could be physiologically specialized by its host, but the results of inoculation experiments lead to the rejection of this hypothesis since this isolate was pathogenic to other hosts. Even though *F. carica* was highly susceptible to all isolates tested, except for of the isolates from *C. guianensis* and *T. cacao*, population of isolates of this host only had two genotypes. *Ficus carica* is cultivated largely in the Brazilian states of São Paulo and Rio Grande do Sul (IBGE, 2019), and the isolates have been obtained from several farms in a limited region of São Paulo (Ferreira *et al.*, 2010) where the disease had been reported (Valarini & Tokeshi, 1980). In these areas, the disease occurred in circular patches of dead trees. Probably the fungus was introduced through vegetatively propagated plants and spread to adjacent plants through the root system (Ferreira *et al.*, 2010). The factors involved in the high susceptibility of *F. carica* to *C. fimbriata* have not been studied. In order to better understand the mechanisms of fungal infection and the host defense responses, histopathology and histochemistry investigations must be carried out, especially in hosts that are contrasting for susceptibility to *C. fimbriata*, such as *T. grandis* and *F. carica*.

Mangifera indica was highly susceptible to nearly all isolates tested, but only LPF1156 from *M. indica*, LPF1331 from *A. squamosa*, and LPF1489 from *C. brasilienses* induced wilt and death of plants. The minimum spanning tree analysis based on the *C. fimbriata* SSR profiles marker, indicated that the isolate LPF1489 clustered with the largest clonal complex of *M. indica* isolates, from São Paulo, Mato Grosso do Sul, and Minas Gerais. Similarly, the isolate LPF1331 differs in only one SSR locus from another large *M. indica* clonal complex with isolates from the state of Rio de Janeiro. The population of *M. indica* isolates from Rio de

Janeiro differs substantially from other populations (Ferreira *et al.*, 2010; Oliveira *et al.*, 2015b) and are also aggressive to *A. squamosa*, which was recorded as a host only in this region of Brazil (Silveira *et al.*, 2006).

Despite the fact that *H. brasiliensis* is endemic to Brazil and has been identified as a *C. fimbriata* host (Albuquerque *et al.*, 1972; Pereira & Santos, 1985; Silveira *et al.*, 1985) strong evidence of specialization to the host was not observed. The isolate LPF1394 was the most aggressive in *H. brasiliensis* plants and caused extensive necrotic lesions on the bark of inoculated plants, but we did not observe wilt symptoms. The disease caused in *H. brasiliensis* by *C. fimbriata* is gray mold or moldy rot on tapping panels affecting latex yield. Small cankers on the tapping panel, uneven renewal of the bark, and formation of pustules with latex exudation are the main disease symptoms (Santos *et al.*, 2012; Valdetaro *et al.*, 2015). These damages can be partially controlled by the use of fungicides (Furtado 2007), and currently represents the only available method to manage the disease on *H. brasiliensis*. Among the Brazilian *H. brasiliensis* isolates investigated, only two genotypes were identified depending on the region of origin, Acre or Bahia states. These two uniform populations suggest that the spread of genotypes from one state to another was mediated by humans on propagative material, moreover, rather than infection from natural soilborne inoculum, the tapping panels may have been infected via contaminated tools (Valdetaro *et al.*, 2015).

Variation in aggressiveness presents a challenge in selection and breeding for resistance. Currently, the main control method for *C. fimbriata* is the planting of resistant genotypes (Oliveira *et al.*, 2021; Guimarães *et al.*, 2021). However, most experiments targeting genetic resistance have only considered the highly aggressive isolates belonging to their respective hosts. Our findings showed a high variation in the aggressiveness of isolates among tested hosts, as well as the capacity of an isolate to be pathogenic to a host other than the one from which it was isolated. In order to minimize problems of loss of genetic resistance, it is crucial to carry out a preliminary screening with isolates from different hosts and search for the most aggressive, to obtain a genotype with robust and durable resistance in the field. In addition, inoculations can be performed with a combination (mixture) of aggressive isolates, selected based on test results with isolates from a certain population and/or geographic region. The populations of *C. fimbriata* should be monitored frequently to determine whether new genotypes are being introduced into a region and whether the frequencies of certain genotypes are changing over time. Furthermore, is essential that in the management of the disease, researchers and farmers have a thorough understanding of the history of the area where the crop is to be planted. It is important to avoid nurseries that multiply different tree species using untreated soil or from places where the disease has been reported.

AUTHOR CONTRIBUTIONS STATEMENT

Fernando Montezano Fernandes: Conceptualization, Formal analysis, Investigation, Methodology, Visualization, Writing - Original Draft. **Daiana Maria Queiroz Azevedo:** Conceptualization, Formal analysis, Investigation, Writing - Review & Editing. **Lucio Mauro:** Conceptualization, Investigation, Supervision, Writing - Review & Editing.

Leonardo Sarno Soares Oliveira and **Rafael Ferreira Alfenas:** Writing - Review & Editing. **Jaime Honorato Junior**: Resources, Writing - Review & Editing. **Acelino Couto Alfenas**: Conceptualization, Funding Acquisition, Resources, Supervision, Writing - Review & Editing. All authors provided feedback and approved the final manuscript.

DATA AVAILABILITY STATEMENT

Authors can confirm that all relevant data are included in the article and/or its supplementary information files. The authors report no declarations of interest.

ACKNOWLEDGMENTS

The authors thank to Coordenação de Aperfeiçoamento de Pessoal de Nível Superior (CAPES) for a fellowship granted to first the author. For Fundação de Amparo à Pesquisa do Estado de Minas Gerais (FAPEMIG) and Conselho Nacional de Desenvolvimento Científico e Tecnológico (CNPq). This study was financed in part by the Coordenação de Aperfeiçoamento de Pessoal de Nível Superior - Brasil (CAPES) - Finance Code 001.

REFERENCES

Al Adawi A, Al Jabri R, Deadman M, Barnes I, Wingfield B, Wingfield M, 2013. The mango sudden decline pathogen, *Ceratocystis manginecans*, is vectored by *Hypocryphalus mangiferae* (Coleoptera: Scolytinae) in Oman. *European Journal of Plant pathology.* **135**, 243–251.

Albuquerque FC, Duarte MLR, Silva HM, 1972. Ocorrência do mofo cinzento (*Ceratocystis fimbriata*) da seringueira. *In: Seminário Nacional da Seringueira*, 125–128.

Alfenas AC, Zauza EAV, Mafia RG, Assis TF de A, 2009. *Clonagem e Doenças do Eucalipto* (UFV, Ed,). Viçosa, MG.

Baker CJ, Harrington TC, Krauss U, Alfenas AC, 2003. Genetic variability and host specialization in the Latin American Clade of *Ceratocystis fimbriata*. *Ecology and Population Biology* **93**, 1274–1284.

de Beer ZW, Duong TA, Barnes I, Wingfield BD, Wingfield MJ, 2014. Redefining *Ceratocystis* and allied genera. *Studies in Mycology* **79**, 187–219.

Carvalho MB, 1938. Sobre dois insetos nocivos à mangueira. *Bol. da Secr. da Agric. Indústria e Comércio*, 130–132.

Engelbrecht CJ, Harrington TC, Alfenas AC, 2007a. Ceratocystis wilt of cacao - A disease of increasing importance. *Phytopathology* **97**, 1648–1649.

Engelbrecht CJB, Harrington TC, Alfenas AC, Suarez C, 2007b. Genetic variation in populations of the cacao wilt pathogen, *Ceratocystis cacaofunesta*. *Plant Pathology* **56**, 923–933.

Farr DF, Rossman AY, 2021. Fungal Databases. *U.S. National Fungus Collections*.

Ferreira FA, Demuner AM, Demuner NL, Pigatto S, 1999. Murcha de Ceratocystis em eucalipto no Brasil. *Fitopatologia Brasileira* **24**, 284.

Ferreira MA, Harrington TC, Alfenas AC, Mizubuti ESG, 2011. Movement of Genotypes of *Ceratocystis fimbriata* Within and Among *Eucalyptus* Plantations in Brazil. *PHYTOPATHOLOGY* **101**, 1005–1012.

Ferreira MA, Harrington TC, Piveta G, Alfenas AC, 2017. Genetic variability suggests that three populations of *Ceratocystis fimbriata* are responsible for the Ceratocystis wilt epidemic on kiwifruit in Brazil. *Tropical Plant Pathology* **42**, 86–95.

Ferreira EM, Harrington TC, Thorpe DJ, Alfenas AC, 2010. Genetic diversity and interfertility among highly differentiated populations of *Ceratocystis fimbriata* in Brazil. *Plant Pathology* **59**, 721–735.

Ferreira FA, Maffia LA, Barreto RW, Demuner NL, Pigatto S, 2006. Sintomatologia da murcha de *Ceratocystis fimbriata* em eucalipto. *Revista Árvore* **30**, 155–162.

Firmino AC, Tozze Jr HJ, Furtado EL, 2012. First report of *Ceratocystis fimbriata* causing wilt in *Tectona grandis* in Brazil. *New Disease Reports* **25**.

Fourie A, de Jonge R, van der Nest MA *et al.*, 2020. Genome comparisons suggest an association between *Ceratocystis* host adaptations and effector clusters in unique transposable element families. *Fungal Genetics and Biology* **143**, 103433.

Fourie A, van der Nest MA, de Vos L, Wingfield MJ, Wingfield BD, Barnes I, 2019. QTL mapping of mycelial growth and aggressiveness to distinct hosts in *Ceratocystis* pathogens. *Fungal Genetics and Biology* **131**.

Fourie A, Wingfield MJ, Wingfield BD, Barnes I, 2015. Molecular markers delimit cryptic species in *Ceratocystis* sensu stricto. *Mycological Progress* **14**, 1020.

Gudelj I, Fitt BDL, Van Den Bosch F, 2004. Evolution of sibling fungal plant pathogens in relation to host specialization. *Phytopathology* **94**, 789–795.

Guimarães LMS, Nunes AS, Santos SA *et al.*, 2021. Resistance of mango cultivar Ubá to Ceratocystis fimbriata depends on the pathogen's physiological variability. *Crop*

Protection **143**, 105560.

Halfeld-Vieira BA, Zilli JE, Nechet KL, Pereira GMD, Souza GR, 2012. First record of *Ceratocystis fimbriata* on *Carapa guianensis*. *New Disease Reports* **26**, 13.

Halsted BD, 1890. Some fungous diseases of the sweet potato. The black rot. *New Jersey Agriculture Experiment Station Bulletin* **76**, 7–14.

Harrington TC, Huang Q, Ferreira MA, Alfenas AC, 2015. Genetic Analyses Trace the Yunnan, China Population of *Ceratocystis fimbriata* on Pomegranate and Taro to Populations on *Eucalyptus* in Brazil. *Plant Disease* **99**, 106–111.

Harrington TC, McNew DL, 1997. Self fertility and uni-directional mating-type switching in *Ceratocystis coerulescens*, a filamentous ascomycete. *Current Genetics* **32**, 52–59.

Harrington TC, Thorpe DJ, Alfenas AC, 2011. Genetic variation and variation in aggressiveness to native and exotic hosts among brazilian populations of *Ceratocystis fimbriata*. *Population Biology* **101**, 566.

IBGE - INSTITUTO BRASILEIRO DE GEOGRAFIA E ESTATÍSTICA, 2019. Censo 2019. *Produção Agrícola Municipal*.

Kamvar ZN, Tabima JF, Gr̈unwald NJ, 2014. Poppr: An R package for genetic analysis of populations with clonal, partially clonal, and/or sexual reproduction. *PeerJ* **2014**, 1–14.

Li Q, Harrington TC, McNew D *et al.*, 2016. Genetic Bottlenecks for Two Populations of *Ceratocystis fimbriata* on Sweet Potato and Pomegranate in China. *Plant Disease* **100**, 2266–2274.

Liu FF, Barnes I, Roux J, Wingfield MJ, Chen SF, 2018. Molecular phylogenetics and microsatellite analysis reveal a new pathogenic *Ceratocystis* species in the Asian-Australian clade. *Plant Pathology* **67**, 1097–1113.

Masood A, Saeed S, 2012. BARK BEETLE, *HYPOCRYPHALUS MANGIFERAE* STEBBING (COLEOPTERA: CURCULIONIDAE: SCOLYTINAE) IS A VECTOR OF MANGO

SUDDEN DEATH DISEASE IN PAKISTAN. *Pakistan Journal of Botany* **44**, 813–820.

Molano EPL, Cabrera OG, Jose J *et al.*, 2018. *Ceratocystis cacaofunesta* genome analysis reveals a large expansion of extracellular phosphatidylinositol-specific phospholipase-C genes (PI-PLC). *BMC Genomics* **19**.

Muchovej JJ, Albuquerque FC, Ribeiro GT, 1978. *Genelina arborea* a new host of *Ceratocystis fimbriata*. *Plant Disease* **62**, 717–719.

Nei M, 1973. Analysis of gene diversity in subdivided populations. *Proceedings of the National Academy of Sciences of the United States of America* **70**, 3321–3323.

Oliveira LSS, Damacena MB, Guimarães LMS, Siqueira DL, Alfenas AC, 2016. *Ceratocystis fimbriata* isolates on *Mangifera indica* have different levels of aggressiveness. *European Journal of Plant Pathology* **145**, 847–856.

Oliveira LSS, Guimarães LMS, Ferreira MA, Nunes AS, Pimenta LVA, Alfenas AC, 2015a. Aggressiveness, cultural characteristics and genetic variation of *Ceratocystis fimbriata* on *Eucalyptus* spp. *Forest Pathology* **45**, 505–514.

Oliveira LSS, Harrington T., Ferreira MA *et al.*, 2015b. Species or genotypes? Reassessment of four recently described species of the ceratocystis wilt pathogen, *Ceratocystis fimbriata*, on *Mangifera indica*. *Phytopathology* **105**, 1229–1244.

Oliveira LSS, Harrington TC, Ferreira MA, Freitas RG, Alfenas AC, 2018. Populations of *Ceratocystis fimbriata* on *Colocasia esculenta* and other hosts in the Mata Atlântica region in Brazil. *Plant Pathology* **67**, 97–106.

Oliveira LSS, Pimenta LVA, Guimarães LMS, Souza PVD, Bhering LL, Alfenas AC, 2021. Resistance of kiwifruit cultivars to ceratocystis wilt: An approach considering the genetic diversity and variation in aggressiveness of the pathogen. *Plant Pathology* **70**, 349–357.

Pena JE, Mohyuddin AI, 1997. The mango: botany, production and uses . In: R. E. Litz, ed. *Insect pests*. Wallingford: CAB International., 327–362.

Pereira JCR, Santos AF, 1985. Controle quimico do mofo-cinzento do painel de sangria da seringueira. *Comunicado técnico. n.46.*, 1–4.

Piveta G, Alfenas AC, Muniz M de FB, Valdebenito-Sanhueza RM, Ferreira MA, 2013. Ocorrência de Ceratocystis fimbriata em kiwi (*Actinidia deliciosa*) no Sul do Brasil. *Revista Brasileira de Fruticultura* **35**, 665–669.

Ribeiro IJA, Lourenção AL, Paradela Filho O, Soares NB, 1984. Seca da mangueira: VII. Resistência de cultivares de mangueira ao fungo *Ceratocystis fimbriata* Ell. & Halst. *Bragantia* **43**, 237–243.

Rossetto CJ, Medeiros JW., 1967. Seca da mangueira. II. Existência do complexo, artrópodos do solo – Ceratocystis fimbriata, Scolytidae, no Estado de São Paulo. *Revista da Sociedade Brasileira de Fitopatologia* **1**, 19–32.

Rossetto CJ, Ribeiro I, 1990. Mango wilt. XII. Recommendations for control. *Revista de Agricultura* **65**, 173–180.

Roux J, Harrington TC, Steimel JP, Wingfield MJ, 2001. Genetic variation in the wattle wilt pathogen *Ceratocystis albofundus*. *Mycoscience* **42**, 327–332.

Santos AF, Furtado EL, Ferreira FA, Pereira JCR, Gasparotto L, 2012. *Doenças da seringueira no Brasil* (L Gasparotto, JCR Pereira, Eds,). Brasília, DF: Embrapa.

Silva AC, Betancourth BML, Ferreira DC, Elerati TL, Rodrigues F, Alfenas AC, 2020. Responses of resistant and susceptible hybrid clones of *Eucalyptus urophylla* × *Eucalyptus grandis* to infection by *Ceratocystis fimbriata*. *Annals of Forest Science* **77**, 1–19.

Silva AC, Cândido TS, Sales NLP, Harrington TC, Alfenas AC, 2017. First report of ceratocystis wilt caused by *Ceratocystis fimbriata* on *Caryocar brasiliense* trees in Brazil. *Plant Disease* **101**, 1822.

Silveira AP, Cardoso RMG, Neto FB, Oliveira DA, 1985. Ocorrência e controle químico do mofo cinzento (*Ceratocystis fimbriata* Ell. & Hast.) da seringueira. *Fitopatologia*

Brasileira **10**.

Silveira SF, Harrington TC, Mussi-Dias V, Engelbrecht CJB, Alfenas AC, Silva CR, 2006. *Annona squamosa*, a new host of *Ceratocystis fimbriata*. *Fitopatologia Brasileira* **31**, 394–397.

Simpson MC, Wilken PM, Coetzee MPA, Wingfield MJ, Wingfield BD, 2013. Analysis of microsatellite markers in the genome of the plant pathogen *Ceratocystis fimbriata*. *Fungal Biology* **117**, 545–555.

Specht CA, DrRusso CC, Novotny CP, Ullrich R, 1982. A method for extracting high-molecular-weight deoxyribonucleic acid from fungi. *Analytical Biochemistry* **119**, 158–163.

Steimel J, Engelbrecht CJB, Harrington TC, 2004. Development and characterization of microsatellite markers for the fungus *Ceratocystis fimbriata*. *Molecular Ecology Notes* **4**, 215–218.

Stoddart JA, Taylor JF, 1988. Genotypic diversity: Estimation and prediction in samples. *Genetics* **118**, 705–711.

Teixeira JA, Gonçalves DB, de Queiroz M V., De Araújo EF, 2011. Improved pectinase production in *Penicillium griseoroseum* recombinant strains. *Journal of Applied Microbiology* **111**, 818–825.

Valarini PJ, Tokeshi H, 1980. *Ceratocystis fimbriata*, causal agent of fig dieback, and its control. *Summa Phytopathologica* **6**, 102–106.

Valdetaro DCOF, Harrington TC, Oliveira LSS *et al.*, 2019. A host specialized form of *Ceratocystis fimbriata* causes seed and seedling blight on native *Carapa guianensis* (andiroba) in Amazonian rainforests. *Fungal Biology* **123**, 170–182.

Valdetaro DCOF, Oliveira LSS, Guimarães LMS *et al.*, 2015. Genetic variation, morphology and pathogenicity of *Ceratocystis fimbriata* on *Hevea brasiliensis* in Brazil. *Tropical Plant*

Pathology **40**, 184–192.

Viégas AP, 1960. Seca da mangueira. *Bragantia* **19**, 162–182.

Witthuhn RC, Harrington TC, Wingfield BD, Steimel JP, Wingfield MJ, 2000. Deletion of the *MAT*-2 mating-type gene during uni-directional mating-type switching in *Ceratocystis*. *Current Genetics* **38**, 48–52.

Zauza EA V, Alfenas AC, Harrington TC, Mizubuti ESG, Silva JF, 2004. Resistance of *Eucalyptus* Clones to *Ceratocystis fimbriata*. *Plant Disease* **88**, 758–760.

Zhan J, Thrall PH, Papa¨ıx JP, Xie L, Burdon JJ, 2015. Playing on a Pathogen’s Weakness: Using Evolution to Guide Sustainable Plant Disease Control Strategies. *Annu. Rev. Phytopathol* **53**, 19–43.

Table 1. Host sources, species, and geographic origins of *Ceratocystis fimbriata* s.l. isolates used in this study.

Species	**LPF code**	**Other code**	**Hosts**	**Geographic origin**
C. fimbriata	LPF1443	CF280, PG01	*Actinidia deliciosa*	Rio Grande do Sul, Brazil
	LPF1331	CF011, C1592	*Annona squamosa*	Rio de Janeiro, Brazil
	LPF1489	Pequi1	*Caryocar brasiliensis*	Minas Gerais, Brazil
	LPF1912	SBS-1	*Eucalyptus* spp.	Bahia, Brazil
	LPF1336	CF016, C1782, = CBS115166	*Ficus carica*	São Paulo, Brazil
	LPF1323	CF003, C925	*Gmelina arborea*	Pará, Brazil
	LPF1394	CF074	*Hevea brasiliensis*	Acre, Brazil
	LPF1156	CF234, CEBS13	*Mangifera indica*	Ceará, Brazil
	LPF2199	CE01	*Tectona grandis*	Mato Grosso, Brazil
C. fimbriata f. sp. *carapa*	LPF1560	CarAC-144B²	*Carapa guianensis*	Acre, Brazil
C. cacaofunesta	LPF1332	CF012, C1593	*Theobroma cacao*	Bahia, Brazil

Table 2. Estimated sizes (bp) of alleles of 14 microsatellite (SSR) loci in *Ceratocystis fimbriata* s.l. populations from Brazil.

SSR Locus	*Actinidia*	*Annona*	*Carapa*	*Caryocar*	*Eucalyptus*	*Ficus*	*Gmelina*	*Hevea*	*Mangifera*	*Tectona*	*Theobroma*
AAG8	173, 174, 177, 180, 183, 186	198	183	180	174, 177, 180, 183	180	174	174, 180	174, 177, 180, 186, 198	174, 180	183, 186, 189, 232
CAA9	172, 212, 218, 266, 284	223	159, 190, 251, 263	175	172, 175, 178, 211, 224, 226, 248	202, 206	175	194, 220	175, 178, 197, 206, 209, 223	175	183, 246, 290
CAA80	302, 308, 314, 317, 323	311	296, 299, 317	323	302, 308, 311, 317, 320, 323, 326	323	311	311, 314	288, 293, 311, 317, 320, 323, 329, 331, 332	311, 317	305, 314
CAA10	125, 128, 131, 134	128	128	131	128, 131, 134	131	137	125, 131	128, 131, 134	134	128, 131
CAG15	271, 277, 280, 283, 286, 298	277	252	286	256, 259, 262, 265, 268, 271, 274, 280, 286	301	262	283, 286	268, 271, 277, 286, 289, 292, 295	286, 289, 297	271, 274, 277
CAT1	246, 247, 249, 252, 255, 261	248	248,254	257	257, 261	254	259	261	248, 254, 257, 260, 261	253	258
CCAA15	321, 327, 330, 369	330	324	324	318, 321, 324	330	324	321	306, 321, 324, 330	318, 324	321, 324, 336
CAG5	317, 326, 328	323	317	317	317	335	317	317, 320	317, 320, 323, 326	317	338
GACA6k	200, 213, 215, 219, 221	219	215	221	215, 219, 221	209	215	215, 221	215, 219, 221	231, 215, 219	215, 234
CAT12x	371, 374, 377	380	365, 377	374	374, 377	383	380	374	371, 374, 377, 380	371, 377	374
CAA38	186, 198, 201, 223, 226, 232, 238, 241, 247, 253, 281, 296, 299, 302	168	156, 159, 168, 171, 180, 205, 214	201	146, 174, 192, 201, 211, 229, 238, 247, 255, 267	195	174	208, 305	146, 153, 162, 168, 174, 183, 195, 201, 211, 214, 223, 238	156, 247	226, 245, 269, 271
GACA60	187, 195, 200	221	187, 207	187	187, 200	187	187	187	187, 221	187	187, 195
AAG9	391, 397, 403	391	400	394	397	400	394	397	391, 397, 400, 403, 406	397	406
CAA900	194	194	194	194	194	194	194	194	194	194	194

0

Table 3. Genetic diversity of *Ceratocystis fimbriata* s.l. populations from Brazil based on 14 polymorphic microsatellite loci

Host	No. of isolates	No. of multilocus genotypes	Nei's gene diversity (*H*) index		Genotypic diversity (*G*) index[b]
			All isolates	Clone-corrected[a]	
Actinidia deliciosa	101	43	0.3893	0.5181	5.06
Annona squamosa	1	1	Na[c]	Na	Na
Carapa guianensis	85	15	0.1405	0.1864	5.56
Caryocar brasiliensis	1	1	Na	Na	Na
Eucalyptus sp.	80	49	0.3301	0.3578	11.54
Ficus carica	16	2	0.0232	0.0714	Na
Gmelina arborea	5	1	0.0000	Na	Na
Hevea brasiliensis	20	2	0.3008	0.5714	1.97
Mangifera indica	190	47	0.5459	0.5668	7.46
Tectona grandis	41	5	0.1219	0.2500	2.88
Theobroma cacao	49	8	0.0645	0.2959	1.44
Total	**589**	**173**	**0.6847**	**0.6828**	**42.7**

[a] Clone correction removed isolates that had genotypes identical to other isolates from the same site.

[b] Stoddart & Taylor's genotypic diversity (*G*) index with rarefaction, maximum value of 16 for each population and 589 for total.

[c] Not available.

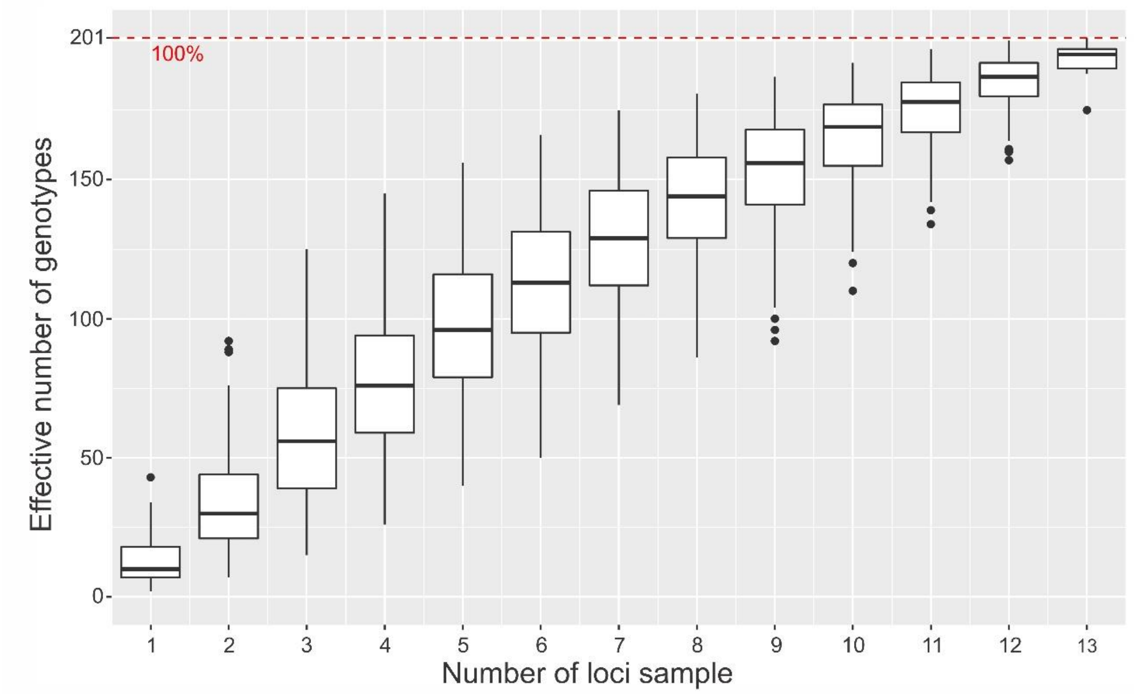

Figure 1. Genotype accumulation curves for *Ceratocystis fimbriata* s.l. populations from Brazil. Dashed line indicates 100% of the number of genotypes identified in each population. The number of loci was randomly sampled (1000 times).

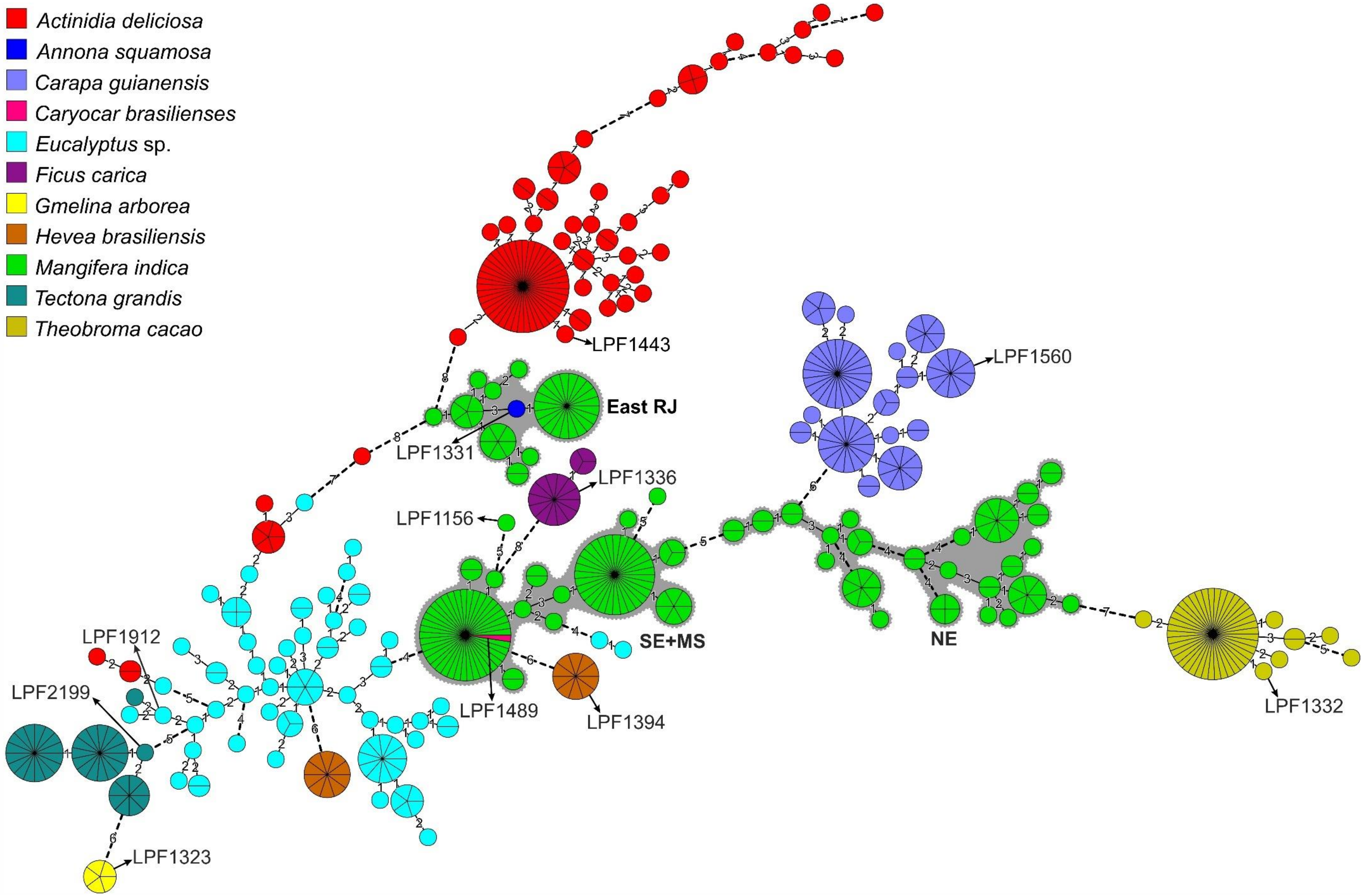
Actinidia deliciosa
Annona squamosa
Carapa guianensis
Caryocar brasilienses
Eucalyptus sp.
Ficus carica
Gmelina arborea
Hevea brasiliensis
Mangifera indica
Tectona grandis
Theobroma cacao
LPF1443
LPF1560
East RJ
LPF1331
LPF1336
LPF1156
SE+MS
NE
LPF1912
LPF2199
LPF1489
LPF1394
LPF1332
LPF1323

Figure 2. Minimum spanning tree generated on alleles of 14 polymorphic loci SSR of 607 isolates of the *Ceratocystis fimbriata* s.l. complex obtained from different host plants and geographic origins in Brazil. Colour codes indicate the host of origin, the number of sections within individual circles represents the number of strains that share the same haplotype. Haplotypes are connected by lines depending on the number of SSR loci that differentiate them. Grey zones encircle *Mangifera indica* populations from three regions of Brazil (NE = Northeastern; SE+MS = Southeastern and Mato Grosso do Sul; EastRJ = Eastern Rio de Janeiro). Arrows indicate the 11 Brazilian isolates analyzed in this study.

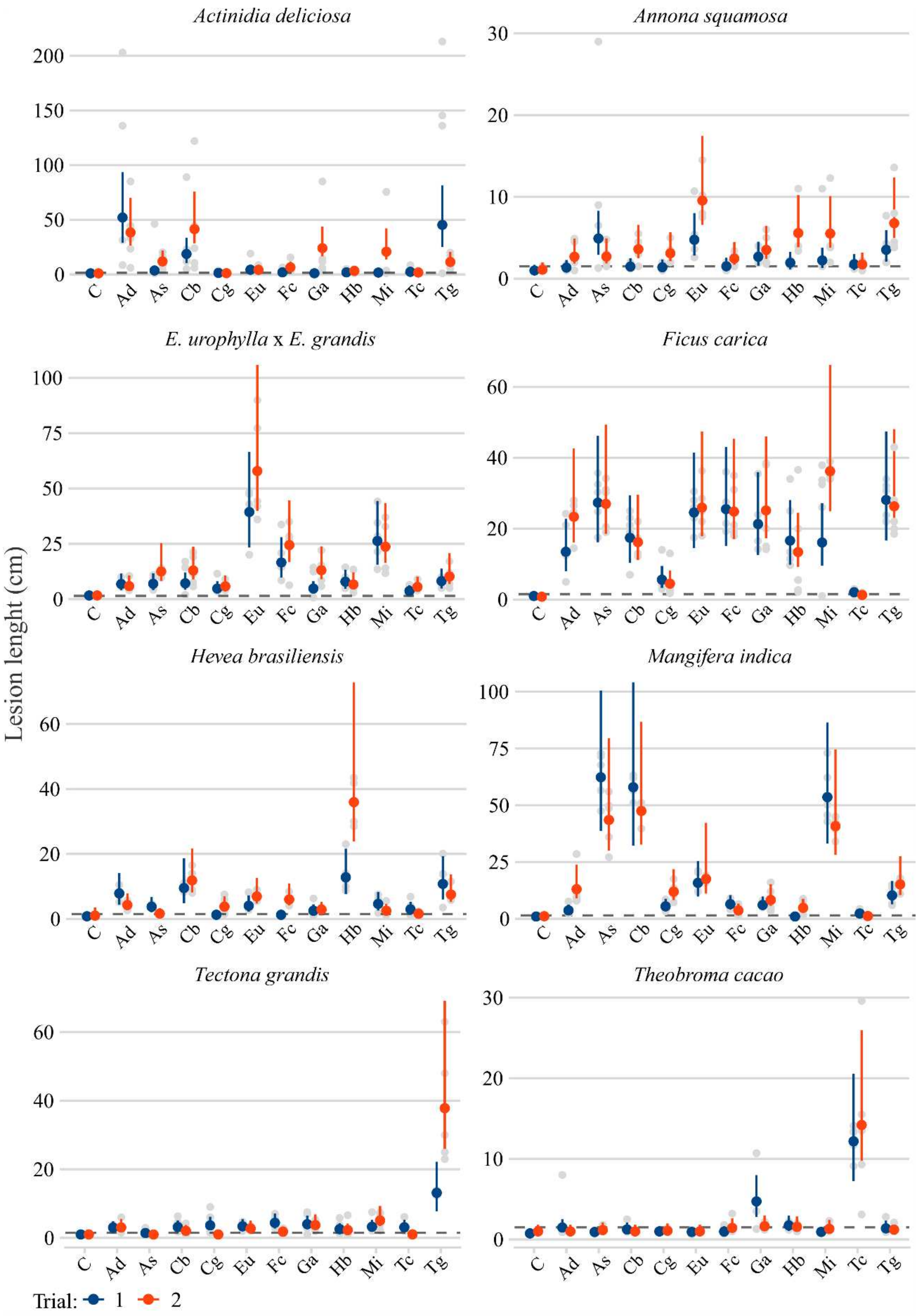

Figure 3. Average length (cm) of xylem discoloration in hosts inoculated with *Ceratocystis fimbriata* s.l. isolates. The blue bars indicate trial one, and the orange bars indicate trial two. The first two letters indicate their host source (C = control; *Ad* = *Actinidia deliciosa* LPF1443;

As = *Annona squamosa* LPF1331; *Cb* = *Caryocar brasiliense* LPF1489; *Cg* = *Carapa guianensis* LPF1560; *Eu* = *Eucalyptus* sp. LPF1912; *Fc* = *Ficus carica* LPF1336; *Ga* = *Gmelina arbórea* LPF1323; *Hb* = *Hevea brasiliensis* LPF1394; *Mi* = *Mangifera indica* LPF1156; *Tc* = *Theobroma cacao* LPF1332; *Tg* = *Tectona grandis* LPF2199).

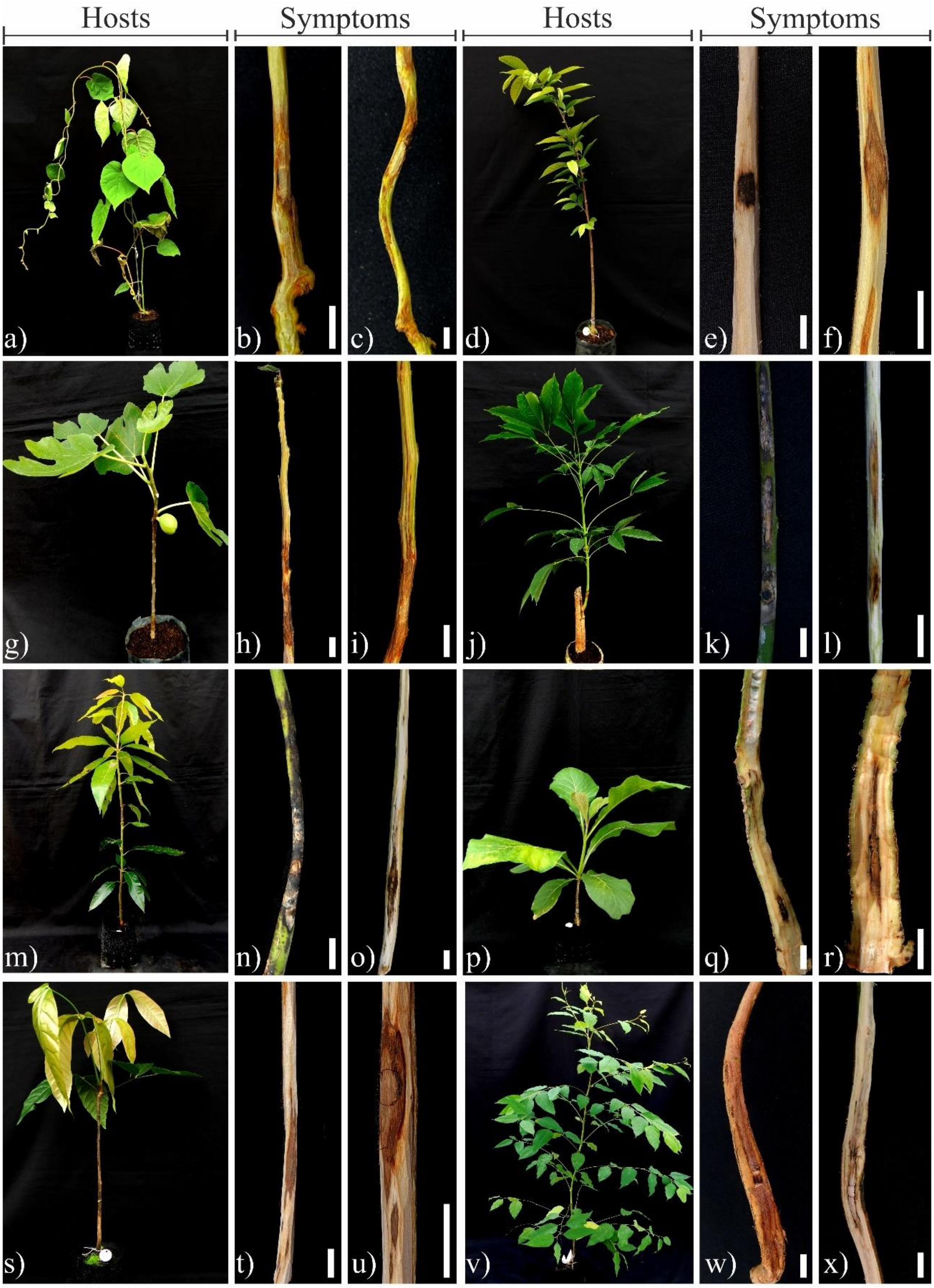

Figure 4. Xylem discoloration symptoms of plants inoculated with isolates of *Ceratocystis fimbriata* s.l. a) *Actinidia deliciosa*. b, c) Stem of *A. deliciosa* with xylem discoloration. d) *Annona squamosa*. e, f) Stem of *A. squamosa* with xylem discoloration. g) *Ficus carica*. h, i) Stem of *F. carica* with xylem discoloration. j) *Hevea brasiliensis*. k) Lesions on the stem bark

in *H. brasiliensis*, l) Stem of *H. brasiliensis* with xylem discoloration. m) *Mangifera indica*. n) Lesions on the stem bark in *M. indica*. o) Stem of *M. indica* with xylem discoloration. p) *Tectona grandis*. q, r) Stem of *T. grandis* with xylem discoloration. s) *Theobroma cacao*. t, u) Stem of *T. cacao* with xylem discoloration. v) *Eucalyptus* sp. w) Lesions on the stem bark in *Eucalyptus* sp. x) Stem of *Eucalyptus* sp. with xylem discoloration

Figure 5. Wilt symptoms of plants inoculated with isolates of *Ceratocystis fimbriata* s.l. a) *Ficus carica.* b) *Eucalyptus* sp. c) *Mangifera indica*. d) *Tectona grandis*.

SUPPLEMENTARY MATERIAL

Supplementary Table S1. Genotyping of *Ceratocystis fimbriata* s.l. using microsatellite markers from Steimel et al. (2004)

Host	**Isolate**	**Localization**	**AAG8**	**CAA9**	**CAA80**	**CAA10**	**CAG15**	**CAT1**	**CCAA15**	**CAG5**	**GACA6k**	**CAT12x**	**CAA38**	**GACA60**	**AAG9**	**CAA900**
Actinidia	A11	RS	180	266	317	125	283	261	327	326	215	371	223	195	403	194
Actinidia	A15	RS	183	218	317	125	280	249	330	326	200	377	296	195	391	194
Actinidia	A16.1	RS	186	266	314	125	283	246	327	317	215	371	223	200	403	194
Actinidia	A17	RS	183	218	317	125	280	249	330	326	200	377	281	195	391	194
Actinidia	A19	RS	183	218	317	125	280	249	330	326	200	377	299	195	391	194
Actinidia	A2	RS	186	266	314	125	286	246	327	317	215	371	223	200	403	194
Actinidia	A26	RS	183	218	317	125	280	249	330	326	200	377	296	195	391	194
Actinidia	A30	RS	183	218	317	125	280	249	330	326	200	377	315	195	391	194
Actinidia	A32	RS	177	218	317	125	280	249	330	326	200	377	296	195	391	194
Actinidia	A44	RS	183	218	317	125	280	249	330	326	200	377	299	195	391	194
Actinidia	A8	RS	183	284	317	125	298	261	327	317	200	371	223	200	391	194
Actinidia	CE07	SC	183	218	323	125	280	252	330	326	200	377	299	195	391	194
Actinidia	FI03	SC	183	218	317	125	277	249	369	326	200	377	353	195	391	194
Actinidia	FI05	SC	183	218	323	125	277	249	330	326	200	377	299	195	391	194
Actinidia	FI11	SC	183	218	317	125	277	255	369	326	200	377	253	195	391	194
Actinidia	FI12	SC	183	218	323	125	277	249	330	326	200	377	302	195	391	194
Actinidia	FI13	SC	183	218	323	125	277	249	330	326	200	377	366	195	391	194
Actinidia	FI16	SC	183	218	302	125	280	249	330	326	200	377	366	195	391	194
Actinidia	FI20	SC	177	218	302	125	283	249	330	326	200	377	232	195	391	194
Actinidia	FI21	SC	177	218	323	125	277	249	330	326	200	377	299	195	391	194
Actinidia	FI22	SC	177	218	302	125	283	249	330	326	200	377	241	195	391	194
Actinidia	JO01	SC	174	218	323	125	277	249	330	326	200	377	186	195	391	194
Actinidia	JO03	SC	180	172	323	131	286	255	327	326	219	377	198	187	391	194
Actinidia	JO13	SC	173	218	302	125	280	249	330	326	200	377	186	195	391	194

Actinidia	P1A1	RS	180	266	314	125	283	246	327	326	221	371	223	200	403	194
Actinidia	P2A1	RS	180	266	314	125	283	246	327	326	221	371	223	195	403	194
Actinidia	PA05	RS	186	218	317	125	280	249	330	326	200	377	299	195	391	194
Actinidia	PA11	RS	186	218	317	125	277	249	330	326	200	377	299	195	391	194
Actinidia	PA12	RS	186	218	317	125	280	249	330	326	200	377	299	195	391	194
Actinidia	PA18	RS	186	218	317	125	280	249	330	326	200	377	299	195	391	194
Actinidia	PA20	RS	186	218	317	125	280	249	330	326	200	377	299	195	391	194
Actinidia	PA25	RS	186	218	317	125	280	249	330	326	200	377	299	195	391	194
Actinidia	PA28	RS	186	218	317	125	280	249	330	326	200	377	299	195	391	194
Actinidia	PA29	RS	186	218	317	125	280	249	330	326	200	377	299	195	391	194
Actinidia	PA30	RS	186	218	317	125	280	249	330	326	200	377	299	195	391	194
Actinidia	PA32	RS	186	218	317	125	280	249	330	326	200	377	299	195	391	194
Actinidia	PA33	RS	186	218	317	125	280	249	330	326	200	377	299	195	391	194
Actinidia	PA34	RS	186	218	317	125	280	249	330	326	200	377	299	195	391	194
Actinidia	PA50	RS	186	218	317	125	280	249	330	326	200	377	299	195	391	194
Actinidia	PB01	RS	180	172	302	134	271	261	321	317	215	377	247	187	397	194
Actinidia	PB02	RS	180	172	302	134	271	261	321	317	215	377	247	187	397	194
Actinidia	PB09	RS	180	172	302	134	271	261	321	317	215	377	247	187	397	194
Actinidia	PB12	RS	180	172	302	134	271	261	321	317	215	377	247	187	397	194
Actinidia	PB13	RS	186	218	317	125	280	249	330	326	200	377	299	195	391	194
Actinidia	PB14	RS	186	218	317	125	280	249	330	326	200	377	299	195	391	194
Actinidia	PB22	RS	186	218	317	125	280	249	330	326	200	377	299	195	391	194
Actinidia	PB25	RS	180	172	302	134	271	249	321	317	215	377	247	187	397	194
Actinidia	PB57	RS	180	172	302	134	271	261	321	317	215	377	247	187	397	194
Actinidia	PB67	RS	186	218	317	125	280	249	330	326	200	377	299	195	391	194
Actinidia	PC03	RS	183	212	302	131	280	261	327	317	215	374	238	187	397	194
Actinidia	PC09	RS	186	218	317	125	280	249	330	326	200	374	299	195	391	194
Actinidia	PC11	RS	186	218	317	125	280	249	330	326	200	377	299	195	391	194

Actinidia	PC12	RS	186	218	317	125	280	249	330	326	200	377	299	195	391	194
Actinidia	PC14	RS	186	218	317	125	280	249	330	326	200	377	299	195	391	194
Actinidia	PC16	RS	186	218	317	125	280	249	330	326	200	377	299	195	391	194
Actinidia	PC17	RS	183	212	302	131	280	261	327	317	215	374	238	187	397	194
Actinidia	PC19	RS	186	218	317	125	280	249	330	326	200	377	299	195	391	194
Actinidia	PC20	RS	186	218	317	125	280	249	330	326	200	377	299	195	391	194
Actinidia	PCT01	RS	186	218	317	125	280	249	330	326	200	377	299	195	391	194
Actinidia	PCT05	RS	186	218	317	125	280	249	330	326	200	377	299	195	391	194
Actinidia	PCT09	RS	186	218	317	125	280	249	330	326	200	377	299	195	391	194
Actinidia	PCT14	RS	186	218	317	125	280	249	330	326	200	377	299	195	391	194
Actinidia	PCT15	RS	186	218	317	125	280	249	330	326	200	377	299	195	391	194
Actinidia	PCT24	RS	186	218	308	125	277	249	330	326	200	377	226	195	391	194
Actinidia	PCT26	RS	186	218	308	125	277	249	330	326	200	377	226	195	391	194
Actinidia	PCT27	RS	186	218	317	125	280	249	330	326	200	377	299	195	391	194
Actinidia	PCT28	RS	186	218	317	125	280	249	330	326	200	377	299	195	391	194
Actinidia	PG01	RS	186	218	317	125	280	249	327	326	200	377	299	195	391	194
Actinidia	PG05	RS	186	218	317	125	280	249	330	326	200	377	299	195	391	194
Actinidia	PG07	RS	186	218	317	125	280	249	330	326	200	377	299	195	391	194
Actinidia	PG09	RS	186	218	317	125	280	249	330	326	200	377	299	195	391	194
Actinidia	PG10	RS	186	218	317	125	280	249	327	326	200	377	299	195	391	194
Actinidia	PG11	RS	186	218	317	125	280	249	330	326	200	377	299	195	391	194
Actinidia	PG17	RS	186	218	317	125	280	249	330	326	200	377	299	195	391	194
Actinidia	PG18	RS	186	218	317	125	280	249	330	326	200	377	299	195	391	194
Actinidia	PG19	RS	186	218	317	125	280	249	330	326	200	377	299	195	391	194
Actinidia	PG21	RS	186	218	314	128	280	249	330	326	200	377	299	195	391	194
Actinidia	PG24	RS	186	218	317	125	280	249	330	328	200	377	299	195	391	194
Actinidia	PG29	RS	186	218	317	125	280	249	330	326	200	377	299	195	391	194
Actinidia	PL01	RS	183	212	302	131	280	261	327	326	213	374	238	187	397	194

Actinidia	PL06	RS	186	218	317	125	280	249	330	326	200	377	299	195	391	194
Actinidia	PL11	RS	186	218	317	125	280	249	330	326	200	377	299	195	391	194
Actinidia	PM08	RS	186	218	317	125	280	249	330	326	200	377	299	195	391	194
Actinidia	PM09	RS	186	218	317	128	277	249	330	326	200	377	309	195	391	194
Actinidia	PM12	RS	186	218	308	125	277	249	330	326	200	377	299	195	391	194
Actinidia	PM15	RS	186	218	317	125	280	249	330	326	200	377	226	195	391	194
Actinidia	PM17	RS	186	218	308	125	277	249	330	326	200	377	226	195	391	194
Actinidia	PM18	RS	186	218	308	125	277	249	330	326	200	377	299	195	391	194
Actinidia	PM20	RS	186	218	314	125	277	249	330	326	200	377	226	195	391	194
Actinidia	PM21	RS	186	218	308	125	277	249	330	326	200	377	226	195	391	194
Actinidia	PM25	RS	186	218	308	125	277	249	330	326	200	377	226	195	391	194
Actinidia	PM28	RS	186	218	317	125	280	249	330	326	200	377	299	195	391	194
Actinidia	PM29	RS	186	218	317	125	280	249	330	326	200	377	299	195	391	194
Actinidia	PM30	RS	186	218	317	128	277	249	330	326	200	377	309	195	391	194
Actinidia	PP01	RS	183	266	314	125	283	249	327	326	219	371	226	195	403	194
Actinidia	PP02	RS	183	266	314	125	283	247	327	326	219	371	226	200	403	194
Actinidia	PP03	RS	183	266	314	125	283	247	327	326	219	371	226	200	403	194
Actinidia	PP05	RS	183	266	314	125	283	249	327	326	219	371	201	200	403	194
Actinidia	PP06	RS	183	266	314	125	283	247	327	326	219	371	226	200	403	194
Actinidia	PP08	RS	183	266	314	125	283	247	327	326	219	371	226	200	403	194
Actinidia	PP14	RS	183	266	314	125	283	247	327	326	219	371	201	200	403	194
Annona	LPF1331		198	223	311	128	277	248	330	323	219	380	168	221	391	194
Carapa	AND2	AC	183	251	317	128	252	254	324	317	215	377	168	187	400	194
Carapa	AND3	AC	183	263	317	128	252	254	324	317	215	377	159	187	400	194
Carapa	AndAC12B	AC	183	263	317	128	252	254	324	317	215	377	159	187	400	194
Carapa	AndAC236A	AC	183	263	317	128	252	254	324	317	215	377	214	187	400	194
Carapa	AndAC144B2	AC	183	263	317	128	252	254	324	317	215	377	159	187	400	194
Carapa	AndACSPO1G	AC	183	251	317	128	252	254	324	317	215	377	168	187	400	194

Carapa	AndAC144C3	AC	183	263	317	128	252	254	324	317	215	377	159	187	400	194
Carapa	AndACSPO3D	AC	183	263	317	128	252	254	324	317	215	377	159	187	400	194
Carapa	AndAC359D	AC	183	263	317	128	252	254	324	317	215	377	156	187	400	194
Carapa	AndAC127-2	AC	183	251	317	128	252	254	324	317	215	377	168	187	400	194
Carapa	AndRR13	RR	183	190	299	128	252	254	324	317	215	377	159	187	400	194
Carapa	AndRR74	RR	183	190	296	128	252	254	324	317	215	377	205	187	400	194
Carapa	AndAMMa2	AM	183	190	296	128	252	248	324	317	215	377	159	187	400	194
Carapa	AndAMMa3	AM	183	190	296	128	252	248	324	317	215	377	159	187	400	194
Carapa	C3601	AC	183	263	317	128	252	254	324	317	215	377	214	187	400	194
Carapa	C3602	AC	183	263	317	128	252	254	324	317	215	377	159	187	400	194
Carapa	C3603	AC	183	263	317	128	252	254	324	317	215	377	159	187	400	194
Carapa	C3604	AC	183	263	317	128	252	254	324	317	215	377	159	187	400	194
Carapa	C3605	AC	183	263	317	128	252	254	324	317	215	377	159	187	400	194
Carapa	C3606	AC	183	251	317	128	252	254	324	317	215	377	168	187	400	194
Carapa	C3607	AC	183	263	317	128	252	254	324	317	215	377	159	187	400	194
Carapa	C3608	AC	183	263	317	128	252	254	324	317	215	377	159	187	400	194
Carapa	C3609	AC	183	251	317	128	252	254	324	317	215	377	168	187	400	194
Carapa	C3615	AC	183	251	317	128	252	254	324	317	215	377	168	187	400	194
Carapa	AndAC127-1	AC	183	251	317	128	252	254	324	317	215	377	168	187	400	194
Carapa	C3613	RR	183	190	299	128	252	254	324	317	215	377	159	187	400	194
Carapa	C3614	RR	183	190	296	128	252	254	324	317	215	377	205	187	400	194
Carapa	C3553	RR	183	190	299	128	252	254	324	317	215	377	180	187	400	194
Carapa	C3554	RR	183	190	299	128	252	254	324	317	215	377	159	187	400	194
Carapa	C3555	RR	183	190	299	128	252	254	324	317	215	377	159	187	400	194
Carapa	C3556	RR	183	190	299	128	252	254	324	317	215	377	159	187	400	194
Carapa	C3557	RR	183	190	299	128	252	254	324	317	215	377	159	187	400	194
Carapa	C3558	RR	183	190	299	128	252	254	324	317	215	377	159	187	400	194
Carapa	C3559	RR	183	190	299	128	252	254	324	317	215	377	159	187	400	194

Carapa	C3560	RR	183	190	299	128	252	254	324	317	215	377	159	187	400	194
Carapa	C3561	RR	183	190	299	128	252	254	324	317	215	377	159	187	400	194
Carapa	C3562	RR	183	190	299	128	252	254	324	317	215	377	159	187	400	194
Carapa	C3563	RR	183	190	299	128	252	254	324	317	215	377	159	187	400	194
Carapa	C3564	RR	183	190	299	128	252	254	324	317	215	377	205	187	400	194
Carapa	C3565	RR	183	190	299	128	252	254	324	317	215	377	159	187	400	194
Carapa	C3566	RR	183	190	299	128	252	254	324	317	215	377	159	187	400	194
Carapa	C3567	RR	183	190	299	128	252	254	324	317	215	377	159	187	400	194
Carapa	C3568	RR	183	190	299	128	252	254	324	317	215	377	205	187	400	194
Carapa	C3569	RR	183	190	299	128	252	248	324	317	215	377	205	187	400	194
Carapa	C3570	RR	183	190	299	128	252	254	324	317	215	377	205	187	400	194
Carapa	C3571	RR	183	159	299	128	252	254	324	317	215	377	205	187	400	194
Carapa	C3572	RR	183	190	299	128	252	254	324	317	215	377	205	187	400	194
Carapa	C3573	RR	183	190	299	128	252	254	324	317	215	377	205	187	400	194
Carapa	C3574	RR	183	190	299	128	252	254	324	317	215	377	205	187	400	194
Carapa	C3575	RR	183	190	299	128	252	248	324	317	215	377	205	187	400	194
Carapa	C3576	RR	183	190	299	128	252	254	324	317	215	377	205	187	400	194
Carapa	C3577	RR	183	190	299	128	252	254	324	317	215	377	205	187	400	194
Carapa	C3578	RR	183	190	299	128	252	248	324	317	215	377	205	187	400	194
Carapa	C3579	RR	183	190	299	128	252	248	324	317	215	377	205	187	400	194
Carapa	C3580	RR	183	190	299	128	252	248	324	317	215	377	205	187	400	194
Carapa	C3581	RR	183	190	299	128	252	254	324	317	215	377	205	187	400	194
Carapa	C3582	RR	183	190	299	128	252	248	324	317	215	377	205	187	400	194
Carapa	C3583	RR	183	190	299	128	252	254	324	317	215	377	205	187	400	194
Carapa	C3584	RR	183	190	299	128	252	248	324	317	215	377	205	187	400	194
Carapa	C3585	RR	183	190	299	128	252	254	324	317	215	377	205	187	400	194
Carapa	C3586	RR	183	190	299	128	252	254	324	317	215	377	205	187	400	194
Carapa	C3587	RR	183	190	299	128	252	254	324	317	215	377	205	187	400	194

Carapa	C3588	RR	183	190	299	128	252	254	324	317	215	377	205	187	400	194
Carapa	C3589	RR	183	190	299	128	252	248	324	317	215	377	205	187	400	194
Carapa	C3590	RR	183	190	299	128	252	254	324	317	215	377	171	187	400	194
Carapa	C3591	RR	183	190	299	128	252	254	324	317	215	377	205	187	400	194
Carapa	C3592	RR	183	190	299	128	252	248	324	317	215	377	205	187	400	194
Carapa	C3593	RR	183	190	299	128	252	254	324	317	215	377	159	187	400	194
Carapa	C3594	RR	183	190	299	128	252	254	324	317	215	377	159	187	400	194
Carapa	C3595	RR	183	190	299	128	252	254	324	317	215	377	159	187	400	194
Carapa	C3596	RR	183	190	299	128	252	254	324	317	215	377	159	187	400	194
Carapa	C3597	RR	183	190	299	128	252	254	324	317	215	377	159	187	400	194
Carapa	C3598	RR	183	190	299	128	252	254	324	317	215	377	159	187	400	194
Carapa	C3599	RR	183	190	299	128	252	254	324	317	215	365	159	207	400	194
Carapa	C3600	RR	183	190	299	128	252	254	324	317	215	377	180	187	400	194
Carapa	C3610	RR	183	190	296	128	252	248	324	317	215	377	159	187	400	194
Carapa	C3611	RR	183	190	296	128	252	248	324	317	215	377	159	187	400	194
Carapa	AndAMAndP1	AM	183	263	299	128	252	254	324	317	215	377	214	187	400	194
Carapa	AndAMAndP2	AM	183	263	299	128	252	254	324	317	215	377	214	187	400	194
Carapa	AndAMAndP4	AM	183	190	317	128	252	254	324	317	215	377	171	187	400	194
Carapa	AndAMAndP5	AM	183	263	299	128	252	254	324	317	215	377	214	187	400	194
Carapa	AndAMAndP7	AM	183	190	317	128	252	254	324	317	215	377	171	187	400	194
Carapa	AND4A		183	190	299	128	252	254	324	317	215	377	159	187	400	194
Carapa	AND5A		183	190	299	128	252	254	324	317	215	377	159	187	400	194
Carapa	AND10A		183	190	296	128	252	248	324	317	215	377	159	187	400	194
Caryocar	LPF1489	MG	180	175	323	131	286	257	324	317	221	374	201	187	397	194
Eucalyptus	2135	MG	180	224	317	128	268	261	324	317	215	377	211	187	397	194
Eucalyptus	2136	MG	174	224	317	128	268	261	324	317	215	377	211	187	397	194
Eucalyptus	8B10	MG	180	175	323	131	274	261	321	317	215	377	238	187	397	194
Eucalyptus	8B15	MG	180	175	311	131	271	261	318	317	215	377	238	187	397	194

Eucalyptus	8B2	MG	180	172	302	131	271	261	318	317	219	377	247	187	397	194
Eucalyptus	8B24	MG	180	175	317	128	259	261	321	317	215	377	238	187	397	194
Eucalyptus	8B26	MG	180	175	302	134	286	261	321	317	215	377	247	187	397	194
Eucalyptus	8B27	MG	180	175	317	128	259	261	321	317	215	377	238	187	397	194
Eucalyptus	8B28	MG	180	175	320	134	274	261	321	317	215	377	247	187	397	194
Eucalyptus	8B32	MG	180	175	317	134	271	261	324	317	215	377	238	187	397	194
Eucalyptus	8B40	MG	180	175	317	134	274	261	324	317	219	377	247	187	397	194
Eucalyptus	8B5	MG	180	175	311	134	274	261	324	317	215	377	255	187	397	194
Eucalyptus	8B8	MG	180	175	311	134	274	261	324	317	215	377	255	187	397	194
Eucalyptus	8B9	MG	180	172	317	134	286	261	324	317	215	377	255	187	397	194
Eucalyptus	CAV10	BA	180	175	311	131	259	261	321	317	215	377	238	187	397	194
Eucalyptus	CAV12	BA	180	175	311	131	259	261	321	317	215	377	238	187	397	194
Eucalyptus	CAV13	BA	180	175	311	131	259	261	321	317	215	377	238	187	397	194
Eucalyptus	CAV19	BA	180	175	311	131	259	261	321	317	215	377	238	187	397	194
Eucalyptus	CAV22	BA	180	175	311	131	259	261	321	317	215	377	238	187	397	194
Eucalyptus	CAV26	BA	180	172	311	131	259	261	321	317	215	377	174	200	397	194
Eucalyptus	CAV28	BA	180	172	311	131	259	261	321	317	215	377	201	200	397	194
Eucalyptus	CAV30	BA	180	226	317	128	259	261	321	317	215	377	247	200	397	194
Eucalyptus	CAV33	BA	180	226	317	128	259	261	321	317	215	377	247	200	397	194
Eucalyptus	CAV41	BA	180	172	311	131	259	261	321	317	215	377	201	200	397	194
Eucalyptus	CAV47	BA	177	175	317	128	259	261	318	317	215	377	238	187	397	194
Eucalyptus	CAV9	BA	180	175	311	131	259	261	321	317	215	377	238	187	397	194
Eucalyptus	PT10	MG	180	175	317	131	271	261	324	317	215	377	238	187	397	194
Eucalyptus	PT11	MG	180	175	323	131	271	261	321	317	215	377	238	187	397	194
Eucalyptus	PT12	MG	180	172	317	131	271	261	321	317	215	377	238	187	397	194
Eucalyptus	PT13	MG	180	248	326	128	265	257	324	317	215	374	238	187	397	194
Eucalyptus	PT15	MG	183	211	302	131	280	261	324	317	215	374	238	187	397	194
Eucalyptus	PT17	MG	180	175	323	131	274	261	321	317	215	377	247	187	397	194

Eucalyptus	PT18	MG	180	248	326	128	265	257	324	317	215	374	267	187	397	194
Eucalyptus	PT19	MG	180	175	317	134	259	261	321	317	215	377	247	187	397	194
Eucalyptus	PT2	MG	180	175	323	131	259	261	321	317	215	377	238	187	397	194
Eucalyptus	PT21	MG	180	175	317	134	274	261	324	317	215	377	238	187	397	194
Eucalyptus	PT22	MG	180	175	323	134	274	261	321	317	215	377	247	187	397	194
Eucalyptus	PT23	MG	180	175	317	128	259	261	321	317	215	377	247	187	397	194
Eucalyptus	PT3	MG	180	175	323	134	274	261	321	317	215	377	247	187	397	194
Eucalyptus	PT5	MG	180	175	323	128	271	257	324	317	215	377	192	187	397	194
Eucalyptus	PT6	MG	180	175	323	134	274	261	321	317	215	377	247	187	397	194
Eucalyptus	PT7	MG	180	175	323	134	274	261	321	317	215	377	247	187	397	194
Eucalyptus	PT8	MG	180	172	317	131	271	261	321	317	215	377	238	187	397	194
Eucalyptus	SBS1	BA	180	175	317	134	286	261	324	317	215	377	247	187	397	194
Eucalyptus	2061	BA	180	175	308	131	259	261	324	317	215	377	229	200	397	194
Eucalyptus	2062	BA	180	178	311	131	259	261	324	317	215	377	229	187	397	194
Eucalyptus	2063	BA	180	178	308	131	259	261	324	317	215	377	229	187	397	194
Eucalyptus	2064	BA	180	175	311	128	262	261	321	317	215	377	238	187	397	194
Eucalyptus	2065	BA	180	175	311	131	262	261	324	317	215	377	229	200	397	194
Eucalyptus	2066	BA	180	178	308	131	262	261	324	317	215	377	229	187	397	194
Eucalyptus	2067	BA	180	178	308	131	259	261	324	317	215	377	229	187	397	194
Eucalyptus	2068	BA	180	178	308	134	262	261	324	317	215	377	201	187	397	194
Eucalyptus	2069	BA	180	178	308	131	262	261	324	317	215	377	229	187	397	194
Eucalyptus	2070	BA	180	178	308	131	262	261	324	317	215	377	229	187	397	194
Eucalyptus	2071	BA	183	175	320	131	259	261	324	317	221	374	146	187	397	194
Eucalyptus	2072	BA	180	178	308	131	262	261	324	317	215	377	229	187	397	194
Eucalyptus	2073	BA	180	178	308	131	262	261	324	317	215	377	229	187	397	194
Eucalyptus	2074	BA	180	175	308	131	262	261	324	317	215	377	229	200	397	194
Eucalyptus	2075	BA	180	175	311	131	259	261	324	317	215	377	229	200	397	194
Eucalyptus	2076	BA	180	178	308	131	259	261	324	317	215	377	229	187	397	194

Eucalyptus	2078	BA	180	178	308	131	259	261	324	317	215	377	229	187	397	194
Eucalyptus	2079	BA	180	178	308	131	259	261	324	317	215	377	229	187	397	194
Eucalyptus	2080	BA	180	175	311	134	259	261	324	317	215	377	201	187	397	194
Eucalyptus	2081	BA	180	178	308	131	259	261	324	317	215	377	229	187	397	194
Eucalyptus	2082	BA	180	178	308	131	259	261	324	317	215	377	229	187	397	194
Eucalyptus	2083	BA	180	178	308	131	259	261	324	317	215	377	229	187	397	194
Eucalyptus	2084	BA	180	178	308	131	259	261	324	317	215	377	229	187	397	194
Eucalyptus	2085	BA	180	175	320	131	259	261	324	317	221	374	146	187	397	194
Eucalyptus	2086	BA	180	175	320	131	259	261	324	317	221	374	146	187	397	194
Eucalyptus	1440	BA	180	175	311	134	259	261	321	317	215	377	238	187	397	194
Eucalyptus	1442, CBS 115174	BA	180	175	311	134	259	261	321	317	215	377	238	187	397	194
Eucalyptus	2077	BA	180	175	311	134	259	261	321	317	215	377	238	187	397	194
Eucalyptus	1345	BA	180	175	311	131	259	261	321	317	215	377	247	187	397	194
Eucalyptus	C2115	BA	180	175	320	131	259	261	324	317	215	377	238	187	397	194
Eucalyptus	2137	PA	180	178	317	131	256	261	321	317	215	377	211	187	397	194
Eucalyptus	1985	BA	180	175	308	131	259	261	324	317	215	377	229	187	397	194
Eucalyptus	C2123	BA	180	178	308	131	259	261	324	317	215	377	229	187	397	194
Eucalyptus	C2124	BA	180	178	308	131	259	261	324	317	215	377	229	187	397	194
Eucalyptus	2018	BA	180	175	311	134	259	261	324	317	215	377	229	200	397	194
Eucalyptus	2020	BA	180	175	311	134	259	261	324	317	215	377	229	200	397	194
Ficus	LPF1336		180	202	323	131	301	254	330	335	209	383	195	187	400	194
Ficus	1893	SP	180	202	323	131	301	254	330	335	209	383	195	187	400	194
Ficus	1894	SP	180	202	323	131	301	254	330	335	209	383	195	187	400	194
Ficus	1896	SP	180	202	323	131	301	254	330	335	209	383	195	187	400	194
Ficus	1897	SP	180	202	323	131	301	254	330	335	209	383	195	187	400	194
Ficus	1898	SP	180	202	323	131	301	254	330	335	209	383	195	187	400	194
Ficus	1851	SP	180	202	323	131	301	254	330	335	209	383	195	187	400	194
Ficus	1852	SP	180	202	323	131	301	254	330	335	209	383	195	187	400	194

Ficus	1853	SP	180	202	323	131	301	254	330	335	209	383	195	187	400	194
Ficus	1854	SP	180	202	323	131	301	254	330	335	209	383	195	187	400	194
Ficus	1855	SP	180	202	323	131	301	254	330	335	209	383	195	187	400	194
Ficus	1856	SP	180	206	323	131	301	254	330	335	209	383	195	187	400	194
Ficus	1857	SP	180	206	323	131	301	254	330	335	209	383	195	187	400	194
Ficus	1858	SP	180	206	323	131	301	254	330	335	209	383	195	187	400	194
Ficus	1895	SP	180	202	323	131	301	254	330	335	209	383	195	187	400	194
Ficus	1899	SP	180	202	323	131	301	254	330	335	209	383	195	187	400	194
Gmelina	916	PA	174	175	311	137	262	259	324	317	215	380	174	187	394	194
Gmelina	917	PA	174	175	311	137	262	259	324	317	215	380	174	187	394	194
Gmelina	918	PA	174	175	311	137	262	259	324	317	215	380	174	187	394	194
Gmelina	924	PA	174	175	311	137	262	259	324	317	215	380	174	187	394	194
Gmelina	925	PA	174	175	311	137	262	259	324	317	215	380	174	187	394	194
Hevea	A01	BA	174	194	311	125	283	261	321	317	215	374	208	187	397	194
Hevea	A05	BA	174	194	311	125	283	261	321	317	215	374	208	187	397	194
Hevea	A16	BA	174	194	311	125	283	261	321	317	215	374	208	187	397	194
Hevea	A21	BA	174	194	311	125	283	261	321	317	215	374	208	187	397	194
Hevea	A35	BA	174	194	311	125	283	261	321	317	215	374	208	187	397	194
Hevea	A40	BA	174	194	311	125	283	261	321	317	215	374	208	187	397	194
Hevea	A50	BA	174	194	311	125	283	261	321	317	215	374	208	187	397	194
Hevea	A58	BA	174	194	311	125	283	261	321	317	215	374	208	187	397	194
Hevea	A64	BA	174	194	311	125	283	261	321	317	215	374	208	187	397	194
Hevea	A74	BA	174	194	311	125	283	261	321	317	215	374	208	187	397	194
Hevea	RB02	AC	180	220	314	131	286	261	321	320	221	374	305	187	397	194
Hevea	RB05	AC	180	220	314	131	286	261	321	320	221	374	305	187	397	194
Hevea	RB08	AC	180	220	314	131	286	261	321	320	221	374	305	187	397	194
Hevea	RB09	AC	180	220	314	131	286	261	321	320	221	374	305	187	397	194
Hevea	RB11	AC	180	220	314	131	286	261	321	320	221	374	305	187	397	194

Hevea	RB13	AC	180	220	314	131	286	261	321	320	221	374	305	187	397	194
Hevea	RB16	AC	180	220	314	131	286	261	321	320	221	374	305	187	397	194
Hevea	RB17	AC	180	220	314	131	286	261	321	320	221	374	305	187	397	194
Hevea	RB19	AC	180	220	314	131	286	261	321	320	221	374	305	187	397	194
Hevea	RB21	AC	180	220	314	131	286	261	321	320	221	374	305	187	397	194
Mangifera	LPF1156	CE	174	175	331	131	295	254	324	317	215	374	201	187	400	194
Mangifera	CBSP1-8	SP	174	206	329	128	286	257	324	317	221	374	214	187	397	194
Mangifera	CBSP1-12	SP	174	206	329	128	286	257	324	317	221	374	214	187	397	194
Mangifera	CBSP1-7	SP	174	206	329	128	286	257	324	317	221	374	146	187	397	194
Mangifera	CBSP1-18	SP	174	206	329	128	286	257	324	317	221	374	214	187	397	194
Mangifera	CBSP1-6	SP	180	175	323	131	286	257	324	317	221	374	201	187	397	194
Mangifera	CBSP1-9	SP	174	206	329	128	286	257	324	317	221	374	214	187	397	194
Mangifera	CBSP1-10	SP	174	206	329	128	286	257	324	317	221	374	214	187	397	194
Mangifera	CBSP1-11	SP	174	206	329	128	286	257	324	317	221	374	146	187	397	194
Mangifera	CBSP1-16	SP	174	206	329	128	286	257	324	317	221	374	214	187	397	194
Mangifera	CBSP2-20	SP	174	206	329	128	286	257	324	317	221	374	146	187	397	194
Mangifera	CBSP3-1	SP	180	175	323	131	286	257	324	317	221	374	214	187	397	194
Mangifera	CBSP4-1	SP	180	175	323	131	286	257	324	317	221	374	201	187	397	194
Mangifera	CBSP4-3	SP	180	175	323	131	286	257	324	317	221	374	201	187	397	194
Mangifera	CBSP5-7	SP	180	175	323	131	286	257	324	317	221	374	201	187	397	194
Mangifera	CBSP5-1	SP	180	175	323	131	286	257	324	317	221	374	201	187	397	194
Mangifera	CBSP5-3	SP	180	175	323	131	286	257	324	317	221	374	201	187	397	194
Mangifera	CBSP5-4	SP	180	175	323	131	286	257	324	317	221	374	201	187	397	194
Mangifera	CBSP5-5	SP	180	175	323	131	286	257	324	317	221	374	201	187	397	194
Mangifera	CBSP5-6	SP	180	175	323	131	286	257	324	317	221	374	201	187	397	194
Mangifera	CBSP5-9	SP	180	175	323	131	286	257	324	317	221	374	201	187	397	194
Mangifera	CBSP5-10	SP	180	175	323	131	286	257	324	317	221	374	201	187	397	194
Mangifera	CBSP5-11	SP	180	175	323	131	286	257	324	317	221	374	201	187	397	194

Mangifera	CBSP5-12	SP	180	175	323	131	286	257	324	317	221	374	201	187	397	194
Mangifera	CBSP5-13	SP	180	175	323	131	286	257	324	317	221	374	201	187	397	194
Mangifera	CBSP6-1	SP	180	175	323	131	286	257	324	317	221	374	201	187	397	194
Mangifera	CBSP6-2	SP	180	175	323	131	286	257	324	317	221	374	201	187	400	194
Mangifera	CBSP7-3	SP	174	206	329	128	286	257	324	317	221	374	214	187	397	194
Mangifera	CBSP7-4	SP	174	206	329	128	286	257	324	317	221	374	214	187	400	194
Mangifera	CBSP7-5	SP	174	206	329	128	286	257	324	317	221	374	214	187	397	194
Mangifera	CBSP7-6	SP	174	206	329	128	286	257	324	317	221	374	214	187	400	194
Mangifera	CBSP8-2	SP	180	175	323	131	286	257	324	317	221	374	201	187	397	194
Mangifera	CBSP8-3	SP	180	175	323	131	286	257	324	317	221	374	201	187	397	194
Mangifera	CBSP8-4	SP	180	175	323	131	286	257	324	317	221	374	201	187	397	194
Mangifera	CBSP9-1	SP	180	175	323	131	286	257	324	317	221	374	201	187	397	194
Mangifera	CBSP9-3	SP	180	175	323	131	286	257	324	317	221	374	201	187	397	194
Mangifera	CBSP9-4	SP	180	175	323	131	286	257	324	317	221	374	201	187	397	194
Mangifera	CBSP9-6	SP	180	175	323	131	286	257	324	317	221	374	201	187	397	194
Mangifera	CBSP9-7	SP	180	175	323	131	286	257	324	317	221	374	201	187	397	194
Mangifera	CBSP10-1	SP	180	175	323	131	286	257	324	317	221	374	201	187	397	194
Mangifera	CBSP10-2	SP	180	175	323	131	286	257	324	317	221	374	201	187	397	194
Mangifera	CBSP10-3	SP	174	206	329	128	286	257	324	317	221	374	214	187	397	194
Mangifera	CBSP11-2	SP	180	175	323	131	286	257	324	317	221	374	201	187	397	194
Mangifera	CBSP11-6	SP	180	175	323	131	286	257	324	317	221	374	201	187	397	194
Mangifera	CBSP11-7	SP	180	175	323	131	286	257	324	317	221	374	201	187	397	194
Mangifera	CBSP11-8	SP	180	175	323	131	286	257	324	317	221	374	201	187	397	194
Mangifera	CBSP11-10	SP	180	175	323	131	286	257	324	317	221	374	201	187	397	194
Mangifera	CBSP11-12	SP	180	175	323	131	286	257	324	317	221	374	201	187	397	194
Mangifera	CBSP12-1	SP	180	175	323	131	286	257	324	317	221	374	201	187	397	194
Mangifera	CBSP12-2	SP	174	206	323	128	286	257	324	317	221	374	214	187	397	194
Mangifera	CBSP13-1	SP	180	175	323	131	286	257	324	317	221	374	201	187	397	194

Mangifera	CBSP13-2	SP	180	175	323	131	286	257	324	317	221	374	201	187	397	194
Mangifera	CBSP14-2	SP	174	206	329	128	286	257	324	317	221	374	214	187	397	194
Mangifera	994	SP	174	206	329	128	286	257	324	317	221	374	214	187	397	194
Mangifera	1847	SP	174	206	329	128	286	257	324	317	221	374	214	187	397	194
Mangifera	MAG1	MS	174	206	329	128	286	257	324	317	221	374	214	187	397	194
Mangifera	MAG2	MS	174	206	329	128	286	257	324	317	221	374	214	187	397	194
Mangifera	MAG3	MS	174	206	329	128	286	257	324	317	221	374	214	187	397	194
Mangifera	MAG4	MS	174	206	329	128	286	257	324	317	221	374	214	187	397	194
Mangifera	MAG5	MS	174	206	329	128	286	257	324	317	221	374	214	187	397	194
Mangifera	1688	SP	180	175	323	131	286	257	324	317	221	374	201	187	397	194
Mangifera	1657	SP	180	175	323	131	286	257	324	317	221	374	201	187	397	194
Mangifera	1656	SP	180	175	323	131	286	257	324	317	221	374	201	187	397	194
Mangifera	1784	SP	180	175	323	131	271	257	324	317	221	374	201	187	397	194
Mangifera	1785	SP	180	175	323	131	271	257	324	317	221	374	201	187	397	194
Mangifera	CBMG1-1	MG	174	206	329	128	286	257	324	317	221	374	214	187	400	194
Mangifera	CBMG1-2	MG	174	206	329	128	286	257	324	317	221	374	214	187	400	194
Mangifera	CBMG1-3	MG	174	206	329	128	286	257	324	317	221	374	214	187	400	194
Mangifera	CBMG1-4	MG	174	206	329	128	286	257	324	317	221	374	214	187	397	194
Mangifera	CBMG1-5	MG	174	206	329	128	286	257	324	317	221	374	214	187	397	194
Mangifera	CBMG1-6	MG	174	206	329	128	286	257	324	317	221	374	214	187	397	194
Mangifera	CBMG1-7	MG	174	206	329	128	286	257	324	317	221	374	214	187	397	194
Mangifera	CBMG2-9	MG	180	206	323	128	289	257	324	317	221	374	201	187	397	194
Mangifera	CBMG2-10	MG	180	206	323	128	289	257	324	317	221	374	201	187	397	194
Mangifera	CBMG3-11	MG	180	209	323	128	286	257	324	317	221	374	238	187	397	194
Mangifera	CBMS1-1	MS	174	206	329	128	286	257	324	317	221	374	214	187	397	194
Mangifera	CBMS1-3	MS	180	175	323	131	286	257	324	317	221	374	201	187	397	194
Mangifera	CBMS1-5	MS	174	206	329	128	286	257	324	317	221	374	214	187	397	194
Mangifera	CBMS1-6	MS	180	175	323	131	286	257	324	317	221	374	201	187	397	194

Mangifera	CBMS1-16	MS	174	206	329	128	286	257	324	317	221	374	214	187	397	194
Mangifera	CBMS1-17	MS	174	206	329	128	286	257	324	317	221	374	214	187	397	194
Mangifera	CBMS1-18	MS	174	206	329	128	286	257	324	317	221	374	214	187	397	194
Mangifera	CBMS2-7	MS	174	206	329	128	286	257	324	317	221	374	214	187	397	194
Mangifera	CBMS2-9	MS	174	206	329	128	286	257	324	317	221	374	214	187	397	194
Mangifera	CBMS2-11	MS	174	206	329	128	286	257	324	317	221	374	214	187	397	194
Mangifera	CBMS2-12	MS	174	206	329	128	286	257	324	317	221	374	214	187	397	194
Mangifera	CBMS2-13	MS	180	175	323	128	286	257	324	317	221	374	201	187	397	194
Mangifera	CBMS2-14	MS	180	175	323	131	286	257	324	317	221	374	201	187	397	194
Mangifera	CBMS3-6	MS	180	175	323	131	286	257	324	317	221	374	214	187	397	194
Mangifera	CBMS4-1	MS	174	206	329	128	286	257	324	317	221	374	195	187	397	194
Mangifera	CBMS4-2	MS	174	206	329	128	286	257	324	317	221	374	214	187	397	194
Mangifera	NEPB1-2	PB	177	178	320	128	286	257	324	317	215	377	174	187	397	194
Mangifera	NEPB1-3	PB	177	175	317	128	292	261	321	320	215	374	162	187	400	194
Mangifera	NEPB1-6	PB	174	175	323	128	268	261	306	320	215	374	214	187	397	194
Mangifera	NEPB1-7	PB	177	178	320	128	286	257	324	317	215	377	174	187	400	194
Mangifera	NEPB1-8	PB	177	178	288	128	295	261	324	320	215	374	201	187	406	194
Mangifera	NEPB1-9	PB	177	178	320	128	286	257	324	317	215	377	146	187	397	194
Mangifera	NEPB1-10	PB	177	178	320	128	286	257	324	317	215	377	146	187	397	194
Mangifera	NEPB1-12	PB	177	175	317	128	292	261	321	320	215	374	162	187	400	194
Mangifera	NEPB1-15	PB	177	175	317	128	292	261	321	320	215	374	162	187	400	194
Mangifera	NEPB1-18	PB	177	175	317	128	292	261	321	320	215	374	162	187	400	194
Mangifera	NEPB2-2	PB	177	178	320	128	286	257	324	317	215	377	174	187	397	194
Mangifera	1970	PB	177	178	317	128	295	257	324	320	215	374	201	187	397	194
Mangifera	1968	PB	174	175	323	128	268	257	306	320	215	374	223	187	397	194
Mangifera	1969	PB	174	175	323	128	268	257	306	320	215	374	223	187	397	194
Mangifera	NEAL1-2	AL	174	175	323	128	268	261	306	320	215	374	214	187	397	194
Mangifera	NEAL1-3	AL	174	175	323	128	268	261	306	320	215	374	214	187	403	194

Mangifera	NEAL1-5	AL	174	175	323	128	268	261	306	320	215	374	214	187	397	194
Mangifera	NEAL1-6	AL	174	175	323	128	268	261	306	320	215	374	214	187	397	194
Mangifera	NEAL1-8	AL	174	175	323	128	268	261	306	320	215	374	223	187	397	194
Mangifera	NEAL1-9	AL	174	175	323	128	268	261	306	320	215	374	223	187	397	194
Mangifera	NEAL1-10	AL	174	175	323	128	268	261	306	320	215	374	214	187	397	194
Mangifera	NEAL1-12	AL	174	175	323	128	268	261	306	320	215	374	214	187	397	194
Mangifera	NEAL1-13	AL	174	175	323	128	268	261	306	320	215	374	214	187	400	194
Mangifera	NEAL1-14	AL	174	175	323	128	268	261	306	320	215	374	214	187	397	194
Mangifera	NEAL1-16	AL	174	175	323	128	268	261	306	320	215	374	214	187	397	194
Mangifera	NEAL1-17	AL	174	175	323	128	268	261	306	320	215	374	214	187	397	194
Mangifera	NEAL1-18	AL	174	175	323	128	268	261	306	320	215	374	214	187	403	194
Mangifera	NEBA1-6	BA	177	175	320	134	286	257	321	317	215	371	153	187	397	194
Mangifera	NEBA1-7	BA	177	175	320	134	286	257	321	317	215	371	153	187	400	194
Mangifera	NEBA1-8	BA	177	175	320	134	286	257	321	317	215	371	153	187	400	194
Mangifera	NEBA1-9	BA	177	175	320	134	286	257	321	317	215	371	153	187	400	194
Mangifera	NEBA1-10	BA	177	175	320	134	286	257	321	317	215	371	153	187	400	194
Mangifera	NEBA1-12	BA	177	175	320	134	286	257	321	317	215	371	153	187	400	194
Mangifera	NEBA1-13	BA	177	175	320	134	286	257	321	317	215	371	153	187	400	194
Mangifera	NEBA1-14	BA	177	175	320	134	286	257	321	317	215	371	153	187	400	194
Mangifera	NECE1-1	CE	174	175	293	134	286	257	324	317	221	371	174	187	397	194
Mangifera	NECE2-1	CE	177	175	323	128	295	257	324	320	215	374	201	187	400	194
Mangifera	NECE2-2	CE	177	175	323	128	295	261	324	320	215	374	183	187	400	194
Mangifera	NECE2-3	CE	177	175	320	128	286	261	324	317	215	371	195	187	400	194
Mangifera	NECE2-4	CE	177	175	320	128	286	261	324	317	215	371	174	187	397	194
Mangifera	NECE2-5	CE	177	175	320	128	286	261	324	320	215	371	174	187	400	194
Mangifera	NECE2-6	CE	177	175	320	128	286	261	324	320	215	371	174	187	400	194
Mangifera	NECE2-7	CE	177	175	320	128	286	261	324	320	215	371	174	187	400	194
Mangifera	NECE2-8	CE	174	206	329	128	286	257	324	317	221	374	214	187	400	194

Mangifera	NECE2-12	CE	177	175	323	128	295	261	324	320	215	374	183	187	400	194
Mangifera	NECE2-13	CE	177	178	332	128	295	254	324	320	215	374	201	187	400	194
Mangifera	NECE2-15	CE	177	175	320	128	286	261	324	317	215	371	174	187	400	194
Mangifera	NEPE1-1	PE	177	178	288	128	295	260	324	320	215	374	201	187	400	194
Mangifera	NEPE1-2	PE	177	178	288	128	295	260	324	320	215	374	201	187	400	194
Mangifera	NEPE1-3	PE	177	178	288	128	295	260	324	320	215	374	201	187	400	194
Mangifera	NEPE1-4	PE	177	178	288	128	295	260	324	320	215	374	201	187	400	194
Mangifera	NEPE1-5	PE	177	178	288	128	295	260	324	320	215	374	201	187	400	194
Mangifera	NEPE1-6	PE	177	178	317	128	295	260	324	320	215	374	201	187	397	194
Mangifera	NEPE1-7	PE	177	178	317	128	295	260	324	320	215	374	211	187	400	194
Mangifera	NEPE1-10	PE	177	178	288	128	295	260	324	320	215	374	201	187	400	194
Mangifera	NEPE1-11	PE	177	178	317	128	295	260	324	320	215	374	201	187	397	194
Mangifera	NEPE1-12	PE	177	178	288	128	295	260	324	320	215	374	201	187	400	194
Mangifera	NEPE1-13	PE	177	178	317	128	295	260	324	320	215	374	201	187	400	194
Mangifera	NEPE1-14	PE	177	178	317	128	295	260	324	320	215	374	201	187	400	194
Mangifera	NEPE1-15	PE	177	178	320	128	286	257	324	317	215	377	174	187	400	194
Mangifera	ERRJ1-2	RJ	186	223	311	128	286	248	321	323	219	380	168	187	391	194
Mangifera	ERRJ1-4	RJ	186	223	311	128	286	248	321	323	219	380	211	187	391	194
Mangifera	ERRJ1-5	RJ	186	223	311	128	286	248	321	323	219	380	168	187	391	194
Mangifera	ERRJ1-6	RJ	186	223	311	128	286	248	321	323	219	380	168	187	391	194
Mangifera	ERRJ1-7	RJ	186	197	311	128	286	248	321	323	219	380	168	187	391	194
Mangifera	ERRJ1-8	RJ	186	223	311	128	286	248	321	323	219	380	211	187	391	194
Mangifera	ERRJ1-10	RJ	186	223	311	128	286	248	330	323	219	380	168	187	391	194
Mangifera	ERRJ2-1	RJ	198	223	311	128	277	248	330	326	219	380	168	221	391	194
Mangifera	ERRJ2-2	RJ	198	223	311	128	277	248	330	326	219	380	168	221	391	194
Mangifera	ERRJ2-4	RJ	198	223	311	128	277	248	330	326	219	380	168	221	391	194
Mangifera	ERRJ2-5	RJ	186	223	311	128	286	248	321	323	219	380	168	187	391	194
Mangifera	ERRJ3-6	RJ	186	223	311	128	286	248	330	323	219	380	168	187	391	194

Mangifera	ERRJ3-7	RJ	186	223	311	128	286	248	330	323	219	380	168	187	391	194
Mangifera	ERRJ3-8	RJ	186	223	311	128	286	248	330	323	219	380	168	187	391	194
Mangifera	ERRJ3-9	RJ	186	223	311	128	286	248	330	323	219	380	168	187	391	194
Mangifera	ERRJ3-10	RJ	186	223	311	128	286	248	330	326	219	380	168	187	391	194
Mangifera	ERRJ4-2	RJ	198	223	311	128	277	248	330	326	219	380	168	221	391	194
Mangifera	ERRJ5-1	RJ	198	223	311	128	277	248	330	326	219	380	168	221	391	194
Mangifera	ERRJ6-1	RJ	186	223	311	128	286	248	321	323	219	380	168	187	391	194
Mangifera	ERRJ7-1	RJ	186	223	311	128	286	248	321	323	219	380	168	187	391	194
Mangifera	1554	RJ	198	223	311	128	277	248	330	326	219	380	168	221	391	194
Mangifera	1555	RJ	198	223	311	128	277	248	330	326	219	380	168	221	391	194
Mangifera	1556	RJ	198	223	311	128	277	248	330	326	219	380	168	221	391	194
Mangifera	1557	RJ	198	223	311	128	277	248	330	326	219	380	168	221	391	194
Mangifera	1558	RJ	198	223	311	128	277	248	330	326	219	380	168	221	391	194
Mangifera	1559	RJ	198	223	311	128	277	248	330	326	219	380	168	221	391	194
Mangifera	1588	RJ	198	223	311	128	277	248	330	326	219	380	168	221	391	194
Mangifera	1589	RJ	198	223	311	128	277	248	330	326	219	380	168	221	391	194
Mangifera	1590	RJ	198	223	311	128	277	248	330	326	219	380	168	221	391	194
Mangifera	1591	RJ	186	223	311	128	277	261	330	323	219	371	168	187	391	194
Mangifera	2112	RJ	198	223	311	128	277	248	330	326	219	380	168	221	391	194
Mangifera	1658	RJ	198	223	311	128	277	248	330	326	219	380	168	221	391	194
Mangifera	1659	RJ	198	223	311	128	277	248	330	326	219	380	168	221	391	194
Mangifera	1660	RJ	198	223	311	128	277	248	330	326	219	380	168	221	391	194
Mangifera	1661	RJ	198	223	311	128	277	248	330	326	219	380	168	221	391	194
Mangifera	1662	RJ	186	223	311	128	286	248	330	323	219	377	168	187	391	194
Mangifera	1663	RJ	186	223	311	128	286	248	330	323	219	371	168	187	391	194
Mangifera	1664	RJ	198	223	311	128	277	248	330	326	219	380	168	221	391	194
Mangifera	1671	RJ	198	223	311	128	277	248	330	326	219	380	168	221	391	194
Tectona	TecMT5	MT	174	175	311	134	297	253	324	317	215	371	156	187	397	194

Tectona	TecMT8	MT	174	175	311	134	297	253	324	317	215	371	156	187	397	194
Tectona	TecMT15	MT	174	175	317	134	289	253	324	317	213	371	156	187	397	194
Tectona	TecMT16	MT	174	175	317	134	289	253	324	317	213	371	156	187	397	194
Tectona	TecMT22	MT	174	175	317	134	289	253	324	317	213	371	156	187	397	194
Tectona	TecMT23	MT	174	175	317	134	289	253	324	317	213	371	156	187	397	194
Tectona	TecMT24	MT	174	175	317	134	289	253	324	317	213	371	156	187	397	194
Tectona	TecMT29	MT	174	175	317	134	289	253	324	317	213	371	156	187	397	194
Tectona	TecMT35	MT	174	175	317	134	289	253	318	317	213	371	156	187	397	194
Tectona	TecMT354	MT	174	175	317	134	289	253	318	317	213	371	156	187	397	194
Tectona	TecMT355	MT	174	175	317	134	289	253	318	317	213	371	156	187	397	194
Tectona	TecMT356	MT	174	175	317	134	289	253	318	317	213	371	156	187	397	194
Tectona	TecMT357	MT	174	175	317	134	289	253	318	317	213	371	156	187	397	194
Tectona	TecMT358	MT	174	175	317	134	289	253	318	317	213	371	156	187	397	194
Tectona	TecMT69	MT	174	175	311	134	297	253	324	317	215	371	156	187	397	194
Tectona	C3622	MT	174	175	311	134	297	253	324	317	215	371	156	187	397	194
Tectona	C3623	MT	174	175	311	134	297	253	324	317	215	371	156	187	397	194
Tectona	TecMT7	MT	174	175	311	134	297	253	324	317	215	371	156	187	397	194
Tectona	C3624	MT	174	175	311	134	297	253	324	317	215	371	156	187	397	194
Tectona	TecMT10	MT	174	175	317	134	289	253	324	317	213	371	156	187	397	194
Tectona	C3625	MT	174	175	317	134	289	253	324	317	213	371	156	187	397	194
Tectona	C3626	MT	174	175	317	134	289	253	324	317	213	371	156	187	397	194
Tectona	TecMT18	MT	174	175	317	134	289	253	324	317	213	371	156	187	397	194
Tectona	C3627	MT	174	175	317	134	289	253	324	317	213	371	156	187	397	194
Tectona	C3628	MT	174	175	317	134	289	253	324	317	213	371	156	187	397	194
Tectona	C3629	MT	174	175	317	134	289	253	324	317	213	371	156	187	397	194
Tectona	TecMT28	MT	174	175	317	134	289	253	324	317	213	371	156	187	397	194
Tectona	C3630	MT	174	175	317	134	289	253	324	317	213	371	156	187	397	194
Tectona	TecMT32	MT	174	175	317	134	289	253	318	317	213	371	156	187	397	194

Tectona	C3631	MT	174	175	317	134	289	253	318	317	213	371	156	187	397	194
Tectona	TecMT39	MT	174	175	317	134	289	253	318	317	213	371	156	187	397	194
Tectona	TecMT46	MT	174	175	317	134	289	253	318	317	213	371	156	187	397	194
Tectona	TecMT352	MT	180	175	317	134	286	253	324	317	219	377	247	187	397	194
Tectona	C3616	MT	174	175	317	134	289	253	318	317	213	371	156	187	397	194
Tectona	C3617	MT	174	175	317	134	289	253	318	317	213	371	156	187	397	194
Tectona	C3618	MT	174	175	317	134	289	253	318	317	213	371	156	187	397	194
Tectona	C3619	MT	174	175	317	134	289	253	318	317	213	371	156	187	397	194
Tectona	C3620	MT	174	175	317	134	289	253	318	317	213	371	156	187	397	194
Tectona	LPF2199	MT	174	175	317	134	289	253	324	317	215	371	156	187	397	194
Tectona	C3621	MT	174	175	317	134	289	253	318	317	213	371	156	187	397	194
Tectona	C3632	MT	174	175	311	134	297	253	324	317	215	371	156	187	397	194
Theobroma	1585	BA	186	246	305	128	274	258	336	338	215	374	245	187	406	194
Theobroma	1586	BA	186	246	305	128	274	258	336	338	215	374	245	187	406	194
Theobroma	1587	BA	186	246	305	128	274	258	336	338	215	374	245	187	406	194
Theobroma	C1593/LPF1332		183	246	305	128	274	258	336	338	215	374	245	187	406	194
Theobroma	1593	BA	186	246	305	128	274	258	336	338	215	374	245	187	406	194
Theobroma	1594	BA	186	246	305	128	274	258	336	338	215	374	245	187	406	194
Theobroma	1595	BA	186	246	305	128	274	258	336	338	215	374	245	187	406	194
Theobroma	1596	BA	186	246	305	128	274	258	336	338	215	374	245	187	406	194
Theobroma	1597	BA	186	246	305	128	274	258	336	338	215	374	245	187	406	194
Theobroma	1598	BA	186	246	305	128	274	258	336	338	215	374	226	187	406	194
Theobroma	1599	BA	186	246	305	128	274	258	336	338	215	374	245	187	406	194
Theobroma	1600	BA	186	246	305	128	274	258	336	338	215	374	245	187	406	194
Theobroma	1601	BA	186	246	305	128	274	258	336	338	215	374	245	187	406	194
Theobroma	1718	BA	186	246	305	128	274	258	336	338	215	374	245	187	406	194
Theobroma	1719	BA	186	246	305	128	274	258	336	338	215	374	245	187	406	194
Theobroma	1720	BA	186	246	305	128	274	258	336	338	215	374	245	187	406	194

Theobroma	1721	BA	186	246	305	128	277	258	324	338	215	374	245	187	406	194
Theobroma	1722	BA	186	246	305	128	274	258	336	338	215	374	245	187	406	194
Theobroma	1723	BA	186	246	305	128	274	258	336	338	215	374	245	187	406	194
Theobroma	1724	BA	186	246	314	128	274	258	321	338	215	374	245	187	406	194
Theobroma	1725	BA	186	246	305	128	274	258	336	338	215	374	245	187	406	194
Theobroma	1726	BA	186	246	305	128	274	258	336	338	215	374	245	187	406	194
Theobroma	1727	BA	186	246	305	128	274	258	336	338	215	374	245	187	406	194
Theobroma	1728	BA	186	246	305	128	274	258	336	338	215	374	245	187	406	194
Theobroma	1729	BA	186	246	305	128	274	258	336	338	215	374	245	187	406	194
Theobroma	1730	BA	186	246	305	128	274	258	336	338	215	374	245	187	406	194
Theobroma	1731	BA	186	246	305	128	274	258	336	338	215	374	245	187	406	194
Theobroma	1732	BA	186	246	305	128	274	258	336	338	215	374	245	187	406	194
Theobroma	1733	BA	186	246	305	128	274	258	336	338	215	374	245	187	406	194
Theobroma	1734	BA	186	246	305	128	274	258	336	338	215	374	245	187	406	194
Theobroma	1735	BA	186	246	305	128	274	258	336	338	215	374	245	187	406	194
Theobroma	1736	BA	186	246	305	128	274	258	336	338	215	374	245	187	406	194
Theobroma	1737	BA	186	246	305	128	274	258	336	338	215	374	245	187	406	194
Theobroma	1738	BA	186	246	305	128	274	258	336	338	215	374	245	187	406	194
Theobroma	1739	BA	186	246	305	128	274	258	336	338	215	374	245	187	406	194
Theobroma	1740	BA	186	246	305	128	274	258	336	338	215	374	245	187	406	194
Theobroma	1741	BA	186	246	305	128	274	258	336	338	215	374	245	187	406	194
Theobroma	1742	BA	186	246	305	128	274	258	336	338	215	374	245	187	406	194
Theobroma	1743	BA	186	246	305	128	274	258	336	338	215	374	245	187	406	194
Theobroma	1744	BA	186	246	305	128	274	258	336	338	215	374	245	187	406	194
Theobroma	1745	BA	186	246	305	128	274	258	336	338	215	374	245	187	406	194
Theobroma	1746	BA	186	246	305	128	274	258	336	338	215	374	245	187	406	194
Theobroma	1747	BA	186	246	305	128	274	258	336	338	215	374	245	187	406	194
Theobroma	1748	BA	186	246	305	128	274	258	336	338	215	374	245	187	406	194

Theobroma	1749	BA	186	246	305	128	274	258	336	338	215	374	245	187	406	194
Theobroma	1982	RO	186	183	305	128	271	258	336	338	215	374	271	187	406	194
Theobroma	1983	RO	186	183	305	128	271	258	336	338	215	374	271	187	406	194
Theobroma	1984	RO	232	183	305	128	271	258	336	338	215	374	269	187	406	194
Theobroma	2031	RO	189	290	305	131	271	258	336	338	234	374	271	195	406	194

Supplementary Table S2. Mean xylem discoloration (centimeters) caused by *Ceratocystis fimbriata* s.l. isolates inoculated into eight host plants

Isolate	***Ad.***		***As.***		***Eu***		***Fc***		***Hb***		***Mi***		***Tg***		***Tc***	
	T 1[b]	**T 2**[c]	**T 1**	**T 2**	**T 1**	**T 2**	**T 1**	**T 2**	**T 1**	**T 2**	**T 1**	**T 2**	**T 1**	**T 2**	**T 1**	**T 2**
Mi.LPF1156[a]	1.83bc	20.8abc	3.40abcd	5.52abc	28.4ab	23.7ab	17.7ab	29.2a	5.2abcd	2.5c	20.1a	24.5ab	3.6bc	5.1b	0.9c	1.3b
Ga.LPF1323	1.07c	24.0ab	2.78abcd	3.52abc	7.3de	13.1b	17.3a	17.9a	3.1cde	2.9bc	6.2bcd	8.3bc	4.9ab	3.7b	6.1ab	1.6b
As.LPF1331	11.14bc	11.92abcd	9.42a	2.7abc	7.4cd	12.5ab	22.4a	23.2a	3.8abcd	1.3bc	20.5a	20.3ab	1.5bc	1.0b	0.9c	1.2b
Tc.LPF1332	3.45bc	1.74ef	1.80abcd	1.74bc	2.9de	5.5bc	2.2cd	1.3cd	3.6bcde	1.3bc	2.5de	1.2d	3.4bc	1.0b	12.3a	14.2a
Fc.LPF1336	2.63bc	6.5bcde	1.60abcd	2.46abc	18.4abc	24.4ab	21.0a	19.1a	1.3de	6.0bc	6.7bcd	3.7cd	4.6ab	1.8b	1.0c	1.4b
Hb.LPF1394	2.38bc	3.24def	1.96abcd	5.58abc	8.6bcd	6.6bc	18.7ab	8.4ab	14.5a	28.8a	1.0e	4.8cd	3.0bc	2.3b	1.8bc	1.6b
Ad.LPF1443	94.70a	38.4a	1.38cd	2.68abc	7.0cd	5.9bc	15.3ab	21.3ab	8.1abc	4.3bc	4.1cd	13.0abc	3.0bc	3.0b	2.4bc	1.0b
Cb.LPF1489	32.25a	41.4a	1.50abcd	3.6abc	9.2cd	13.0b	19.0ab	16.2ab	7.2abc	11.8ab	13.4a	27.2a	3.5bc	2.1b	1.3c	1.0b
Cg.LPF1560	1.63bc	1.1f	1.44bcd	3.1abc	5.4de	5.8bc	7.4bc	4.5bc	1.3de	3.8bc	5.8bcd	11.9abc	4.5b	1.0b	1.0c	1.1b
Eu.LPF1912	6.26b	4.2cdef	5.36ab	9.56a	41.3a	57.9a	22.0a	22.0a	4.5abcd	6.9bc	16.2b	17.5abc	3.5b	2.7b	1.0c	1.0b
Tg.LPF2199	123.85a	10.2abcd	4.02abc	6.78ab	8.4bcd	10.3ab	23.9a	24.4a	12.8ab	7.5bc	10.9bc	15.1abc	13.1a	37.8a	1.5bc	1.2b
Control	1.0c	1.0f	1.0d	1.10c	1.7e	1.7c	1.0d	0.8d	0.8e	0.4bc	1.0e	1.1d	1.0c	1.0b	0.8c	0.4b

[a] The two letters before isolate names indicate their host source (Tc = *Theobroma cacao*; Cg = *Carapa guianensis*; Mi = *Mangifera indica*; Ad = *Actinidia deliciosa*; Cb = *Caryocar brasiliense*; Fc = *Ficus carica*; As = *Annona squamosa*; Hb = *Hevea brasiliensis*; Ga = *Gmelina arborea*; Tg = *Tectona grandis*; Eu = *Eucalyptus* sp.).

[b] Trials 1.

[c] Trials 2.

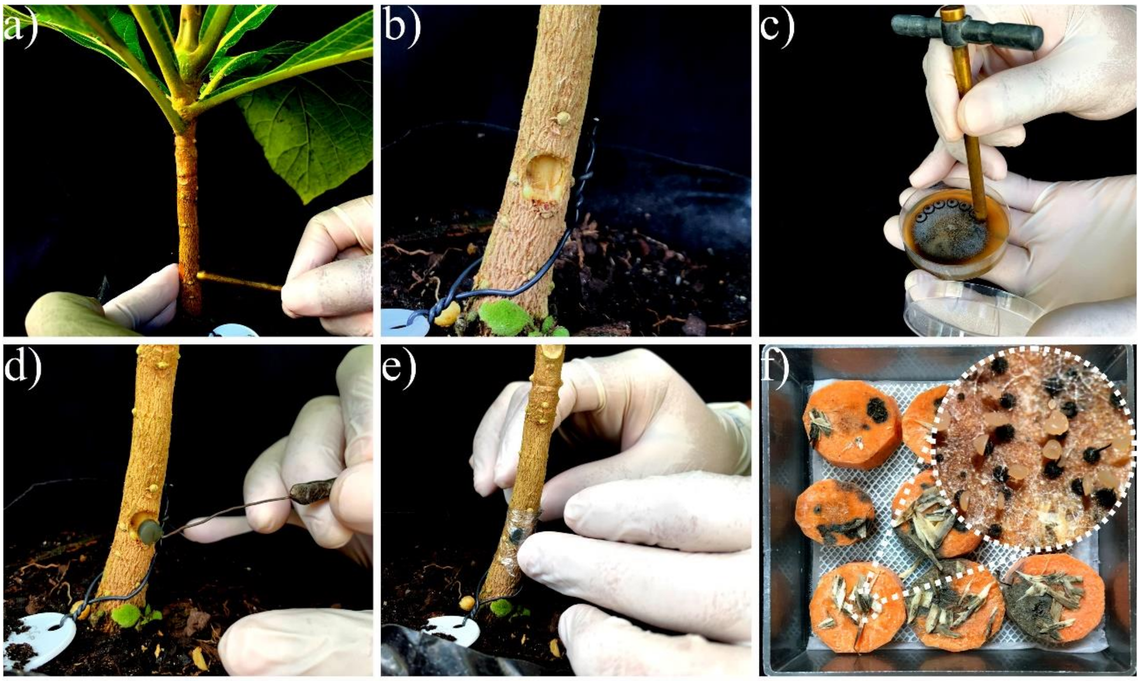

Supplementary Figure S1. Inoculation and isolation of *Ceratocystis fimbriata* in clone C1 of *Tectona grandis*. a-b. Wounding the stem base of the plants with a sterile stylet. c-d. Deposition of a mycelium disc. e. Inoculation site wrapped with parafilm. f. Isolation using the carrot bait method.

CHAPTER 2 - CHROMOSOMAL POLYMORPHISM OF THE *Ceratocystis fimbriata* SPECIES COMPLEX IN BRAZIL

Author names and affiliations: Fernando Montezano Fernandes[a], Marisa Vieira de Queiroz[b], Leandro Lopes da Silva[b], Daiana Maria Queiroz Azevedo[a], Jorge Luis Badel[c], Acelino Couto Alfenas[a,*].

[a] Laboratory of Forest Pathology, Department of Plant Pathology, Universidade Federal de Viçosa, Minas Gerais State, Brazil
[b] Laboratory of Molecular Genetics of Microorganisms, Department of Microbiology, Universidade Federal de Viçosa, Minas Gerais State, Brazil
[c] Laboratory of Molecular Phytobacteriology, Department of Plant Pathology, Universidade Federal de Viçosa, Minas Gerais State, Brazil

*Corresponding author: Acelino C. Alfenas, Laboratory of Forest Pathology, Department of Plant Pathology, Universidade Federal de Viçosa, Minas Gerais State, Brazil; Tel: +55 (31) 3612-2428; E-mail: aalfenas@ufv.br

To be submitted to Fungal Genetics and Biology

ABSTRACT

Ceratocystis fimbriata is an important pathogen that causes wilt in several plant species. Despite the importance of this pathogen, knowledge about its karyotypic polymorphism and genomic architecture is limited. The main objective of this study was to investigate the karyotype of isolates of the *C. fimbriata* species complex from different host plants and geographical origins in Brazil. First, the identity of the isolates was confirmed conducting multilocus phylogeny using DNA sequences of mating type genes, TEF-1α, and β-tubulin. To investigate the chromosomal polymorphism, two conditions of pulsed-field gel electrophoresis (PFGE) were used and the karyotypes of the isolates obtained. The retrotransposon-microsatellite amplified polymorphism (REMAP) molecular marker was utilized to assess the genetic variability among isolates. The two species of isolates utilized in this study, *C. cacaofunesta* and *C. fimbriata* isolates, were successfully distinguished in the multilocus analysis. Polymorphism in chromosome number and size was found, indicating the existence of genomic differences among isolates and occurrence of chromosomal rearrangements in the species complex. The number of chromosomes varied from six to eight and the estimated minimum chromosome sizes were estimated to be between 2.7 to 6.0 Mbp. Small polymorphic chromosomes ranging from 1.0 to 1.8 Mbp were observed in all isolates, raising the hypothesis that they could be supernumerary chromosomes. REMAP analysis revealed a high genetic variability and that isolates from the same host tend to group together in a same cluster. Our results bring new insights into the chromosomal diversity and genome organization of the *C. fimbriata* complex.

Keywords:
Chromosomal rearrangements, genomic architecture, karyotyping, PFGE, REMAP marker.

INTRODUCTION

Ceratocystis fimbriata Ellis & Halsted is a pathogen with wide geographical distribution that causes diseases in several agronomic and forest crops of economic importance in Brazil, such as *Actinidia deliciosa* (A. Chev) CF Lianget & AR Ferguson (Piveta et al., 2013), *Annona squamosa* L. (Silveira et al., 2006), *Carapa guianensis* Aubl. (Halfeld-Vieira et al., 2012; Valdetaro et al., 2019), *Caryocar brasiliense* Cambess. (Silva et al., 2017), *Eucalyptus* spp. (Ferreira et al., 1999), *Ficus carica* L. (Valarini and Tokeshi, 1980), *Gmelina arborea* Roxb. Ex Sm. (Muchovej et al., 1978), *Hevea brasiliensis* L. (Albuquerque et al., 1972), *Mangifera indica* L. (Carvalho, 1938), and *Tectona grandi*s L. f. (Firmino et al., 2012). The pathogen mainly infects the parenchyma, phloem and xylem vessels, and causes discoloration in the radial direction of the wood and wilt symptoms (Ferreira et al., 2006; Silva et al., 2020).

Currently, *C. fimbriata* is recognized as a complex of many cryptic species. The pathogen causing black rot in sweet potatoes [*Ipomoea batatas* (L.) Lam] is treated as *C. fimbriata* sensu stricto (s.s.) while those causing disease in other hosts are treated as *C. fimbriata* sensu lato (s.l.). Four phylogenetic clades are known in this complex: Latin American, North American, Asian-Australian and African (Fourie et al., 2015; Harrington et al., 2011; Liu et al., 2018). These clades can be distinguished based on multilocus phylogeny, morphology, and physiological characteristics of isolates from different hosts. However, the taxonomic position of some of the species remains inconclusive (Baker et al., 2003; Harrington et al., 2011; Kanzi et al., 2020; Oliveira et al., 2015a).

Despite recent advances in genomics of the genus *Ceratocystis* (Fourie et al., 2019; Santos et al., 2020), the genomic organization of *C. fimbriata* is unclear. Improvements in pulsed-field gel electrophoresis (PFGE) (Schwarts and Cantor, 1984) over the years have allowed the study of the karyotype of many plant-pathogenic fungi. This technique can be used to study fungi regardless of their sexual stage (Wieloch, 2006), revealing karyotypic variations with respect to both chromosome size and chromosome number. For instance, the electrophoretic karyotype of twenty-four isolates of *Moniliophthora perniciosa* (=*Crinipellis perniciosa*) revealed chromosomal variability within and among three different biotypes collected from various hosts in South America. These isolates exhibited 8-12 chromosomal bands, whose sizes allowed to estimate a genome size between 30.2 and 46.1Mbp (Rincones et al., 2006). Also, the karyotypes of *Zymoseptoria tritici* (=*Mycosphaerella graminicola*) isolates were analyzed running two PFGE conditions. The chromosome numbers in these isolates varied between 18 and 20, whose sizes were in the range 0.3–6 Mbp. The total genome sizes of the studied isolates was estimated to be 31 to 40 Mbp (Mehrabi et al., 2007). These karyotypic variations are caused by chromosomal rearrangements that can result from structural modifications (deletions, inversions, and duplications), changes in repetitive DNA sequences, and translocation of chromosomal segments within and among chromosomes (Zolan, 1995). Among the known mechanisms that mediate chromosomal rearrangements are transposable elements (TEs) (Mehrabi et al., 2017; Möller and Stukenbrock, 2017).

Transposable elements are present and dispersed in a significant portion of eukaryotic genomes (Muszewska et al., 2019) and are often used as molecular markers in population genetics studies of plant-pathogenic fungi (Daboussi and Capy, 2003; Schulman, 2007). Molecular markers, including the microsatellite probe $(CAT)_5$ (DeScenzo and Harrington, 1994), mitochondrial DNA restriction fragment length polymorphism (RFLP) (Engelbrecht et al., 2007; Roux et al., 2001) and simple sequence repeat (SSR) markers (Steimel et al., 2004), have been widely used to analyze the genetic variability of the genus *Ceratocysti*s. However, there is no molecular markers based on TEs for *C. fimbriata*. Molecular marker based on TEs, in contrast to other markers, detect large changes in the genome. Due to their capacity to move in the host genome and to increase their copy number, TEs can generate insertion mutations and gene disruptions, increase gene expression, and promote chromosomal rearrangements through recombination causing translocations, inversions or deletions (Hua-Van et al., 2005). The most abundant group among TEs are retrotransposons, which are divided into two main classes, according to the presence or absence of flanking long terminal repeats (LTRs) (Rohde, 1996). Transposition of LTR retrotransposons in the genome is a random process and occurs continuously during species evolution (Kalendar et al., 2021). The LTR sequences are widely conserved and can be exploited to develop retrotransposon-based markers (Santos et al., 2012).

Retrotransposon-microsatellite amplified polymorphism (REMAP) markers have been used to assess the genetic variability in phytopathogenic fungi. These REMAP markers utilize primers targeted to SSR motifs in conjunction with LTR-specific primers to identify polymorphic segments spanning between the retrotransposon and the SSR (Kalendar et al., 1999). Recently, the TEs content of the *C. fimbriata* genome was revealed and the presence of retrotransposons in all analyzed isolates was confirmed (Fourie et al., 2020; Santos et al., 2020). Therefore, the REMAP technique can be used to investigate the occurrence of retrotransposons integration in the *C. fimbriata* genome as well as to study the genetic variability of this important phytopathogen.

We hypothesized that *C. fimbriata* isolates exhibit variability in chromosome number and size. As *C. fimbriata* is a fungus with a relatively small genome (31.6 Mbp) (Santos et al., 2020), PFGE can be used to investigate such a variability. To confirm our hypothesis, we determined the karyotype of isolates of the *C. fimbriata* species complex from different host plants and geographic origins in Brazil using PFGE. Because chromosomal variation can be caused by TEs, we also assessed the variability of the same isolates using REMAP markers. Prior to PFGE and REMAP, the identity of the isolates was confirmed by multilocus phylogeny.

MATERIALS AND METHODS

Fungal isolates and culture conditions

Fungal isolates used in this study belong to the Fungal Collection of the Laboratory of Forest Pathology/Bioagro of the Universidade Federal de Viçosa, Minas Gerais, Brazil. Fourteen isolates of the *C. fimbriata* complex obtained from different host plants and geographic origins in Brazil were analyzed. The isolates were chosen based on previous studies showed that these isolates are pathogenic to their corresponding hosts (Baker et al., 2003; Oliveira et al., 2015a; Oliveira et al., 2016, 2021; Silveira et al., 2006; Valdetaro et al., 2015, 2019). Information on isolates studied is summarized in Table 1. Isolates were grown on MEYA culture medium (2% malt extract, 0.2% yeast extract, and 2% agar) maintaining the plates in a growth room (25 ± 2 ºC, photoperiod 12 h light/12 h dark).

DNA extraction, amplification and sequencing

The isolates were cultured in 250 mL Erlenmeyer flasks containing 100 mL of MEY liquid medium (2% malt extract and 0.2% yeast extract) at 25°C under constant agitation at 150 rpm for 120 h. The mycelium was collected for DNA extraction as previously described by Specht et al., (1982), with modifications (Teixeira et al., 2011). The quality and quantity of the total DNA were assessed using a NanoDrop 2000c spectrophotometer (Thermo Scientific) and by electrophoresis in 0.8% (w v^{-1}) agarose gel.

Partial sequences of the nuclear genes encoding β-tubulin and portions of the TEF-1α, MAT1 (*MAT1-1-2*) and MAT2 (*MAT1-2-1*) regions were amplified and sequenced from self-fertile isolates using the BT1-α/ BT1-β; EFCF1/ EFCF6; CFMAT1-F/ CFMAT1-R; x9978a/ CFM2-1F primers (Supplementary Table S1). Each PCR reaction was prepared in a 15 µL total volume containing 7.5 µL GoTaq Colorless Master Mix (Promega), 1.5 µL of each primer (10 µM; Sigma Aldrich), 2 µL of genomic DNA (15 ng μL^{-1}) and 2.5 µl of nuclease-free water. The PCR was performed in a Veriti 96 thermocycler (Applied Biosystems).

The PCR procedure for β-tubulin gene was as follows: initial denaturation at 94°C for 4 min, 30 cycles of 94°C for 50 s, 55°C for 50 s, 72°C for 50 s, and a final extension at 72°C for 10 min (Glass and Donaldson, 1995). The PCR procedure for TEF-1α gene followed Harrington (2007) with slight modifications: initial denaturation at 85°C for 2 min followed by 94°C for 95s, 36 cycles of 68°C for 60s, 72°C for 90 s, and 94°C for 35 s, and a final extension at 72°C for 15 min. The PCR procedure for *MAT1-1-2* and *MAT1-2-1* gene was as follows: initial denaturation at 94°C for 120s, 36 cycles of 94°C for 60s, 60°C for 60 s, 72°C for 120 s, and a final extension at 72°C for 10 min (Harrington et al., 2014).

The PCR products were resolved on 1% (w v^{-1}) agarose gels in 1X TAE (40 mM Tris-base, 20 mM acetic acid, 1.0 mM EDTA, pH 8.0) buffer, stained with ethidium bromide and photographed using an L-PIX gel documentation system (Locus Biotechnology). The size of the amplified fragments was determined by comparison to a 1 Kb plus DNA Ladder (Invitrogen, CA, USA). PCR products were purified using Ilustra$^{\text{TM}}$ GFX$^{\text{TM}}$ PCR DNA and sequenced on an ABI PRISM 3100 sequencer. Reagents and equipment utilized for DNA sequencing were from Applied Biosystems. Consensus sequences were assembled using SeqAssem (Hepperle, 2004). All sequences were checked and adjusted manually, and ambiguous nucleotide positions were clarified using sequences from both DNA strands. For the first identification, consensus sequences were tested against the GenBank database using the MEGA BLAST software.

Phylogenetic analysis

Sequences of the β-tubulin ,TEF-1α, MAT1 (*MAT1-1-2*) and MAT2 (*MAT1-2-1*) regions of the 14 Brazilian isolates analyzed in this study were compared with those of isolates from the Fungal Collection of the Laboratory of Forest Pathology/Bioagro and reference sequences from species representative of the *C. fimbriata* complex deposited at GenBank (http://www.ncbi.nlm.nih.gov). *Ceratocystis destructans* from the North American clade was used as the outgroup taxon. The sequences were aligned using MUSCLE (Edgar, 2004) implemented in MEGA 7 software (Kumar et al., 2016). A concatenated data matrix (β-tubulin + TEF-1α + MAT1 + MAT2) was constructed using AliView software (Larsson, 2014). Two analyses were performed: Maximum Likelihood (ML) and Bayesian Inference (BI).

ML analyses were conducted in the RAxML v. 8.2.9 (Stamatakis, 2014) platform available on CIPRES Science Gateway Portal (Miller et al., 2010). The default parameters were used, and bootstrapping was performed using the quick bootstrapping algorithm with the automatic halt option (1,000 initial replicates). The trees were visualized in FigTree (Rambaut and Drummond, 2018). Clade support was inferred from 1000 bootstrap (BS) replicates. BS values greater than or equal to 70% were considered significant.

The BI was performed using MrBayes v3.2.6 (Ronquist et al., 2012) using the Markov chain Monte Carlo method (MCMC). The best model of nucleotide substitution was chosen based on the Akaike Information Criterion (AIC) of MrModelTest 3.2 (Nylander, 2004). The HKY+G models were selected for β-tubulin and MAT2, HKY+I+G for TEF-1α and K80+G for MAT1. Two parallel runs of four Markov chains were performed for 10,000,000 generations and sampled every 1000 generations. For the resulting 10,000 trees, 25 % were discarded as burn-in and the remaining 7500 trees were used to calculate the posterior probability (PP) of the branches of the concatenated tree. Branches with at least 0.70 of PP were considered well supported. The BI phylogenetic analyses were performed using the CIPRES Science Gateway Portal (Miller et al., 2010).

Preparation of intact chromosomal DNA and pulsed-field gel electrophoresis

Intact chromosomal DNA of the 14 isolates of the *C. fimbriata* complex was prepared according to Brody and Carbon (1989), with modifications. The fungal isolates were cultured in 1000 mL Erlenmeyer flasks in a volume of 500 mL of dextrose potato broth medium (200 g potato; 20 g L^{-1} dextrose). The medium was inoculated with $1x10^6$ conidia and incubated at 25°C with agitation at 250 rpm for 12-15 h. The mycelium was collected by filtration using a 200-mesh sieve and washed with ultrapure water to completely remove the conidia. To obtain protoplasts, 800-1000 mg of mycelium was suspended in 5 mL of osmotic stabilizer (0.8 M KCl in phosphate buffer 0.01 M, pH 5.8) containing 25 mg mL^{-1} Lysing Enzymes L1412 (Sigma Aldrich®) and 10 mg mL^{-1} bovine serum albumin (BSA) and incubated at 30°C with agitation at 80 rpm for 3-4 h.

The protoplasts were filtered using a syringe with gauze and centrifuged at 5000 g for 10 min. Centrifugation in 5 mL osmotic stabilizer (0.8 M KCl in phosphate buffer 0.01 M, pH 5.8) was conducted twice. The pellet was resuspended in ST buffer (sorbitol 1 M; Tris-HCl, 0.01 M, pH 7.5) to a final concentration of $1x10^8$ protoplasts mL^{-1}. An equal volume of 1.4% InCert agarose (FMC) in ST buffer prewarmed to 42°C was added to the protoplast suspension and the mixture was poured into a plug mold and solidified at 4°C for 10 min. The blocks containing the protoplasts were treated in 1 mL of NDS solution [50 mM EDTA (pH 8.0); 10 mM Tris-HCl (pH 8.0); 1% N-lauroyl sarcosine] and 1 mg mL^{-1} of proteinase K and incubated overnight at 50°C. The blocks were washed twice with 50 mM EDTA (pH 8.0) at 50°C for 30 min and the tubes containing the blocks were stored in 50 mM EDTA pH 8.0 at 4°C. The PFGE was carried out using a CHEF-DR III (Clamped Homogeneous Electric Fields - Dynamic Regulation) system (Bio-Rad).

Two electrophoresis programs were used to resolve the *C. fimbriata* chromosomes. Program A was employed to separate the small chromosomes using pulses in a block: 60/120 s, 24 h, 6 V cm^{-1} at an included angle of 120°. The gel was prepared with 1.5% (w v^{-1})

chromosomal-grade agarose (Bio-Rad) in 0.5 X TBE (45 mM Tris-borate, 1.0 mM EDTA, pH 8.0). The buffer was maintained in circulation at 10°C. *Saccharomyces cerevisiae* (Bio-Rad, USA) chromosomes were run in parallel as standard size markers. Program B was utilized to separate the large chromosomes using pulses divided into three blocks: B1 was conducted at 3300 s, 73 h and 1.4 V cm^{-1}; B2 at 2800 s, 48 h, and 1.4 V cm^{-1}; and B3 at 2200 s, 73 h and 1.4 V cm^{-1} at an included angle of 120°. The gel was prepared with 0.8% (w v^{-1}) chromosomal-grade agarose (Bio-Rad) in 1X TBE (90 mM Tris-borate, 2.0 mM EDTA, pH 8.0). The buffer was replaced every 72 h and maintained in circulation at 10°C. *Schizosaccharomyces pombe* (Bio-Rad, USA) and *Aspergillus nidulans* (Queiroz et al., 2000) chromosomes were run in parallel as standard size markers. In both runs, 200 µM of thiourea was added to both the agarose gel and the electrophoresis buffer to ensure minimal DNA degradation (Fawley and Wilcox, 2002). After chromosome separation, the gel was stained with ethidium bromide (1.0 µg mL^{-1}) and visualized in an L-PIX gel documentation system (Locus Biotechnology). Densitometric analysis of the gels was performed with Gel Analyzer 1D version 19.1 (Lazar et al., 2010) and chromosomal band sizes were estimated by comparison with the nearest bands of the *S. cerevisae*, *S. pombe* and *A. nidulans* chromosomes. The PFGE for each isolate with each program was conducted at least twice to establish the repeatability of the banding patterns (number and size of distinct chromosomes).

REMAP amplification

In order to investigate the TE-associated genetic diversity of the 14 Brazilian isolates of the *C. fimbriata* complex, REMAP (Kalendar et al., 1999) with primer CLIRAP4 (5'-CTTTTGACGAGGCCATGC-3') (Santos et al., 2012) in combination with primer MS1 (5'-GGCGGCGGCGGCGGCGGCGGCT-3') (Santana et al., 2012) was conducted. The REMAP reactions were performed in a final 25 µl volume containing 1.0 µl DNA (40 ng µl^{-1}), 12.5 µl of GoTaq® Master Mix (Promega), 1.0 µl of each primer (10 µM) and nuclease-free water. The PCR reactions were performed in a PTC-100-MJ Research thermocycler programmed to undergo an initial denaturation step at 94°C for 2 min, six cycles at 94°C for 30 s, 50°C for 30 s, and 72°C for 2 min. Twenty-four cycles were added to these six initial cycles, with an extension at 72°C for 30 s added at the end of every six cycles. A final extension step at 72°C for 10 min was included. Differences in amplicon patterns among the isolates were analyzed by running electrophoresis on a 1.5% (w v^{-1}) agarose gel at 3 V cm^{-1} for 210 min in 1X TBE (90 mM Tris-borate, 2.0 mM EDTA, pH 8.0) buffer. The gel was stained with ethidium bromide (1.0 µg mL^{-1}) and visualized in an L-PIX gel documentation system (Locus Biotechnology). The size of the amplified fragments was estimated by comparison with a 1Kb DNA ladder (KASVI®) molecular marker. The experiment was conducted three times to confirm the reproducibility of the band profiles.

Fragment profiles obtained with REMAP were used to construct a binary matrix, assigning a value of 1 to presence and 0 to absence of a band. Faint bands were excluded from the analysis. Dendrogram construction was performed with PAST 3.06 (Hammer et al., 2001) using the Dice similarity coefficient (Dice, 1945), the unweighted pair group method with arithmetic means (UPGMA) method and correlations were expressed as percentage similarity.

RESULTS

Phylogenetic analyses

All targeted DNA loci were successfully amplified and sequenced from our C. fimbriata samples. ML and BI phylogenetic analyses were performed for each gene data set and resulted in almost identical trees with topology consistent as reported by Oliveira *et al.*, (2015), Ferreira *et al.*, (2017) and Valdetaro *et al.*, (2019) (BI trees are not shown). Phylogenetic analyses of the β-tubulin gene sequences were performed with a data matrix containing 47 taxa, 564 characters including gaps, 514 of which were conserved, 49 variable, eight parsimony-informative and 41 singletons. Phylogenetic variation among the 14 *C. fimbriata* isolates was observed (Supplementary Figure S1) and a clear separation of *C. fimbriata* from isolates of *C. cacaofunesta* was observed.

For the MAT1 gene, phylogenetic analyses were performed with a data matrix containing 47 taxa, 1040 characters including gaps, of which 880 were conserved, 155 variables, 23 parsimony-informative, and 132 singletons. Some subclades were formed by isolates from the same hosts, showing different haplotypes and intraspecific variation within this group (Supplementary Figure S2). The *Actinidia* sp isolate (LPF1424), *G. arborea* (LPF1323, 1321), *H. brasiliensis* (LPF1394) and T. cacao (LPF1329) ware separated into a well-supported subclade with other isolates from the same host. The MAT2 gene data matrix consisted of 47 taxa,1109 characters including gaps, of which 840 were conserved, 269 variables, 43 parsimony-informative, and 226 singletons. In this analysis, the positioning of the isolates was the same observed for the MAT1 tree (Supplementary Figure S3). Likewise, isolates of *C. guianensis* were positioned in a separate subclade. The TEF-1α sequence matrix consisted of 36 taxa, 1387 characters including gaps, of which 1273 were conserved, 105 variables, 28 parsimony-informative, and 75 singletons (Supplementary Figure S4). The TEF-1α gene was also able to distinguish *C. cacaofunesta* from *C. fimbriata* even as the MAT1 and MAT2 genes. The combined matrix (β-tubulin + TEF-1α + MAT1 + MAT2) successfully distinguished the two species of isolates utilized in this investigation (Figure 1).

Molecular karyotype and chromosomal polymorphism of *C. fimbriata* s.l.

Densitometric analysis of the bands separated by PFGE revealed that the 14 isolates of *C. fimbriata* obtained from different host plants and geographic origins in Brazil displayed remarkable differences in chromosomal profiles. Two conditions and several runs of electrophoresis were used to resolve the karyotypes and to obtain reliable banding profiles of the isolates. When program A was used for separation of small chromosomes, a band with size close to 2,200 Kbp (Figure 2a) was observed in all isolates analyzed, which indicated the upper limit for distinction from larger chromosomes. The estimated sizes of the small chromosomes varied from 1.2 to 1.8 Mbp (Figure 2a).

Running the genomic DNA under the conditions of program B, with considerably long switching intervals and low voltage, enabled the separation of all chromosomes in a single run. Under these conditions, polymorphism in number and size of the large chromosomes was also observed among isolates (Figure 2b). The isolates exhibited six to eight chromosomal bands with estimated sizes ranging from 2.7 to 6.0 Mbp (Table 2). The small chromosomes ≤ 1.8 Mbp observed in the electrophoretic profile obtained with program B were the same as those observed with program A (Figures 2a and b). However, program B was not able to reveal polymorphism in the size of these chromosomes. The molecular sizes of chromosomes larger than 2.7 Mbp were estimated by comparison with those of *S. pombe* and *A. nidulans*. Based on the two PFGE conditions utilized, it was concluded that the number of chromosome bands resolved ranged from seven to nine for the isolates analyzed. These results suggest that chromosomal rearrangements frequently occurred during the evolution of the *Ceratocystis* genomes.

Densitometric analysis of the gels showed that the relative intensity of ultraviolet fluorescence was higher for some bands (Figure 3). These results suggested that each of these brighter bands represent at least two chromosomes, which could be homologous or heterologous chromosomes of similar sizes.

A schematic representation of the band profiles was generated in order to facilitate karyotype visualization and comparison among all isolates of the *C. fimbriata* complex analyzed (Figure 4). No chromosomal band was common to all isolates. Nonetheless, a set of three bands of similar sizes, ranging from 3.7 to 4.3 Mbp, were observed in several isolates; the same occurred with the two bands of intermediate sizes between 2.7 and 3.1 Mbp (Figure 4, arrows). Interestingly, the electrophoretic karyotypes of the two isolates from *G. arborea* were the same, while those from *T. grandis* and *Eucalyptus* sp. exhibited differences in the sizes of the small chromosomes.

Estimated genome sizes

The minimum sizes of the genomes were estimated as the sum of the individual chromosomal bands. The minimum genome sizes of the *C. fimbriata* isolates varied from 26.0 to 35.1 Mbp. The smallest size was observed for an isolate obtained from *F. carica* and the largest for an isolate from *A. deliciosa*. These estimated genome sizes are within a range that has been estimated for diverse *Ceratocystis* isolates using whole-genome sequencing (Figure 5).

Genetic variation based on REMAP

Based on the banding pattern obtained with REMAP, the number of well-defined amplicons varied from seven to ten depending on the isolate. A total of 13 fragments, with sizes varying from 300 and 2,000 bp, were amplified and showed high reproducibility, seven (53%) of which were polymorphic (Supplementary Figure S5). A UPGMA dendrogram based on the seven polymorphic loci showed eight clusters; five of these clusters were each formed by isolates from the same host (Figure 6). The only isolate of *C. cacaofunesta* grouped in the same cluster as those of *C. fimbriata* isolates from *H. brasiliensis*, *Eucalyptus* sp. and *C. brasiliense*. Isolates LPF1321 and LPF1323 from *G. arborea* grouped together in a single cluster. Isolates LPF1594 and LPF2199 from *T. grandis* also grouped together, but in the same cluster as isolates from *M. indica* and *Eucalyptus* sp.

DISCUSSION

The results of the phylogenetic analysis based on concatenated matrix (β-tubulin + TEF-1α + MAT1 + MAT2) sequences support the conclusion that the 14 isolates analyzed in the study belong to the *C. fimbriata* species complex. Despite being isolated from different hosts, they are closely related to reference isolates from sweet potato (type isolate), classified as *C. fimbriata* (Halsted, 1890). The reference isolates of *C. cacaofunesta* and *C. fimbriata* remained in distinct subclades well supported (BS > 75; PP > 0.8). Separation of *C. cacaofunesta* has been achieved in phylogenetic analysis of the *C. fimbriata* complex using the housekeeping genes β-tubulin and TEF-1α (Fourie et al., 2014) as well as mating-type genes (*MAT1-1-2* and *MAT1-2-1*) (Harrington et al., 2014). Our results exhibited a considerable intraspecific variation among the isolates analyzed, some of which were clustered based on their hosts. It is well known that *C. fimbriata* to have substantial genetic variability, which has already been associated with hosts and geographical origin (Ferreira et al., 2010; Oliveira et al., 2015b). *Ceratocystis cacaofunesta* is considered a distinct species within the *C. fimbriata* complex due to host specialization, infecting exclusively *T. cacao* plants in the Upper Amazon, and are not interfertile with tester strains of *C. fimbriata* from Brazil and elsewhere (Baker et al., 2003; Engelbrecht and Harrington, 2005; Ferreira et al., 2010). Physiological specialization was also confirmed for a population of *C. fimbriata* isolates from *C. guianensis*, however mating studies showed that they were interfertile with the sweet potato type, on which the species name is based and therefore it was named as *C. fimbriata* f. sp. *carapa* (Valdetaro et al., 2019).

The electrophoretic karyotype of the 14 isolates, determined using two different PFGE running conditions, varied considerably. These isolates exhibited 7-9 chromosomal bands with estimated sizes between 1.2 to 6.0 Mbp, with at least one chromosome smaller than 1.8 Mbp. Most isolates showed a unique karyotype, except for the two isolates obtained from *G. arborea* (collected in the same geographic region), whose karyotypes were identical. It is noteworthy that other isolates obtained from the same host (LPF2199 and LPF1594 from *T. grandis* and LPF1912 and LPF1611 from *Eucalyptus* sp.) possess identical complements of chromosomes larger than 2.2 Mbp, suggesting that high variability occurs when small chromosomes are considered. The number of chromosomes of the *C. fimbriata* isolates is relatively small when compared to the karyotypes previously described for other fungi. For instance, *Zymoseptoria tritici* (=*Mycosphaerella graminicola*)(Mehrabi et al., 2007), *Fusarium solani* (Suga et al., 2002), *Cochliobolus heterostrophus* (=*Bipolaris maydis*) (Tzeng et al. 1992) and *Colletotrichum lindemuthianum* (O'Sullivan et al., 1998) have 21, 12, 16 and 12 chromosomes, respectively.

The first linkage map for *C. fimbriata* and *C. manginecas*, considered a lineage within *C. fimbriata* complex (Oliveira et al., 2015b), was recently revealed in a study to map genes linked with mycelial growth rate and aggressiveness using both whole-genome sequencing and QTLs of SNPS (Fourie et al., 2019). The authors confirmed the presence of nine linkage groups (LG) in this study, with sizes ranging from 5.4 to 1.1 Mbp, providing the first indication of the number of putative chromosomes in the species. However, only the LPF1682 isolate of *A. deliciosa* exhibited the presence of 9 chromosomes. A reduced number of chromosomes found in our study might represent a genetic variation that occurs in the population of *C. fimbriata* isolates because the total of the bands resulted in a very near value for those isolates who had their genome sequenced. The minimum haploid genome size of each isolate was calculated by summing the sizes of the individual chromosomal bands observed with PFGE. Based on whole-genome sequencing, the genome sizes of *C. fimbriata* isolates CMW 15049 from *I. batatas*, LPF1912 from *Eucalyptus* sp. and isolate C1593 of *C. cacaofunesta* from *T. cacao* were estimated to be 28.1, 31.8, and 30.5 Mbp, respectively (Kanzi et al., 2020; Molano et al., 2018; Santos et al., 2020). In the present study, the minimum genome size of isolate LPF1912 was estimated by PFGE as 32.7 Mbp. Nonetheless, the estimated genome size using PFGE is not as accurate as that estimated by whole-genome sequencing. Recently, the genome of *C. guianensis* isolate LPF1560 was sequenced, and its size was estimated to be 28.9 Mbp (unpublished data), similar to the sum of bands which was 29.0 Mbp. Similarly, the sum of the chromosome sizes of isolate LPF1329 of *C. cacaofunesta* studied here was 29.5 Mbp whereas that of isolate C1593 whose whole-genome was sequenced was estimated as 30.5 Mbp. In addition to the use of different techniques, this genome size variation may also be related to the use of different isolates, since chromosomal variation can occur between isolates of the same species, as demonstrated in this study.

Variations in chromosome length and number are common in natural populations of plant pathogenic fungi. These variations result from chromosomal rearrangements that can be mediated by mechanisms as diverse as meiotic recombination, double-stranded breaks (DSBs) which trigger (Fourie et al., 2015) DNA repair processes, and TEs (Mehrabi et al., 2017; Möller and Stukenbrock, 2017). The *C. fimbriata* sexual cycle has been elucidated (Webster and Butler, 1967) and the breaking and fusion of DNA strands between non-sister chromatids as a result of crossing-over during recombination may be a factor that generate the karyotypic variation observed among isolates of this species (McClintock, 1941; Mehrabi et al., 2017). It is known that recombination between homologous chromosomes of different sizes can result in new karyotype variants (Perkins, 1997).

Repetitive elements in the *C. fimbriata* genome can also potentially mediate recombination and cause chromosomal rearrangements. During meiosis, pairing of repeat sequences resulting from transposon insertions on different chromosomes may lead to translocations and chromosome length polymorphisms (Wittenberg et al., 2009). In addition, deletions of DNA fragments located between repetitive sequences may be the result of intrachromosomal mitotic recombination, which occurs during crossing over between two repeat sequences on the same chromosome. Recently, large structural rearrangements in the genomes of *C. fimbriata* isolate CMW14799 from *I. batatas* and *C. manginecans* isolates CMW46461 and CMW22563 from *Acacia mangium* and CMW17570 from *Prosopis cineraria*, were evidenced using Illumina and Oxford Nanopore sequencing technologies. Based on sequence alignment and split reads, chromosomal rearrangements, including inversions within chromosomes and reciprocal translocations between different chromosomes, were identified. A high content of TEs was found (between 13 and 20% of the total genome) in both species, which acted in insertions/deletions of unique genomic segments as well as in rearrangements of chromosomes (Fourie et al., 2020).

As expected, the present study revealed that the *C. fimbriata* species complex displays extensive polymorphisms in chromosome number and size. The presence of the small polymorphic chromosomes whose sizes ranged from 1.2 to 1.8 Mbp was demonstrated; we hypothesized that they could be supernumerary chromosomes. Several plant pathogenic fungi have isolate-specific chromosomes, which are highly variable within and among species and have been referred to as conditionally dispensable (CD), supernumerary, lineage-specific (LS), accessory or B chromosomes to differentiate them from the core chromosomes that are shared among all members of a species (Covert, 1998; Croll and McDonald, 2012). Supernumerary chromosomes are characterized by their lower gene density and G+C content, abundance of repetitive sequences (Coleman et al., 2009; Feurtey et al., 2020) and presence of genes that encode specific virulence determinants in some fungal species. Despite they are variable in size, they tend to be smaller than core-chromosomes ranging from ~400 kb to 3 Mb in plant pathogenic fungi (Bertazzoni et al., 2018; Covert, 1998). For instance, in the plant-pathogenic fungi *Nectria haematococca* (= *Fusarium solani*) (Coleman et al., 2009) and *Alternaria alternata* (Wang et al., 2019) supernumerary (polymorphic) chromosomes with sizes ranging from 1.57-0.56 and 1.0-2.0 Mbp, respectively, conferring host-specific virulence have been reported. Also, supernumerary chromosome LS14 found in isolates of *Fusarium oxysporum* f. sp. *lycopersici*, harbors genes that contribute to pathogenicity by encoding small effector proteins that are secreted to the xylem sap of infected tomato plants; strains whose LS14 chromosome was deleted displayed complete loss of pathogenicity (Vlaardingerbroek et al., 2016). Many effector genes of plant-pathogenic fungi have been found inserted in genomic regions rich in repeat sequences and TEs (Langner et al., 2021). Recently, a repertoire of effector genes was predicted to be encoded in the *C. fimbriata* and *C. manginecans* genomes (Fourie et al., 2020). These genes were not overrepresented in specific supercontigs of the genome assemblies, but were specifically close to putative sub-telomeric extremities with high TE density. Therefore, prediction studies must be combined with higher resolution sequencing and *in situ* gene mapping approaches in order to determine more conclusively the chromosomal locations of these *C. fimbriata* putative effector genes.

Knowledge about the processes underlying gain or loss of supernumerary chromosomes in fungi is limited. In *Z. tritici*, it was observed that the accessory chromosomes undergo significant structural rearrangements, including fusions and large insertions. In addition, segregation of some supernumerary chromosomes was distorted, with nondisjunction during meiosis leading to their frequent loss (Croll et al., 2013). In *S. cerevisiae*, duplication of large chromosomal fragments and fusion between sequences from two different chromosomes occasionally result in the formation of supernumerary chromosomes that are highly unstable during mitosis (Koszul et al., 2006). Horizontal transfer of entire supernumerary chromosomes between pathogenic and non-pathogenic *Fusarium* species has also been demonstrated (Ma et al., 2010).

Since TEs may be involved in chromosomal rearrangements, REMAP was used to investigate the genetic variability of the isolates whose karyotype had been defined by PFGE. The REMAP-based cluster analysis revealed that the studied isolates exhibited high genetic variability; eight clusters formed when only 14 isolates were interrogated. Even though isolates from the same host (*T. grandis* and *G. arborea*) tend to cluster together, those obtained from *Eucalyptus* were separated into different clusters. Previously, investigation of a *C. fimbriata* population with SSR markers showed low genetic variability, but the isolates grouped according to host source and geographic origin (Ferreira et al., 2010; Oliveira et al., 2015b; Oliveira et al., 2021, 2018). However, the small number of isolates analyzed here limits the possibility to draw clear conclusions on the usefulness of REMAP to access the genetic variability of *C. fimbriata*. Further studies with larger *C. fimbriata* populations are required to determine whether clustering associated with host source and geographic origin is observed using REMAP. Nonetheless, the genetic variability observed with REMAP raises the possibility that chromosomal rearrangements in *C. fimbriata* may be caused by mechanisms that involve the presence of multiple copies of retrotransposons. This interpretation is supported by the finding that 1.19% of the genome of isolate LPF1912 from Eucalyptus sp. is comprised of LTR-type retrotransposons as estimated by whole-genome sequencing (Santos et al., 2020). Furthermore, Fourie et al. (2020) found that most TEs present in the genome of *C. fimbriata* (CMW14799) and *C. manginecans* (CMW46461, CMW22563, CMW17570) belong to Class I (retrotransposons).

In this work, we report the chromosomal polymorphism of a Brazilian population of the *C. fimbriata* species complex using molecular karyotyping. Nonetheless, extensive karyotype analysis of a larger number of isolates, including some from the Latin American, North American, Asian-Australian and African clades is desirable to gain a more comprehensive picture of the extent of such a polymorphism. Interrogation of the *C. fimbriata* genome with REMAP indicated that this marker has potential for use in research aimed at understanding the TE-associated genetic variability, which may provide important insights into the mechanisms underlying chromosomal rearrangements. Our results provide new perspectives about the genome architecture of the *C. fimbriata* species complex. Future investigation using technology that allows sequencing of individual chromosomes could provide crucial information to elucidate the role of chromosomal polymorphisms and supernumerary chromosomes for the biology of the *C. fimbriata* species complex, including its plant pathogenicity.

CREDIT AUTHORSHIP CONTRIBUTIONS STATEMENT

Fernando Montezano Fernandes: Conceptualization, Methodology, Validation, Formal analysis, Investigation, Writing - Original Draft. **Marisa Vieira de Queiroz:** Conceptualization, Methodology, Resources, Writing - Review & Editing, Supervision, Project administration. **Daiana Maria Queiroz Azevedo:** Conceptualization, Methodology, Formal analysis, Investigation. **Leandro Lopes da Silva:** Conceptualization, Methodology, Formal analysis, Investigation. **Jorge Luis Badel**: Conceptualization, Writing - Review & Editing. **Acelino Couto Alfenas**: Conceptualization, Resources, Writing - Review & Editing, Supervision, Project administration, Funding acquisition.

DECLARATION OF COMPETING INTEREST

The authors report no declarations of interest.

ACKNOWLEDGMENTS

The authors thank to Coordenação de Aperfeiçoamento de Pessoal de Nível Superior (CAPES) for a fellowship granted to first the author. For Fundação de Amparo à Pesquisa do Estado de Minas Gerais (FAPEMIG) and Conselho Nacional de Desenvolvimento Científico e Tecnológico (CNPq). This study was financed in part by the Coordenação de Aperfeiçoamento de Pessoal de Nível Superior - Brasil (CAPES) - Finance Code 001. We are also grateful for the technical and scientific support offered by Dra. Patrícia Pereira Fontes.

REFERENCES

Albuquerque, F.C., Duarte, M.L.R., Silva, H.M., 1972. Ocorrência do mofo cinzento (*Ceratocystis fimbriata*) da seringueira. Semin. Nac. da Sering. 125–128.

Baker, C.J., Harrington, T.C., Krauss, U., Alfenas, A.C., 2003. Genetic variability and host specialization in the Latin American Clade of *Ceratocystis fimbriata*. Ecol. Popul. Biol. 93, 1274–1284. https://doi.org/10.1094/PHYTO.2003.93.10.1274.

Bertazzoni, S., Williams, A.H., Jones, D.A., Syme, R.A., Tan, K.-C., Hane, J.K., 2018. Accessories Make the Outfit: Accessory Chromosomes and Other Dispensable DNA Regions in Plant-Pathogenic Fungi. Mol. Plant-Microbe Interact. 31, 779–788. https://doi.org/10.1094/MPMI-06-17-0135-FI

Brody, H., Carbon, J., 1989. Electrophoretic karyotype of *Aspergillus nidulans*. Proc. Nati. Acad. Sci. USA 86, 6260–6263. https://doi.org/10.1073/pnas.86.16.6260

Carvalho, M.B., 1938. Sobre dois insetos nocivos à mangueira. Bol. da Secr. da Agric. Indústria e Comércio 130–132.

Coleman, J.J., Rounsley, S.D., Rodriguez-Carres, M., Kuo, A., Wasmann, C.C., Grimwood, J., Schmutz, J., Taga, M., White, G.J., Zhou, S., Schwartz, D.C., Freitag, M., Ma, L., Danchin, E.G.J., Henrissat, B., Coutinho, P.M., Nelson, D.R., Straney, D., Napoli, C.A., Barker, B.M., Gribskov, M., Rep, M., Kroken, S., Molnár, I., Rensing, C., Kennell, J.C., Zamora, J., Farman, M.L., Selker, E.U., Salamov, A., Shapiro, H., Pangilinan, J., Lindquist, E., Lamers, C., Grigoriev, I. V., Geiser, D.M., Covert, S.F., Temporini, E., VanEtten, H.D., 2009. The Genome of *Nectria haematococca*: contribution of supernumerary chromosomes to gene expansion. PLoS Genet. 5, e1000618. https://doi.org/10.1371/journal.pgen.1000618

Covert, S.F., 1998. Supernumerary chromosomes in filamentous fungi. Curr. Genet. 33, 311–319. https://doi.org/10.1007/s002940050342

Croll, D., McDonald, B.A., 2012. The accessory genome as a cradle for adaptive evolution in pathogens. PLoS Pathog. 8, e1002608. https://doi.org/10.1371/journal.ppat.1002608

Croll, D., Zala, M., McDonald, B.A., 2013. Breakage-fusion-bridge cycles and large insertions contribute to the rapid evolution of accessory chromosomes in a fungal pathogen. PLoS Genet. 9. https://doi.org/10.1371/journal.pgen.1003567

Daboussi, M.J., Capy, P., 2003. Transposable elements in filamentous fungi. Annu. Rev. Microbiol. 57, 275–299. https://doi.org/10.1146/annurev.micro.57.030502.091029

DeScenzo, R.A., Harrington, T.C., 1994. Use of (CAT)5 as a DNA fingerprinting probe for fungi. Phytopathology 84, 534–540. https://doi.org/10.1094/Phyto-84-534

Dice, L.R., 1945. Measures of the amount of ecologic association between species. Ecology 26, 297–302. https://doi.org/10.2307/1932409

Edgar, R.C., 2004. MUSCLE: multiple sequence alignment with high accuracy and high throughput. Nucleic Acids Res. 32, 1792–1797. https://doi.org/10.1093/NAR/GKH340

Engelbrecht, C.J.B., Harrington, T.C., 2005. Intersterility, morphology and taxonomy of *Ceratocystis fimbriata* on sweet potato, cacao and sycamore. Mycologia 97, 57–69. https://doi.org/10.3852/mycologia.97.1.57

Engelbrecht, C.J.B., Harrington, T.C., Alfenas, A.C., Suarez, C., 2007. Genetic variation in populations of the cacao wilt pathogen, *Ceratocystis cacaofunesta*. Plant Pathol. 56, 923–933. https://doi.org/10.1111/j.1365-3059.2007.01735.x

Fawley, W.N., Wilcox, M.H., 2002. Pulsed-field gel electrophoresis can yield DNA fingerprints of degradation-susceptible *Clostridium difficile* strains. J. Clin. Microbiol. 40, 3546–3547. https://doi.org/10.1128/JCM.40.9.3546-3547.2002

Ferreira, E.M., Harrington, T.C., Thorpe, D.J., Alfenas, A.C., 2010. Genetic diversity and interfertility among highly differentiated populations of *Ceratocystis fimbriata* in Brazil.

Plant Pathol. 59, 721–735. https://doi.org/10.1111/j.1365-3059.2010.02275.x

Ferreira, F.A., Demuner, A.M., Demuner, N.L., Pigatto, S., 1999. Murcha de Ceratocystis em eucalipto no Brasil. Fitopatol. Bras. 24, 284.

Ferreira, F.A., Maffia, L.A., Barreto, R.W., Demuner, N.L., Pigatto, S., 2006. Sintomatologia da murcha de *Ceratocystis fimbriata* em eucalipto. Rev. Árvore 30, 155–162. https://doi.org///dx.doi.org/10.1590/S0100-67622006000200001

Ferreira, M.A., Harrington, T.C., Piveta, G., Alfenas, A.C., 2017. Genetic variability suggests that three populations of *Ceratocystis fimbriata* are responsible for the Ceratocystis wilt epidemic on kiwifruit in Brazil. Trop. Plant Pathol. 42, 86–95. https://doi.org/10.1007/s40858-017-0131-y

Feurtey, A., Lorrain, C., Croll, D., Eschenbrenner, C., Freitag, M., Habig, M., Haueisen, J., Möller, M., Schotanus, K., Stukenbrock, E.H., 2020. Genome compartmentalization predates species divergence in the plant pathogen genus *Zymoseptoria*. BMC Genomics 21, 588. https://doi.org/10.1186/s12864-020-06871-w

Firmino, A.C., Tozze Jr, H.J., Furtado, E.L., 2012. First report of *Ceratocystis fimbriata* causing wilt in *Tectona grandis* in Brazil. New Dis. Reports 25. https://doi.org/10.5197/j.2044-0588.2012.025.024

Fourie, A., de Jonge, R., van der Nest, M.A., Duong, T.A., Wingfield, M.J., Wingfield, B.D., Barnes, I., 2020. Genome comparisons suggest an association between *Ceratocystis* host adaptations and effector clusters in unique transposable element families. Fungal Genet. Biol. 143, 103433. https://doi.org/10.1016/j.fgb.2020.103433

Fourie, A., van der Nest, M.A., de Vos, L., Wingfield, M.J., Wingfield, B.D., Barnes, I., 2019. QTL mapping of mycelial growth and aggressiveness to distinct hosts in *Ceratocystis* pathogens. Fungal Genet. Biol. 131. https://doi.org/10.1016/j.fgb.2019.103242

Fourie, A., Wingfield, M.J., Wingfield, B.D., Barnes, I., 2015. Molecular markers delimit cryptic species in *Ceratocystis* sensu stricto. Mycol. Prog. 14, 1020. https://doi.org/10.1007/s11557-014-1020-0

Fourie, A., Wingfield, M.J., Wingfield, B.D., Barnes, I., 2014. Molecular markers delimit cryptic species in *Ceratocystis sensu stricto*. Mycol. Prog. 14, 1–18. https://doi.org/10.1007/S11557-014-1020-0

Glass, N.L., Donaldson, G.C., 1995. Development of primer sets designed for use with the PCR to amplify conserved genes from filamentous ascomycetes. Appl. Environ. Microbiol. 61, 1323–1330. https://doi.org/10.1128/AEM.61.4.1323-1330.1995.

Halfeld-Vieira, B.A., Zilli, J.E., Nechet, K.L., Pereira, G.M.D., Souza, G.R., 2012. First record of *Ceratocystis fimbriata* on *Carapa guianensis*. New Dis. Reports 26, 13. https://doi.org/10.5197/j.2044-0588.2012.026.013

Halsted, B.D., 1890. Some fungous diseases of the sweet potato. The black rot. New Jersey Agric. Exp. Stn. Bull. 76, 7–14.

Hammer, D.A.T., Ryan, P.D., Hammer, Ø., Harper, D.A.T., 2001. Past: paleontological statistics software package for education and data analysis. Palaeontol. Electron. 4, 178.

Harrington, T.C., 2007. The genus Ceratocystis. Where does the oak wilt fungus fit?, in: Billings, R.F., Appel, D.N. (Eds.), The Proceedings of the 2nd National Oak Wilt Symposium. Texas Forest Service, Austin, TX, p. 166.

Harrington, T.C., Kazmi, M.R., Al-Sadi, A.M., Ismail, S.I., 2014. Intraspecific and intragenomic variability of ITS rDNA sequences reveals taxonomic problems in *Ceratocystis fimbriata* sensu stricto. Mycologia 106, 224–242. https://doi.org/10.3852/13-189

Harrington, T.C., Thorpe, D.J., Alfenas, A.C., 2011. Genetic variation and variation in aggressiveness to native and exotic hosts among brazilian populations of *Ceratocystis fimbriata*. Popul. Biol. 101, 566. https://doi.org/10.1094/PHYTO-08-10-0228

Hepperle, D., 2004. SeqAssem©. A sequence analysis tool, contig assembler and trace data visualization tool for molecular sequences.

Hua-Van, A., Le Rouzic, A., Maisonhaute, C., Capy, P., 2005. Abundance, distribution and dynamics of retrotransposable elements and transposons: Similarities and differences. Cytogenet. Genome Res. 110, 426–440. https://doi.org/10.1159/000084975

Kalendar, R., Grob, T., Regina, M., Suoniemi, A., Schulman, A., 1999. IRAP and REMAP: two new retrotransposon-based DNA fingerprinting techniques. Theor. Appl. Genet. 98, 704–711. https://doi.org/10.1007/s001220051124

Kalendar, R., Muterko, A., Boronnikova, S., 2021. Retrotransposable Elements: DNA Fingerprinting and the Assessment of Genetic Diversity, in: Besse, P. (Ed.), Molecular Plant Taxonomy. Methods in Molecular Biology. Humana Press Inc., pp. 263–286. https://doi.org/10.1007/978-1-0716-0997-2_15

Kanzi, A.M., Trollip, C., Wingfield, M.J., Barnes, I., Van Der Nest, M.A., Wingfield, B.D., 2020. Phylogenomic incongruence in *Ceratocystis*: A clue to speciation? BMC Genomics 21, 362. https://doi.org/10.1186/s12864-020-6772-0

Koszul, R., Dujon, B., Fischer, G., 2006. Stability of large segmental duplications in the yeast genome. Genetics 172, 2211–2222. https://doi.org/10.1534/genetics.105.048058

Kumar, S., Stecher, G., Tamura, K., 2016. MEGA7: molecular evolutionary genetics analysis version 7.0 for bigger datasets. Mol. Biol. Evol. 33, 1870–1874. https://doi.org/10.1093/molbev/msw054

Langner, T., Harant, A., Gomez-Luciano, L.B., Shrestha, R.K., Malmgren, A., Latorre, S.M., Burbano, H.A., Win, J., Kamoun, S., 2021. Genomic rearrangements generate hypervariable mini-chromosomes in host-specific isolates of the blast fungus. PLoS Genet. 17. https://doi.org/10.1371/JOURNAL.PGEN.1009386

Larsson, A., 2014. AliView: a fast and lightweight alignment viewer and editor for large datasets. Bioinformatics 30, 3276–3278. https://doi.org/10.1093/BIOINFORMATICS/BTU531

Lazar, I., Horvath-Lazar, E., Lazar, I., 2010. Gel Analyzer 19.1 [WWW Document]. www.gelanalyzer.com. URL http://www.gelanalyzer.com/#section-citation (accessed 5.18.21).

Liu, F.F., Barnes, I., Roux, J., Wingfield, M.J., Chen, S.F., 2018. Molecular phylogenetics and microsatellite analysis reveal a new pathogenic *Ceratocystis* species in the Asian-Australian clade. Plant Pathol. 67, 1097–1113. https://doi.org/10.1111/ppa.12820

Ma, L.J., Van Der Does, H.C., Borkovich, K.A., Coleman, J.J., Daboussi, M.J., Di Pietro, A., Dufresne, M., Freitag, M., Grabherr, M., Henrissat, B., Houterman, P.M., Kang, S., Shim, W.B., Woloshuk, C., Xie, X., Xu, J.R., Antoniw, J., Baker, S.E., Bluhm, B.H., Breakspear, A., Brown, D.W., Butchko, R.A.E., Chapman, S., Coulson, R., Coutinho, P.M., Danchin, E.G.J., Diener, A., Gale, L.R., Gardiner, D.M., Goff, S., Hammond-Kosack, K.E., Hilburn, K., Hua-Van, A., Jonkers, W., Kazan, K., Kodira, C.D., Koehrsen, M., Kumar, L., Lee, Y.H., Li, L., Manners, J.M., Miranda-Saavedra, D., Mukherjee, M., Park, G., Park, J., Park, S.Y., Proctor, R.H., Regev, A., Ruiz-Roldan, M.C., Sain, D., Sakthikumar, S., Sykes, S., Schwartz, D.C., Turgeon, B.G., Wapinski, I., Yoder, O., Young, S., Zeng, Q., Zhou, S., Galagan, J., Cuomo, C.A., Kistler, H.C., Rep, M., 2010. Comparative genomics reveals mobile pathogenicity chromosomes in *Fusarium*. Nature 464, 367–373. https://doi.org/10.1038/nature08850

McClintock, B., 1941. The stability of broken ends of chromosomes in *Zea mays*. Genetics 26, 234–82.

Mehrabi, R., Mirzadi Gohari, A., Kema, G.H.J., 2017. Karyotype variability in plant-pathogenic fungi. Annu. Rev. Phytopathol. 55, 483–503. https://doi.org/10.1146/annurev-phyto-080615-095928

Mehrabi, R., Taga, M., Kema, G.H.J., 2007. Electrophoretic and cytological karyotyping of the foliar wheat pathogen *Mycosphaerella graminicola* reveals many chromosomes with a large size range. Mycologia 99, 868–876. https://doi.org/10.1080/15572536.2007.11832518

Miller, M.A., Pfeiffer, W., Schwartz, T., 2010. Creating the CIPRES Science Gateway for inference of large phylogenetic trees, in: Proceedings of the Gateway Computing Environments Workshop (GCE). New Orleans, pp. 1–8. https://doi.org/10.1109/GCE.2010.5676129

Molano, E.P.L., Cabrera, O.G., Jose, J., do Nascimento, L.C., Carazzolle, M.F., Teixeira, P.J.P.L., Alvarez, J.C., Tiburcio, R.A., Tokimatu Filho, P.M., de Lima, G.M.A., Guido, R.V.C., Corrêa, T.L.R., Leme, A.F.P., Mieczkowski, P., Pereira, G.A.G., 2018. *Ceratocystis cacaofunesta* genome analysis reveals a large expansion of extracellular phosphatidylinositol-specific phospholipase-C genes (PI-PLC). BMC Genomics 19. https://doi.org/10.1186/s12864-018-4440-4

Möller, M., Stukenbrock, E.H., 2017. Evolution and genome architecture in fungal plant pathogens. Nat. Rev. Microbiol. 15, 756–771. https://doi.org/10.1038/nrmicro.2017.76

Muchovej, J.J., Albuquerque, F.C., Ribeiro, G.T., 1978. *Genelina arborea* a new host of *Ceratocystis fimbriata*. Plant Dis. 62, 717–719.

Muszewska, A., Steczkiewicz, K., Stepniewska-Dziubinska, M., Ginalski, K., 2019. Transposable elements contribute to fungal genes and impact fungal lifestyle. Sci. Rep. 9. https://doi.org/10.1038/s41598-019-40965-0

O’Sullivan, D., Tosi, P., Creusot, F., Cooke, M., Phan, T.H., Dron, M., Langin, T., 1998. Variation in genome organization of the plant pathogenic fungus *Colletotrichum* *lindemuthianum*. Curr. Genet. 33, 291–298. https://doi.org/10.1007/s002940050339

Oliveira, L.S.S., Damacena, M.B., Guimarães, L.M.S., Siqueira, D.L., Alfenas, A.C., 2016. *Ceratocystis fimbriata* isolates on *Mangifera indica* have different levels of aggressiveness. Eur. J. Plant Pathol. 145, 847–856. https://doi.org/10.1007/s10658-016-0873-2

Oliveira, L.S.S., Guimarães, L.M.S., Ferreira, M.A., Nunes, A.S., Pimenta, L.V.A., Alfenas, A.C., 2015a. Aggressiveness, cultural characteristics and genetic variation of *Ceratocystis fimbriata* on *Eucalyptus* spp. For. Pathol. 45, 505–514. https://doi.org/10.1111/efp.12200

Oliveira, L.S.S., Harrington, T.., Ferreira, M.A., Damacena, M.B., Al-Sadi, A.M., Al-Mahmooli, I.H.., Alfenas, A.C., 2015b. Species or genotypes? Reassessment of four recently described species of the ceratocystis wilt pathogen, *Ceratocystis fimbriata*, on *Mangifera indica*. Phytopathology 105, 1229–1244. https://doi.org/10.1094/PHYTO-03-15-0065-R

Oliveira, L.S.S., Harrington, T.C., Ferreira, M.A., Freitas, R.G., Alfenas, A.C., 2018. Populations of *Ceratocystis fimbriata* on *Colocasia esculenta* and other hosts in the Mata Atlântica region in Brazil. Plant Pathol. 67, 97–106. https://doi.org/10.1111/ppa.12706

Oliveira, L.S.S., Pimenta, L.V.A., Guimarães, L.M.S., Souza, P.V.D., Bhering, L.L., Alfenas, A.C., 2021. Resistance of kiwifruit cultivars to ceratocystis wilt: An approach considering the genetic diversity and variation in aggressiveness of the pathogen. Plant Pathol. 70, 349–357. https://doi.org/10.1111/ppa.13305

Perkins, D.D., 1997. Chromosome rearrangements in Neurospora and other filamentous fungi, in: Hall, J.C., Dunlap, J.C., Friedmann, T., Giannelli, F. (Eds.), Advances in Genetics. Academic Press Inc., pp. 239–398. https://doi.org/10.1016/S0065-2660(08)60311-9

Piveta, G., Alfenas, A.C., Muniz, M. de F.B., Valdebenito-Sanhueza, R.M., Ferreira, M.A., 2013. Ocorrência de Ceratocystis fimbriata em kiwi (*Actinidia deliciosa*) no Sul do Brasil.

Rev. Bras. Frutic. 35, 665–669. https://doi.org/10.1590/S0100-29452013000200040

Queiroz, M. V., Pizzirani-Kleiner, A.A., Azevedo, J.L., 2000. Electrophoretic characterization of *Aspergillus nidulans* strains with chromosomal duplications. Genet. Mol. Biol. 23, 293–297. https://doi.org/10.1590/s1415-47572000000200009

Rambaut, A., Drummond, A., 2018. FigTree [WWW Document]. URL http://tree.bio.ed.ac.uk/software/figtree/ (accessed 8.11.21).

Rincones, J., Mazotti, G.D., Griffith, G.W., Pomela, A., Figueira, A., Leal, G.A., Queiroz, M. V., Pereira, J.F., Azevedo, R.A., Pereira, G.A.G., Meinhardt, L.W., 2006. Genetic variability and chromosome-length polymorphisms of the witches' broom pathogen *Crinipellis perniciosa* from various plant hosts in South America. Mycol. Res. 110, 821–832.

Rohde, W., 1996. Inverse sequence-tagged repeat (ISTR) analysis. A novel and universal PCR (polymerase chain reaction)-based technique for genome analysis in the plant and animal kingdom. J. Genet. Breed. 50, 249–261.

Roux, J., Harrington, T.C., Steimel, J.P., Wingfield, M.J., 2001. Genetic variation in the wattle wilt pathogen *Ceratocystis albofundus*. Mycoscience 42, 327–332. https://doi.org/10.1007/BF02461214

Santana, M.F., Araújo, E.F., Souza, J.T., Mizubuti, E.S.G., Queiroz, M.V., 2012. Development of molecular markers based on retrotransposons for the analysis of genetic variability in *Moniliophthora perniciosa*. Eur. J. Plant Pathol. 134, 497–507. https://doi.org/10.1007/s10658-012-0031-4

Santos, L.V., Queiroz, M.V., Santana, M.F., Soares, M.A., Barros, E.G., Araújo, E.F., Langin, T., 2012. Development of new molecular markers for the *Colletotrichum* genus using RetroCl1 sequences. World J. Microbiol. Biotechnol. 28, 1087–1095. https://doi.org/10.1007/s11274-011-0909-x

Santos, S.A., Vidigal, P.M.P., Thrimawithana, A., Betancourth, B.M.L., Guimarães, L.M.S., Templeton, M.D., Alfenas, A.C., 2020. Comparative genomic and transcriptomic analyses reveal different pathogenicity-related genes among three eucalyptus fungal pathogens. Fungal Genet. Biol. 137. https://doi.org/10.1016/j.fgb.2019.103332

Schulman, A.H., 2007. Molecular markers to assess genetic diversity. Euphytica 158, 313–321. https://doi.org/10.1007/s10681-006-9282-5

Schwarts, D.C., Cantor, C.R., 1984. Separation of yeast chromosome-sized DNAs by pulsed field gradient gel electrophoresis. Cell 37, 67–75. https://doi.org/10.1016/0092-8674(84)90301-5.

Silva, A.C., Betancourth, B.M.L., Ferreira, D.C., Elerati, T.L., Rodrigues, F., Alfenas, A.C., 2020. Responses of resistant and susceptible hybrid clones of *Eucalyptus urophylla* × *Eucalyptus grandis* to infection by *Ceratocystis fimbriata*. Ann. For. Sci. 77, 1–19. https://doi.org/10.1007/s13595-020-00932-6

Silva, A.C., Cândido, T.S., Sales, N.L.P., Harrington, T.C., Alfenas, A.C., 2017. First report of ceratocystis wilt caused by *Ceratocystis fimbriata* on *Caryocar brasiliense* trees in Brazil. Plant Dis. 101, 1822. https://doi.org/10.1094/PDIS-03-17-0376-PDN

Silveira, S.F., Harrington, T.C., Mussi-Dias, V., Engelbrecht, C.J.B., Alfenas, A.C., Silva, C.R., 2006. *Annona squamosa*, a new host of *Ceratocystis fimbriata*. Fitopatol. Bras. 31, 394–397. https://doi.org/10.1590/S0100-41582006000400010

Specht, C.A., DrRusso, C.C., Novotny, C.P., Ullrich, R., 1982. A method for extracting high-molecular-weight deoxyribonucleic acid from fungi. Anal. Biochem. 119, 158–163. https://doi.org/doi.org/10.1016/0003-2697(82)90680-7

Stamatakis, A., 2014. RAxML version 8: a tool for phylogenetic analysis and post-analysis of large phylogenies. Bioinformatics 30, 1312–1313.

https://doi.org/10.1093/BIOINFORMATICS/BTU033

Steimel, J., Engelbrecht, C.J.B., Harrington, T.C., 2004. Development and characterization of microsatellite markers for the fungus *Ceratocystis fimbriata*. Mol. Ecol. Notes 4, 215–218. https://doi.org/10.1111/j.1471-8286.2004.00621.x

Suga, H., Ikeda, S., Taga, M., Kageyama, K., Hyakumachi, M., 2002. Electrophoretic karyotyping and gene mapping of seven formae speciales in *Fusarium solani*. Curr. Genet. 41, 254–260. https://doi.org/10.1007/s00294-002-0303-1

Teixeira, J.A., Gonçalves, D.B., de Queiroz, M. V., De Araújo, E.F., 2011. Improved pectinase production in *Penicillium griseoroseum* recombinant strains. J. Appl. Microbiol. 111, 818–825. https://doi.org/10.1111/j.1365-2672.2011.05099.x

Valarini, P.J., Tokeshi, H., 1980. *Ceratocystis fimbriata*, causal agent of fig dieback, and its control. Summa Phytopathol. 6, 102–106.

Valdetaro, D.C.O.F., Harrington, T.C., Oliveira, L.S.S., Guimarães, L.M.S., McNew, D.L., Pimenta, L.V.A., Gonçalves, R.C., Schurt, D.A., Alfenas, A.C., 2019. A host specialized form of *Ceratocystis fimbriata* causes seed and seedling blight on native *Carapa guianensis* (andiroba) in Amazonian rainforests. Fungal Biol. 123, 170–182. https://doi.org/10.1016/j.funbio.2018.12.001

Valdetaro, D.C.O.F., Oliveira, L.S.S., Guimarães, L.M.S., Harrington, T.C., Ferreira, M.A., Freitas, R.G., Alfenas, A.C., 2015. Genetic variation, morphology and pathogenicity of *Ceratocystis fimbriata* on *Hevea brasiliensis* in Brazil. Trop. Plant Pathol. 40, 184–192. https://doi.org/10.1007/s40858-015-0036-6

Vlaardingerbroek, I., Beerens, B., Schmidt, S.M., Cornelissen, B.J.C., Rep, M., 2016. Dispensable chromosomes in *Fusarium oxysporum* f. sp. *lycopersici*. Mol. Plant Pathol. 17, 1455–1466. https://doi.org/10.1111/mpp.12440

Wang, M., Fu, H., Shen, X., Ruan, R., Rokas, A., Li, H., 2019. Genomic features and evolution of the conditionally dispensable chromosome in the tangerine pathotype of *Alternaria alternata*. Mol. Plant Pathol. 20, 1425–1438. https://doi.org/10.1111/mpp.12848

Webster, R.K., Butler, E.E., 1967. The Origin of Self-Sterile, Cross-Fertile Strains and Culture Sterility in *Ceratocystis fimbriata*. Mycologia 59, 212. https://doi.org/doi.org/10.1080/00275514.1967.12018411

Wieloch, W., 2006. Chromosome visualisation in filamentous fungi. J. Microbiol. Methods 67, 1–8. https://doi.org/10.1016/j.mimet.2006.05.022.

Wittenberg, A.H.J., van der Lee, T.A.J., M'Barek, S. Ben, Ware, S.B., Goodwin, S.B., Kilian, A., Visser, R.G.F., Kema, G.H.J., Schouten, H.J., 2009. Meiosis drives extraordinary genome plasticity in the haploid fungal plant pathogen *Mycosphaerella graminicola*. PLoS One 4. https://doi.org/10.1371/journal.pone.0005863

Zolan, M.E., 1995. Chromosome-length polymorphism in fungi. Microbiol. Rev. 59, 686–698.

Table 1. Host sources, species, geographic origins, and GenBank accession numbers of *Ceratocystis fimbriata* s.l. isolates used in this study.

Species	**Hosts**	**LPF code**	**Other code**	**Geographic origin**	**GenBank accessions**			
					β-tubulin	**TEF-1α**	***MAT1***	***MAT2***
C. fimbriata	*Acacia mearnsii*	-	C1181	South African	-	-	-	-
		-	C2042	Paraná, Brazil	-	-	-	-
	Actinidia deliciosa	LPF1424	CF261, PC03	Rio Grande do Sul, Brazil	-	-	-	-
		LPF1443	CF280, PG01	Rio Grande do Sul, Brazil	-	-	-	-
		LPF1465	CF302, PM20	Rio Grande do Sul, Brazil	-	-	MF347680	MF347678
		LPF1682*	A32	Rio Grande do Sul, Brazil	-	-	-	-
	Annona squamosa	LPF1331*	CF011, C1592	Rio de Janeiro, Brazil	-	-	-	-
	Caryocar brasiliensis	LPF1489*	-Pequi1	Minas Gerais, Brazil	-	-	-	-
	Colocasia esculenta	-	C1865	Rio de Janeiro, Brazil				
		-	C1905	São Paulo, Brazil			KF482989	
		-	C1926	São Paulo, Brazil				
	Eucalyptus spp.	LPF1611*	VER11	Bahia, Brazil	-	-	-	-
		LPF1640	TL3	Mato Grosso do Sul, Brazil	-	-	-	-
		LPF1912*	SBS-1	Bahia, Brazil	-	-	-	-
		-	C1985	Bahia,	-	-	-	-

			Brazil				
	-	C1987	Paraná, Brazil	-	-	-	-
Ficus carica	LPF1336*	CF016, C1782, = CBS115166	São Paulo, Brazil	-	-	-	
	LPF1339	CF019, C1899	São Paulo, Brazil	-	-	-	
Gmelina arborea	LPF1321*	CF001, C918	Pará, Brazil	-	-	-	HQ157549
	LPF1322	CF002, C920	Pará, Brazil	-	-	-	-
	LPF1323	CF003, C925	Pará, Brazil	-	-	KF482983	-
Hevea brasiliensis	LPF1370	CF050	Bahia, Brazil	-	-	-	-
	LPF1372	CF052, HevBA-A50	Bahia, Brazil	-	-	MH744816	MH744824
	LPF1394*	CF074	Acre, Brazil	-	-	-	-
	LPF1476	CF313, HevAC-RB08	Acre, Brazil	-	-	MH744815	MH744823
Ipomoea batatas	-	C1476	Papua New Guinea	MG980827	MG980731	KF482992	KF483000
Mangifera indica	LPF1077	CF156, SPLIM7.15	São Paulo, Brazil	-	-	-	-
	LPF1156*	CF234, CEBS13	Ceará, Brazil	-	-		-
	LPF1324	CF004, C994	São Paulo, Brazil	-	-	HQ157551	KF482987
	LPF1328	CF008, C1558	Rio de Janeiro, Brazil	-	-	KF482988	HQ157552
	LPF1335	CF015, C1688	São Paulo, Brazil	-	-	KF482986	-

		-	C1889	São Paulo, Brazil	-	-	-	-
		-	C2759	Pakistan	-	-	KF482991	KF482999
		-	T1S8	Oman	-	-	-	-
	Tectona grandis	LPF1483	CF353, Teca-AM2	Mato Grosso, Brazil	-	-	-	-
		LPF1594*	Teca22, TecMT-QM22	Mato Grosso, Brazil	-	-	MH744814	MH744822
		LPF2199*	CE01	Mato Grosso, Brazil	-			
C. fimbriata f. sp. *carapa*	*Carapa guianensis*	LPF1560*	CarAC-144B[2]	Acre, Brazil	-	-	MH744812	MH744820
		LPF1561	CarAC-144C[3]	Acre, Brazil	-	-	-	-
		LPF1565	CarRR1-RR74	Roraima, Brazil	-	-	MH744813	MH744821
		LPF1567	CarAM-MA[2]	Amazonas, Brazil	-	-	MH746809	MH746810
C. cacaofunesta	*Theobroma cacao*	LPF1329*	CF009, C1587	Bahia, Brazil	-	-	-	-
		LPF1332	CF012, C1593	Bahia, Brazil	-	-	-	-
		LPF1333	CF013, C1597	Bahia, Brazil	-	-	-	C1597
		-	C1004	Ecuador			KF482993	KF483001
		-	C2031	Rôndonia, Brazil	-	HM569616	MH744819	MH744827
Ceratocystis destructans	*Prunus serotina*	-	C1963	Iowa, USA	MG980844	MG980748	KF482996	KF483004

Asterisks (*) indicate the Brazilian isolates analyzed in this study.

Table 2. Chromosome numbers and estimated sizes of 14 *Ceratocystis fimbriata* s.l. isolates examined by pulsed field gel electrophoresis (PFGE). The chromosomal bands were numbered according to decreasing size

Isolate*	**Chromosomal bands (Mbp)****								
	1	**2**	**3**	**4**	**5**	**6**	**7**	**8**	**9**
Mi. LPF1156	6.0	5.7	4.1	3.8	3.7	3.1	3.0	1.4	-
Ga. LPF1321	5.9	5.5	4.2	3.9	3.8	3.2	3.1	1.6	-
Ga. LPF1323	5.9	5.5	4.2	3.9	3.8	3.2	3.1	1.6	-
Tc. LPF1329	5.9	5.7	3.7	3.5	3.4	2.9	2.7	1.3	-
As. LPF1331	5.8	5.1	4.1	3.5	3.1	2.9	1.2	-	-
Fc. LPF1336	5.7	5.1	3.9	3.7	3.1	2.9	1.3	-	-
Hb. LPF1394	5.9	5.2	4.5	3.8	3.7	3.1	3.0	1.4	-
Cb. LPF1489	5.9	5.2	4.2	3.7	3.6	3.1	2.9	1.4	-
Cg. LPF1560	5.9	5.7	3.7	3.4	3.2	2.8	2.7	1.3	-
Tg. LPF1594	5.9	5.6	5.5	4.3	4.0	3.3	3.1	1.5	-
Eu. LPF1611	5.9	5.7	4.4	4.2	4.0	3.3	3.1	1.6	-
Ad. LPF1682	5.7	5.3	5.1	4.2	3.9	3.4	3.0	2.8	1.3
Eu. LPF1912	5.9	5.7	4.4	4.2	4.0	3.3	3.1	1.8	-
Tg. LPF2199	5.9	5.6	4.3	4.2	3.9	3.3	3.1	1.4	-

(*) The two letters before isolate names indicate their host source (*Tc* = *Theobroma cacao*; *Cg* = *Carapa guianensis*; *Mi* = *Mangifera indica*; *Ad* = *Actinidia deliciosa*; *Cb* = *Caryocar brasiliense*; *Fc* = *Ficus carica*; *As* = *Annona squamosa*; *Hb* = *Hevea brasiliensis*; *Ga* = *Gmelina arborea*; *Tg* = *Tectona grandis*; *Eu* = *Eucalyptus* sp.).

(**) Estimated chromosome sizes in mega base pairs (Mbp).

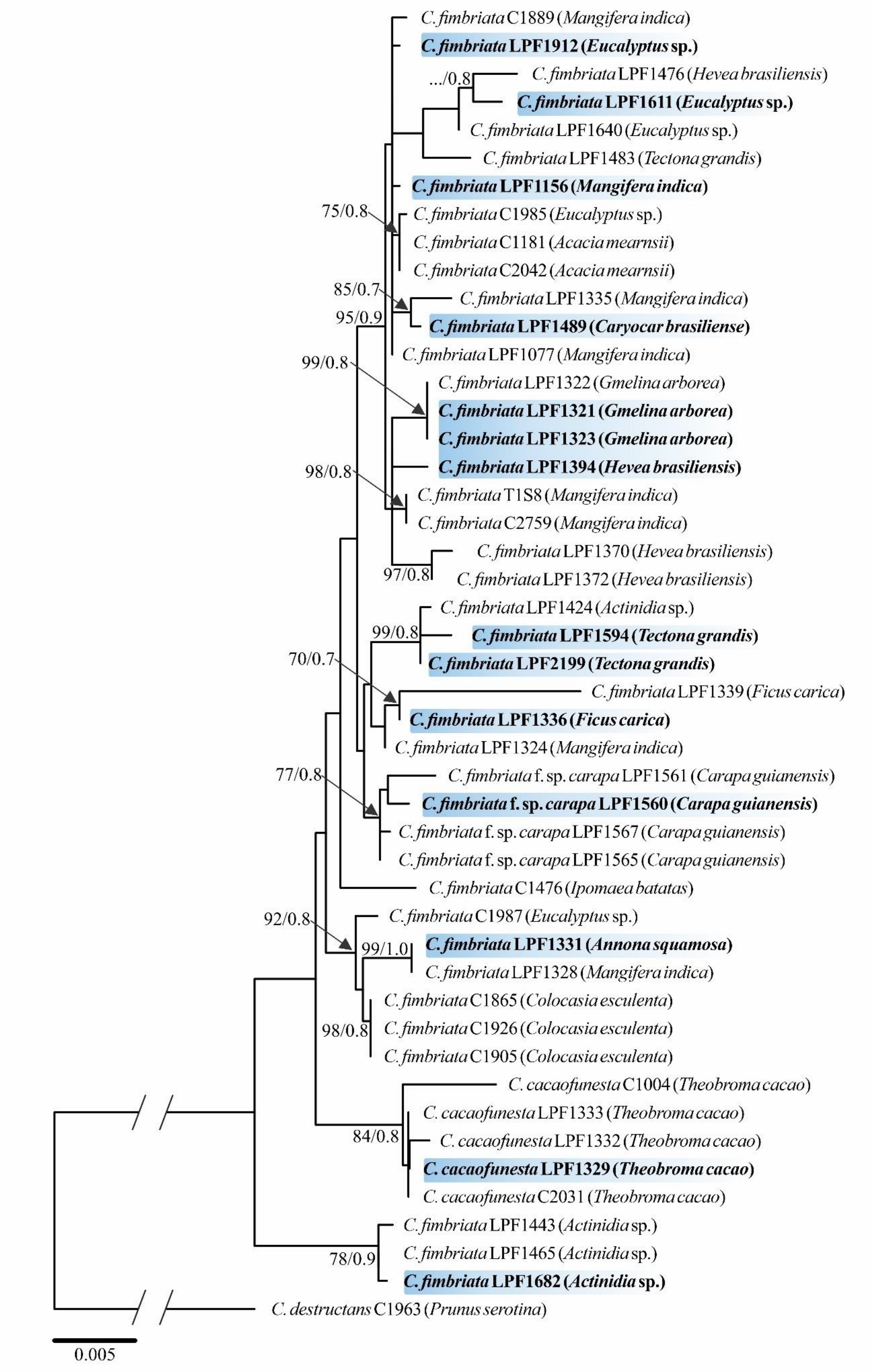
C. fimbriata C1889 (Mangifera indica)
C. fimbriata LPF1912 (Eucalyptus sp.)
.../0.8
C. fimbriata LPF1476 (Hevea brasiliensis)
C. fimbriata LPF1611 (Eucalyptus sp.)
C. fimbriata LPF1640 (Eucalyptus sp.)
C. fimbriata LPF1483 (Tectona grandis)
C. fimbriata LPF1156 (Mangifera indica)
75/0.8
C. fimbriata C1985 (Eucalyptus sp.)
C. fimbriata C1181 (Acacia mearnsii)
C. fimbriata C2042 (Acacia mearnsii)
85/0.7
C. fimbriata LPF1335 (Mangifera indica)
95/0.9
C. fimbriata LPF1489 (Caryocar brasiliense)
C. fimbriata LPF1077 (Mangifera indica)
99/0.8
C. fimbriata LPF1322 (Gmelina arborea)
C. fimbriata LPF1321 (Gmelina arborea)
C. fimbriata LPF1323 (Gmelina arborea)
C. fimbriata LPF1394 (Hevea brasiliensis)
98/0.8
C. fimbriata T1S8 (Mangifera indica)
C. fimbriata C2759 (Mangifera indica)
C. fimbriata LPF1370 (Hevea brasiliensis)
97/0.8
C. fimbriata LPF1372 (Hevea brasiliensis)
C. fimbriata LPF1424 (Actinidia sp.)
99/0.8
C. fimbriata LPF1594 (Tectona grandis)
70/0.7
C. fimbriata LPF2199 (Tectona grandis)
C. fimbriata LPF1339 (Ficus carica)
C. fimbriata LPF1336 (Ficus carica)
C. fimbriata LPF1324 (Mangifera indica)
77/0.8
C. fimbriata f. sp. carapa LPF1561 (Carapa guianensis)
C. fimbriata f. sp. carapa LPF1560 (Carapa guianensis)
C. fimbriata f. sp. carapa LPF1567 (Carapa guianensis)
C. fimbriata f. sp. carapa LPF1565 (Carapa guianensis)
C. fimbriata C1476 (Ipomaea batatas)
92/0.8
C. fimbriata C1987 (Eucalyptus sp.)
99/1.0
C. fimbriata LPF1331 (Annona squamosa)
C. fimbriata LPF1328 (Mangifera indica)
C. fimbriata C1865 (Colocasia esculenta)
98/0.8
C. fimbriata C1926 (Colocasia esculenta)
C. fimbriata C1905 (Colocasia esculenta)
C. cacaofunesta C1004 (Theobroma cacao)
C. cacaofunesta LPF1333 (Theobroma cacao)
84/0.8
C. cacaofunesta LPF1332 (Theobroma cacao)
C. cacaofunesta LPF1329 (Theobroma cacao)
C. cacaofunesta C2031 (Theobroma cacao)
C. fimbriata LPF1443 (Actinidia sp.)
78/0.9
C. fimbriata LPF1465 (Actinidia sp.)
C. fimbriata LPF1682 (Actinidia sp.)
C. destructans C1963 (Prunus serotina)
0.005

Figure 1. Maximum Likelihood (ML) phylogenetic tree based on combined β-tubulin, TEF-1α, MAT1 (*MAT1-1-2*) and MAT2 (*MAT1-2-1*) regions sequences of isolates of the Latin American Clade of the *Ceratocystis fimbriata* complex. The tree was rooted to *C. destructans*, of the North American clade. Bootstrap values greater than 70% are indicated on appropriate branches and PPs > 0.70 for BI are indicated along branches. Bold text indicates the 14 Brazilian isolates analyzed in this study. Fungal species are shown before the isolate name. Host sources of the isolates are shown in parenthesis.

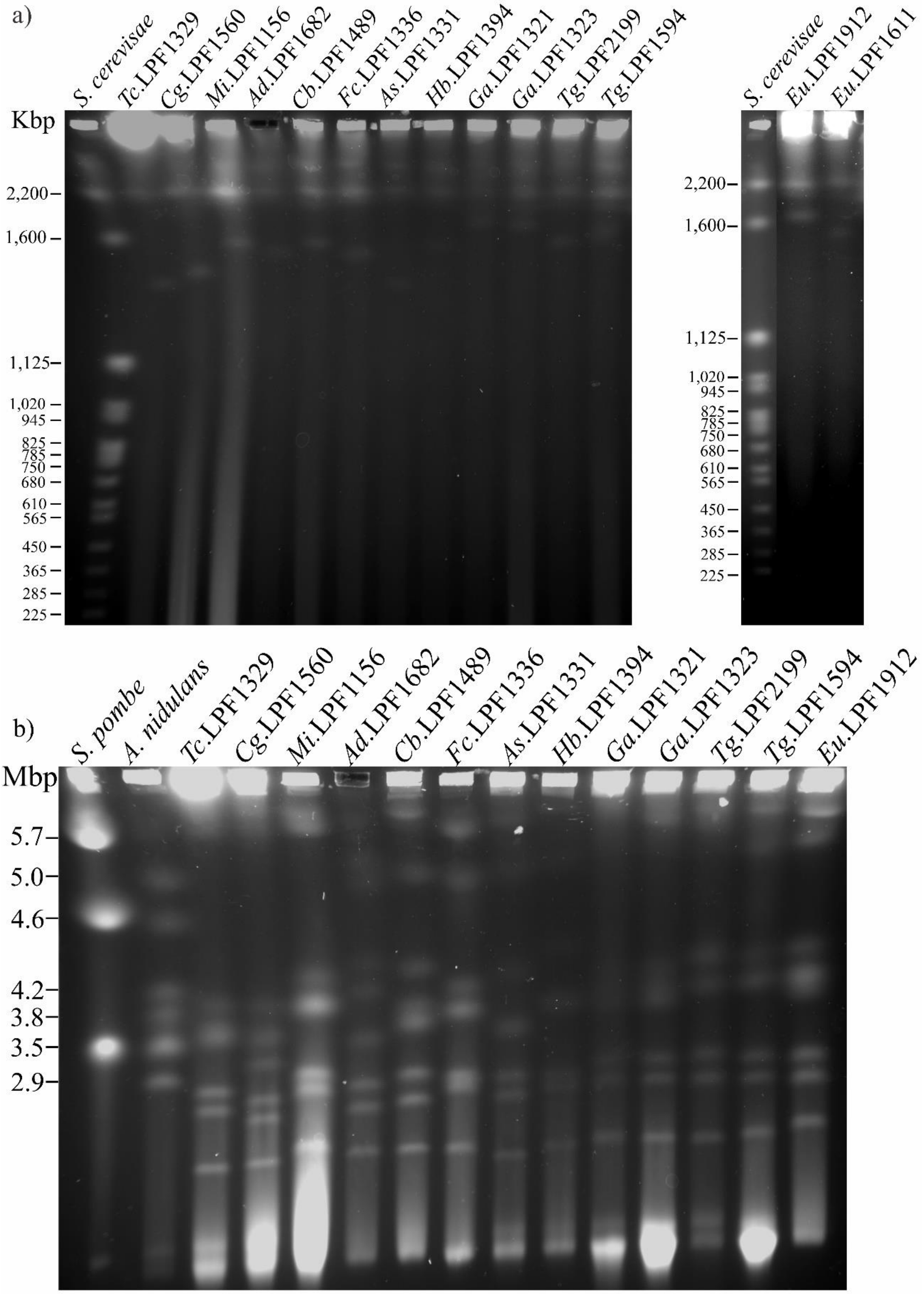

Figure 2. Chromosomal variation in isolates of *Ceratocystis fimbriata* s.l. revealed by pulsed field gel electrophoresis (PFGE). a) Small chromosomes separated using program A. b) Large chromosomes separated using program B. *Saccharomyces cerevisiae*, *Schizosaccharomyces*

pombe and *Aspergillus nidulans* chromosomes were used as chromosome-size DNA standard. The sizes of chromosomal bands in kilobase pairs (Kbp) and megabase pairs (Mbp) of the markers are shown on the left. The first two letters before isolate names indicate their host source (*Tc* = *Theobroma cacao*; *Cg* = *Carapa guianensis*; *Mi* = *Mangifera indica*; *Ad* = *Actinidia deliciosa*; *Cb* = *Caryocar brasiliense*; *Fc* = *Ficus carica*; *As* = *Annona squamosa*; *Hb* = *Hevea brasiliensis*; *Ga* = *Gmelina arborea*; *Tg* = *Tectona grandis*; *Eu* = *Eucalyptus* sp.).

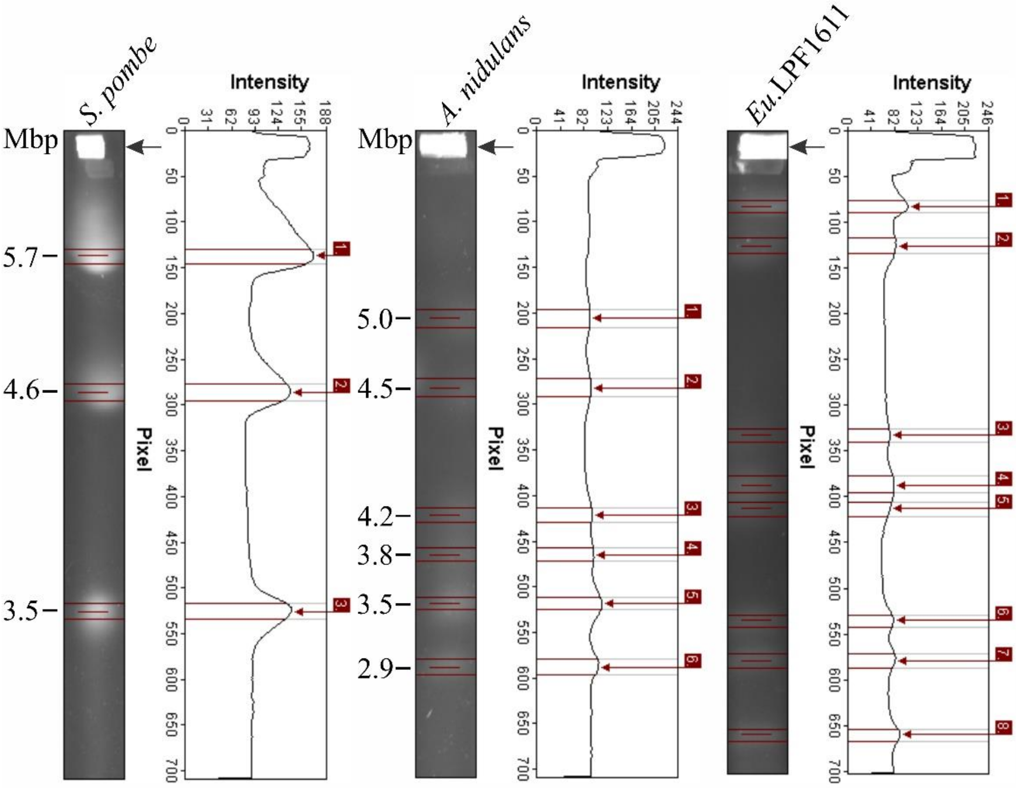

Figure 3. Densitometric analysis of the karyotype of the isolate LPF1611 of *Eucalyptus* sp. Black arrowheads indicate the origin of the gels. The red arrow indicates each chromosomal band to the right of the corresponding peaks on the graph. The chromosomal bands of *Schizosaccharomyces pombe* and *Aspergillus nidulans* were used as chromosome-size DNA standard. The sizes of chromosomal bands in megabase pairs (Mbp) of the markers are shown on the left.

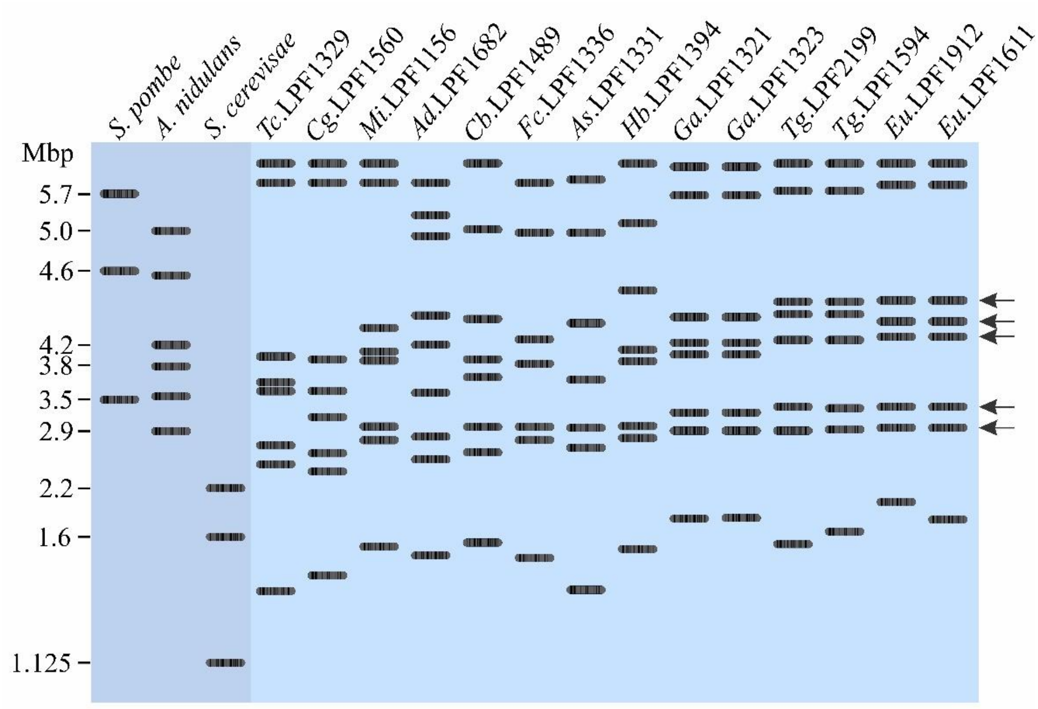

Figure 4. Schematic representation of chromosomal band profiles obtained for *C. fimbriata* s.l. The markers used are grouped on the left side in the dark blue rectangle with the sizes of the chromosomal bands (Mbp). *Saccharomyces cerevisiae*, *Schizosaccharomyces pombe* and *Aspergillus nidulans* chromosomes were used as size markers. The sizes of chromosomal bands are shown on the left. Arrows indicate bands common to several isolates. The first two letters before isolate names indicate their host sources (*Tc* = *Theobroma cacao*; *Cg* = *Carapa guianensis*; *Mi* = *Mangifera indica*; *Ad* = *Actinidia deliciosa*; *Cb* = *Caryocar brasiliense*; *Fc* = *Ficus carica*; *As* = *Annona squamosa*; *Hb* = *Hevea brasiliensis*; *Ga* = *Gmelina arborea*; *Tg* = *Tectona grandis*; *Eu* = *Eucalyptus* sp.).

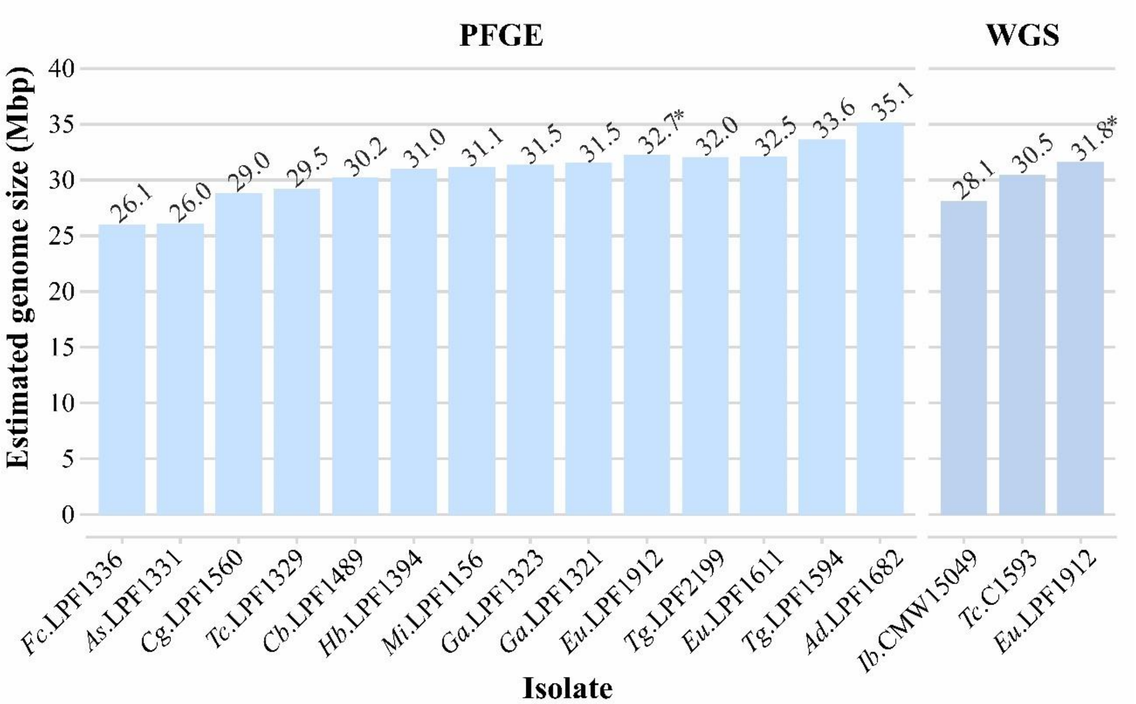

Figure 5. Genome sizes of *Ceratocystis* sp. isolates estimated as the sum of the sizes of individual chromosomes observed by pulsed field gel electrophoresis (PFGE) (left) and by whole-genome sequencing (WGS) (right). Isolates LPF1329 and C1593 are *C. cacaofunesta* and all others are *C. fimbriata*. The two letters before isolate names indicate their host source (*Fc* = *Ficus carica*; *As* = *Annona squamosa*; *Cg* = *Carapa guianensis*; *Tc* = *Theobroma cacao*; *Cb* = *Caryocar brasiliense*; *Hb* = *Hevea brasiliensis*; *Mi* = *Mangifera indica*; *Ga* = *Gmelina arborea*; *Eu* = *Eucalyptus* sp.; *Tg* = *Tectona grandis*; *Ad* = *Actinidia deliciosa*; *Ib* = *Ipomoea batatas*). Asterisks (*) indicate the isolate that has been sequenced and karyotyped.

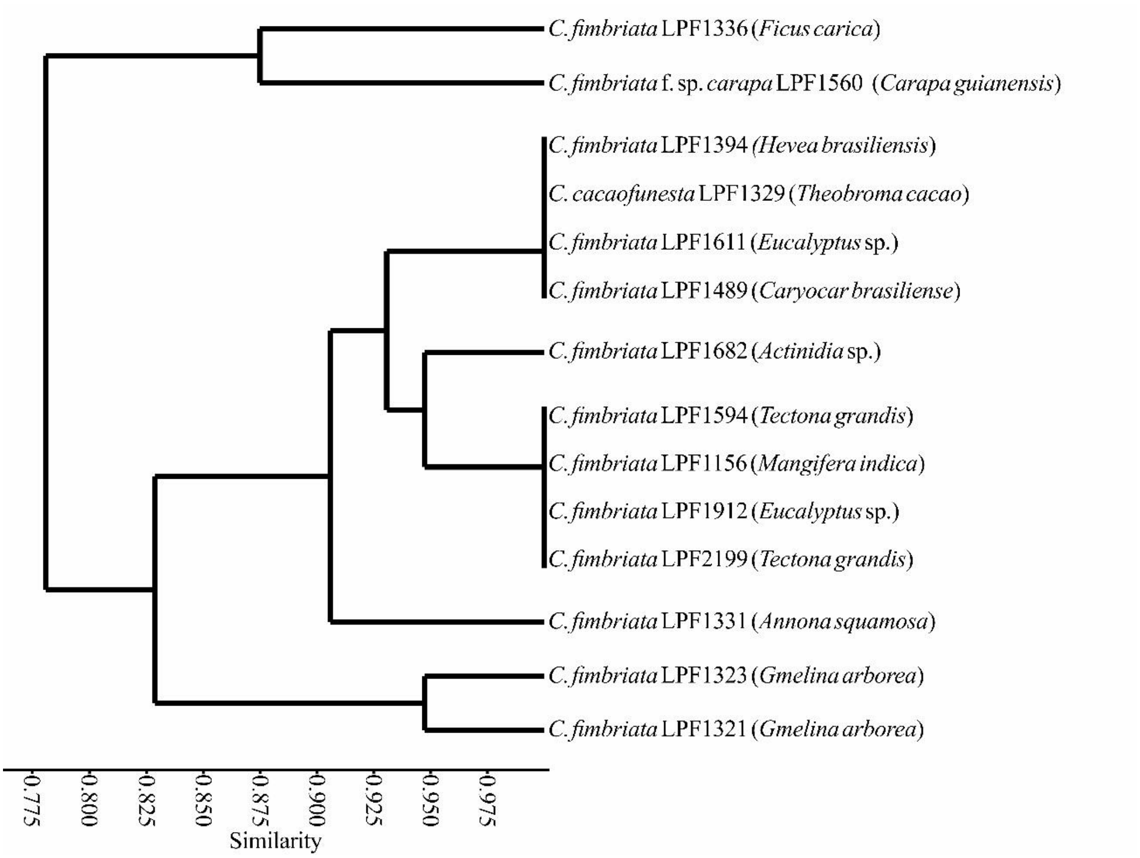

Figure 6. Unweighted pair group method with arithmetic means (UPGMA) dendrogram based on REMAP analysis of 14 *Ceratocystis* isolates. Fungal species are shown before the isolate name. Host sources of the isolates are shown in parenthesis.

SUPPLEMENTARY MATERIAL

Supplementary Table S1: Primers used for phylogenetic analysis of *Ceratocystis* sp. isolates used in this study.

Gene	**Primer**	**Primer sequences (5’-3’)**
β-tubulin	BT1-α	TTCCCCCGTCTCCACTTCTTCATG
	BT1-β	GACGAGATCGTTCATGTTGAACTC
TEF-1α	EFCF1	AGTGCGGTGGTATCGACAAG
	EFCF6	CATGTCACGGACGGCGAAAC
MAT1-1-2	CFMAT1-F	CAGCCTCGATTGAKGGTATGA
	CFMAT1-R	GGCATTTTTACGCTGGTTAG
MAT1-2-1	x9978a	GCTAACCTTCACGCCAATTTTGCC
	CFM2-1F	GTTACAAGTGTTCCCAAAAG

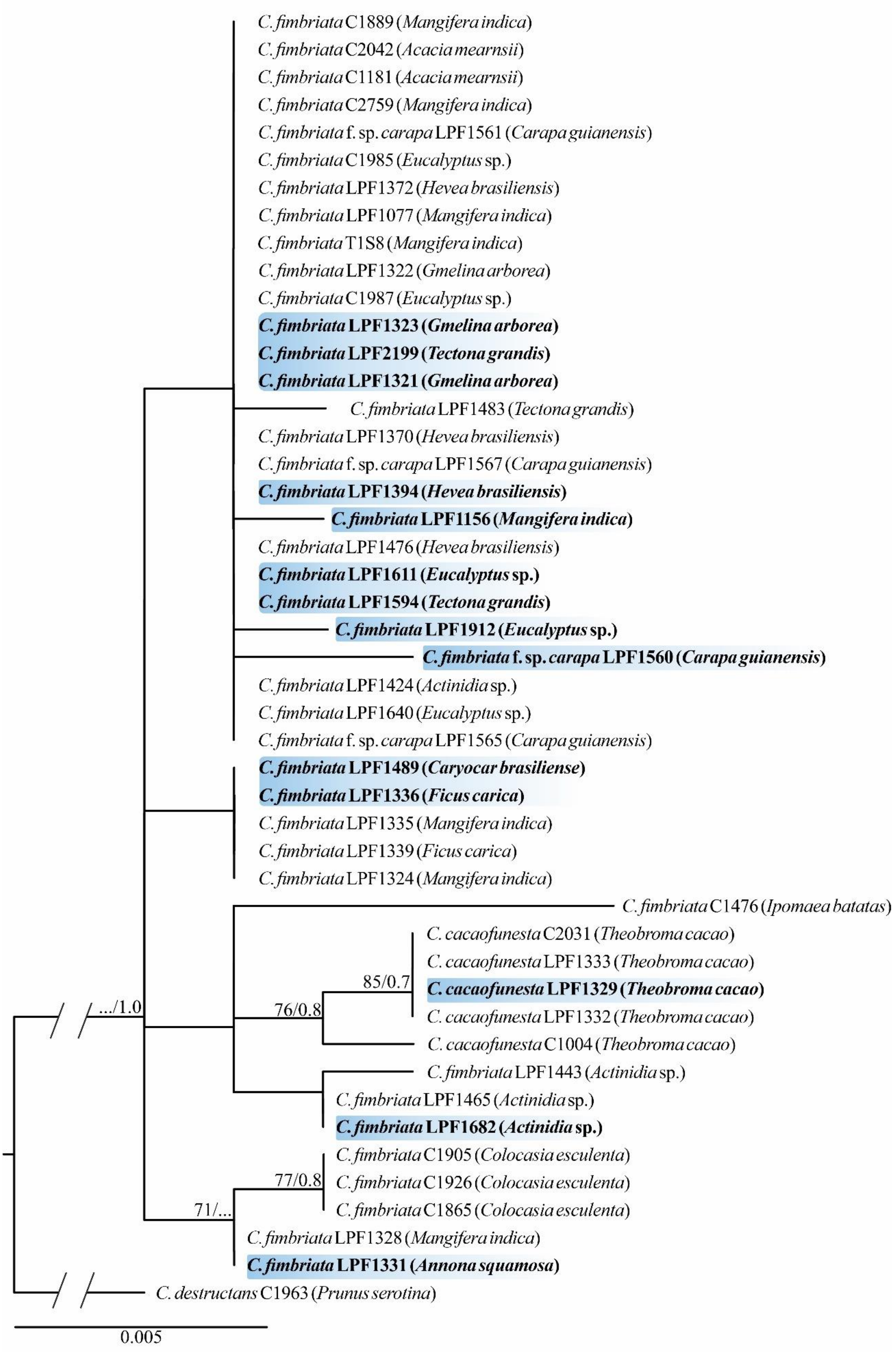
C. fimbriata C1889 (Mangifera indica)
C. fimbriata C2042 (Acacia mearnsii)
C. fimbriata C1181 (Acacia mearnsii)
C. fimbriata C2759 (Mangifera indica)
C. fimbriata f. sp. carapa LPF1561 (Carapa guianensis)
C. fimbriata C1985 (Eucalyptus sp.)
C. fimbriata LPF1372 (Hevea brasiliensis)
C. fimbriata LPF1077 (Mangifera indica)
C. fimbriata T1S8 (Mangifera indica)
C. fimbriata LPF1322 (Gmelina arborea)
C. fimbriata C1987 (Eucalyptus sp.)
C. fimbriata LPF1323 (Gmelina arborea)
C. fimbriata LPF2199 (Tectona grandis)
C. fimbriata LPF1321 (Gmelina arborea)
C. fimbriata LPF1483 (Tectona grandis)
C. fimbriata LPF1370 (Hevea brasiliensis)
C. fimbriata f. sp. carapa LPF1567 (Carapa guianensis)
C. fimbriata LPF1394 (Hevea brasiliensis)
C. fimbriata LPF1156 (Mangifera indica)
C. fimbriata LPF1476 (Hevea brasiliensis)
C. fimbriata LPF1611 (Eucalyptus sp.)
C. fimbriata LPF1594 (Tectona grandis)
C. fimbriata LPF1912 (Eucalyptus sp.)
C. fimbriata f. sp. carapa LPF1560 (Carapa guianensis)
C. fimbriata LPF1424 (Actinidia sp.)
C. fimbriata LPF1640 (Eucalyptus sp.)
C. fimbriata f. sp. carapa LPF1565 (Carapa guianensis)
C. fimbriata LPF1489 (Caryocar brasiliense)
C. fimbriata LPF1336 (Ficus carica)
C. fimbriata LPF1335 (Mangifera indica)
C. fimbriata LPF1339 (Ficus carica)
C. fimbriata LPF1324 (Mangifera indica)
C. fimbriata C1476 (Ipomaea batatas)
C. cacaofunesta C2031 (Theobroma cacao)
C. cacaofunesta LPF1333 (Theobroma cacao)
85/0.7
C. cacaofunesta LPF1329 (Theobroma cacao)
.../1.0
76/0.8
C. cacaofunesta LPF1332 (Theobroma cacao)
C. cacaofunesta C1004 (Theobroma cacao)
C. fimbriata LPF1443 (Actinidia sp.)
C. fimbriata LPF1465 (Actinidia sp.)
C. fimbriata LPF1682 (Actinidia sp.)
C. fimbriata C1905 (Colocasia esculenta)
77/0.8
C. fimbriata C1926 (Colocasia esculenta)
71/...
C. fimbriata C1865 (Colocasia esculenta)
C. fimbriata LPF1328 (Mangifera indica)
C. fimbriata LPF1331 (Annona squamosa)
C. destructans C1963 (Prunus serotina)
0.005

Supplementary Figure S1. Maximum Likelihood (ML) phylogenetic tree based on β-tubulin gene sequences of isolates of the Latin American Clade of the *Ceratocystis fimbriata* complex. The tree was rooted to *C. destructans*, of the North American clade. Bootstrap values greater than 70% are indicated on appropriate branches and PPs > 0.70 for BI are indicated along branches. Bold text indicates the 14 Brazilian isolates analyzed in this study. Fungal species are shown before the isolate name. Host sources of the isolates are shown in parenthesis.

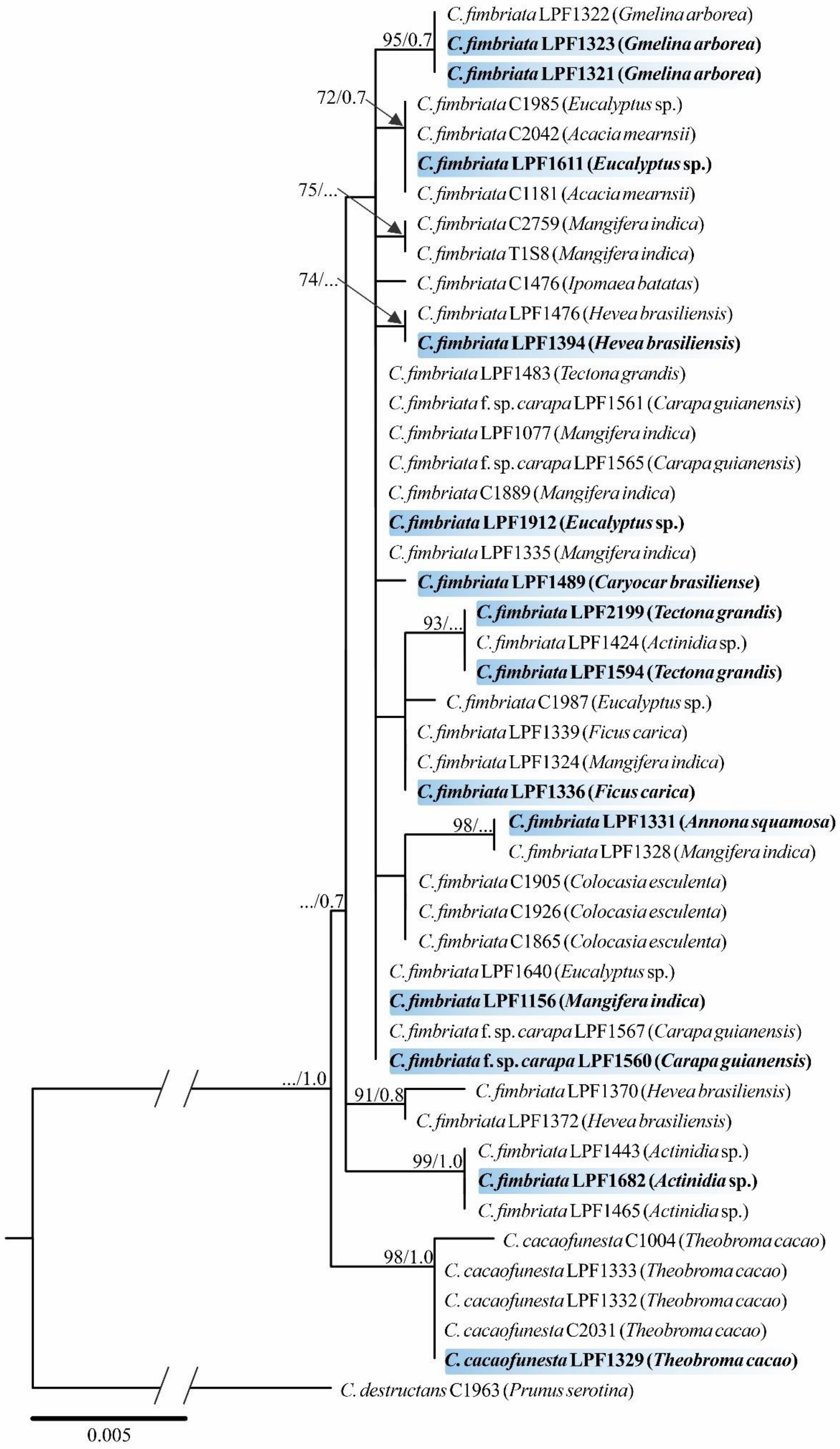
C. fimbriata LPF1322 (Gmelina arborea)
95/0.7
C. fimbriata LPF1323 (Gmelina arborea)
C. fimbriata LPF1321 (Gmelina arborea)
72/0.7
C. fimbriata C1985 (Eucalyptus sp.)
C. fimbriata C2042 (Acacia mearnsii)
C. fimbriata LPF1611 (Eucalyptus sp.)
C. fimbriata C1181 (Acacia mearnsii)
75/...
C. fimbriata C2759 (Mangifera indica)
C. fimbriata T1S8 (Mangifera indica)
C. fimbriata C1476 (Ipomaea batatas)
74/...
C. fimbriata LPF1476 (Hevea brasiliensis)
C. fimbriata LPF1394 (Hevea brasiliensis)
C. fimbriata LPF1483 (Tectona grandis)
C. fimbriata f. sp. carapa LPF1561 (Carapa guianensis)
C. fimbriata LPF1077 (Mangifera indica)
C. fimbriata f. sp. carapa LPF1565 (Carapa guianensis)
C. fimbriata C1889 (Mangifera indica)
C. fimbriata LPF1912 (Eucalyptus sp.)
C. fimbriata LPF1335 (Mangifera indica)
C. fimbriata LPF1489 (Caryocar brasiliense)
C. fimbriata LPF2199 (Tectona grandis)
93/...
C. fimbriata LPF1424 (Actinidia sp.)
C. fimbriata LPF1594 (Tectona grandis)
C. fimbriata C1987 (Eucalyptus sp.)
C. fimbriata LPF1339 (Ficus carica)
C. fimbriata LPF1324 (Mangifera indica)
C. fimbriata LPF1336 (Ficus carica)
98/...
C. fimbriata LPF1331 (Annona squamosa)
C. fimbriata LPF1328 (Mangifera indica)
C. fimbriata C1905 (Colocasia esculenta)
.../0.7
C. fimbriata C1926 (Colocasia esculenta)
C. fimbriata C1865 (Colocasia esculenta)
C. fimbriata LPF1640 (Eucalyptus sp.)
C. fimbriata LPF1156 (Mangifera indica)
C. fimbriata f. sp. carapa LPF1567 (Carapa guianensis)
C. fimbriata f. sp. carapa LPF1560 (Carapa guianensis)
.../1.0
91/0.8
C. fimbriata LPF1370 (Hevea brasiliensis)
C. fimbriata LPF1372 (Hevea brasiliensis)
C. fimbriata LPF1443 (Actinidia sp.)
99/1.0
C. fimbriata LPF1682 (Actinidia sp.)
C. fimbriata LPF1465 (Actinidia sp.)
C. cacaofunesta C1004 (Theobroma cacao)
98/1.0
C. cacaofunesta LPF1333 (Theobroma cacao)
C. cacaofunesta LPF1332 (Theobroma cacao)
C. cacaofunesta C2031 (Theobroma cacao)
C. cacaofunesta LPF1329 (Theobroma cacao)
C. destructans C1963 (Prunus serotina)
0.005

Supplementary Figure S2. Maximum Likelihood (ML) phylogenetic tree based on portions of the MAT1 (*MAT1-1-2*) mating type genes of isolates of the Latin American Clade of the *Ceratocystis fimbriata* complex. The tree was rooted to *C. destructans*, of the North American clade. Bootstrap values greater than 70% are indicated on appropriate branches and PPs > 0.70 for BI are indicated along branches. Bold text indicates the 14 Brazilian isolates analyzed in this study. Fungal species are shown before the isolate name. Host sources of the isolates are shown in parenthesis.

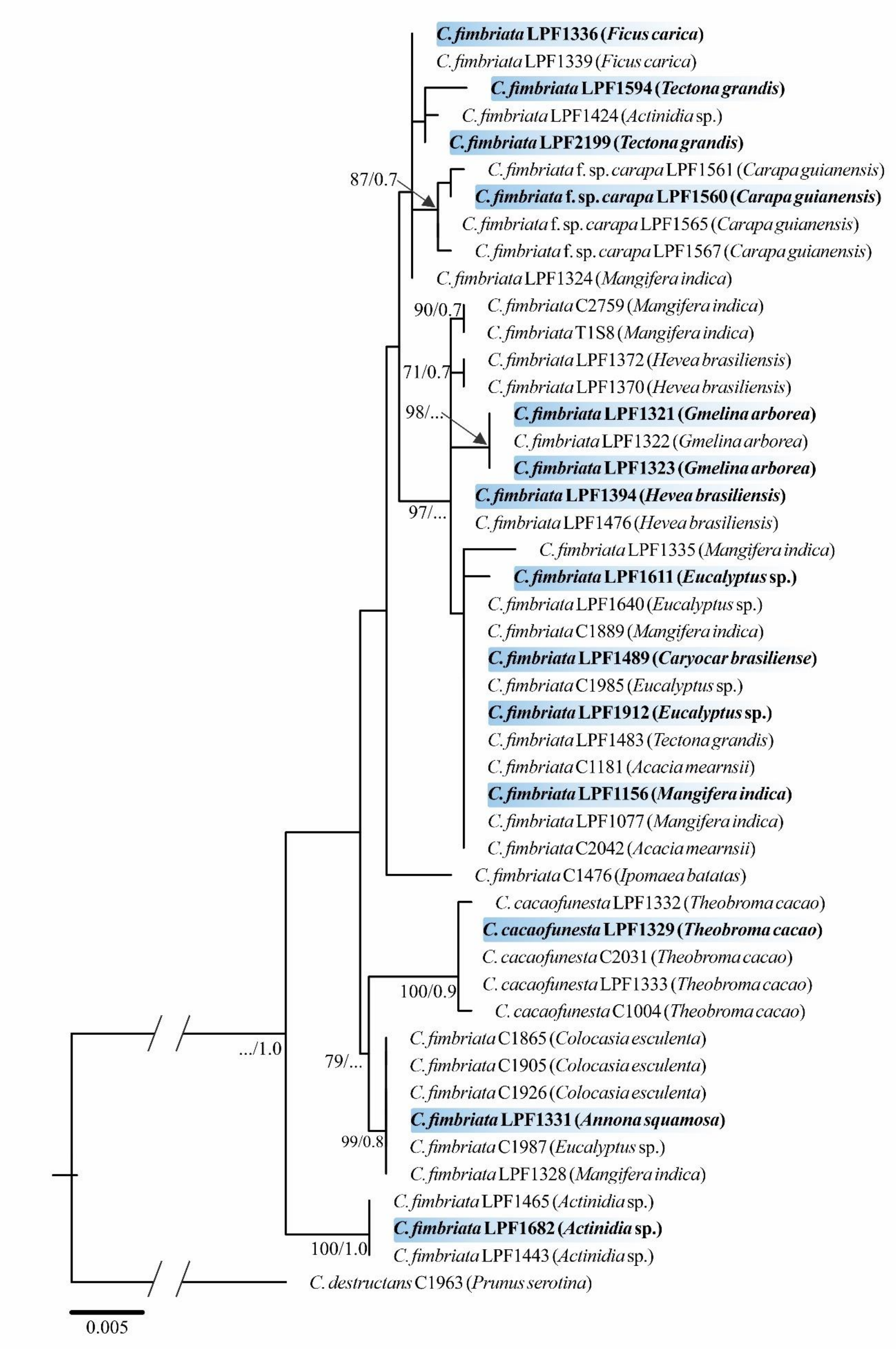
C. fimbriata LPF1336 (Ficus carica)
C. fimbriata LPF1339 (Ficus carica)
C. fimbriata LPF1594 (Tectona grandis)
C. fimbriata LPF1424 (Actinidia sp.)
C. fimbriata LPF2199 (Tectona grandis)
87/0.7
C. fimbriata f. sp. carapa LPF1561 (Carapa guianensis)
C. fimbriata f. sp. carapa LPF1560 (Carapa guianensis)
C. fimbriata f. sp. carapa LPF1565 (Carapa guianensis)
C. fimbriata f. sp. carapa LPF1567 (Carapa guianensis)
C. fimbriata LPF1324 (Mangifera indica)
90/0.7
C. fimbriata C2759 (Mangifera indica)
C. fimbriata T1S8 (Mangifera indica)
71/0.7
C. fimbriata LPF1372 (Hevea brasiliensis)
C. fimbriata LPF1370 (Hevea brasiliensis)
98/...
C. fimbriata LPF1321 (Gmelina arborea)
C. fimbriata LPF1322 (Gmelina arborea)
C. fimbriata LPF1323 (Gmelina arborea)
C. fimbriata LPF1394 (Hevea brasiliensis)
97/...
C. fimbriata LPF1476 (Hevea brasiliensis)
C. fimbriata LPF1335 (Mangifera indica)
C. fimbriata LPF1611 (Eucalyptus sp.)
C. fimbriata LPF1640 (Eucalyptus sp.)
C. fimbriata C1889 (Mangifera indica)
C. fimbriata LPF1489 (Caryocar brasiliense)
C. fimbriata C1985 (Eucalyptus sp.)
C. fimbriata LPF1912 (Eucalyptus sp.)
C. fimbriata LPF1483 (Tectona grandis)
C. fimbriata C1181 (Acacia mearnsii)
C. fimbriata LPF1156 (Mangifera indica)
C. fimbriata LPF1077 (Mangifera indica)
C. fimbriata C2042 (Acacia mearnsii)
C. fimbriata C1476 (Ipomaea batatas)
C. cacaofunesta LPF1332 (Theobroma cacao)
C. cacaofunesta LPF1329 (Theobroma cacao)
C. cacaofunesta C2031 (Theobroma cacao)
100/0.9
C. cacaofunesta LPF1333 (Theobroma cacao)
C. cacaofunesta C1004 (Theobroma cacao)
C. fimbriata C1865 (Colocasia esculenta)
.../1.0
79/...
C. fimbriata C1905 (Colocasia esculenta)
C. fimbriata C1926 (Colocasia esculenta)
C. fimbriata LPF1331 (Annona squamosa)
99/0.8
C. fimbriata C1987 (Eucalyptus sp.)
C. fimbriata LPF1328 (Mangifera indica)
C. fimbriata LPF1465 (Actinidia sp.)
C. fimbriata LPF1682 (Actinidia sp.)
100/1.0
C. fimbriata LPF1443 (Actinidia sp.)
C. destructans C1963 (Prunus serotina)
0.005

Supplementary Figure S3. Maximum Likelihood (ML) phylogenetic tree based on portions of the MAT2 (*MAT1-2-1*) mating type genes of isolates of the Latin American Clade of the *Ceratocystis fimbriata* complex. The tree was rooted to *C. destructans*, of the North American clade. Bootstrap values greater than 70% are indicated on appropriate branches and PPs > 0.70 for BI are indicated along branches. Bold text indicates the 14 Brazilian isolates analyzed in this study. Fungal species are shown before the isolate name. Host sources of the isolates are shown in parenthesis.

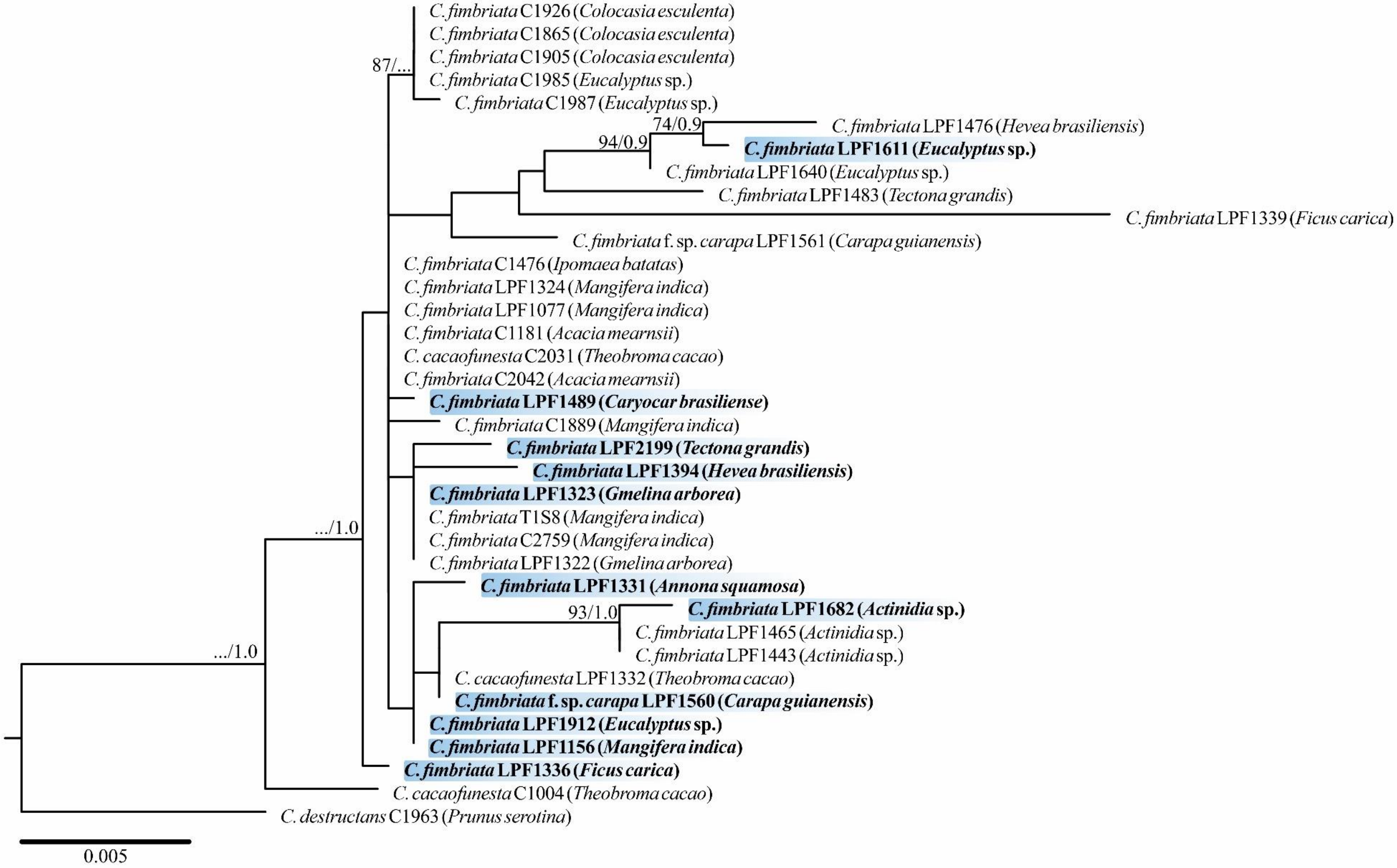
C. fimbriata C1926 (Colocasia esculenta)
C. fimbriata C1865 (Colocasia esculenta)
C. fimbriata C1905 (Colocasia esculenta)
87/...
C. fimbriata C1985 (Eucalyptus sp.)
C. fimbriata C1987 (Eucalyptus sp.)
74/0.9
C. fimbriata LPF1476 (Hevea brasiliensis)
94/0.9
C. fimbriata LPF1611 (Eucalyptus sp.)
C. fimbriata LPF1640 (Eucalyptus sp.)
C. fimbriata LPF1483 (Tectona grandis)
C. fimbriata LPF1339 (Ficus carica)
C. fimbriata f. sp. carapa LPF1561 (Carapa guianensis)
C. fimbriata C1476 (Ipomaea batatas)
C. fimbriata LPF1324 (Mangifera indica)
C. fimbriata LPF1077 (Mangifera indica)
C. fimbriata C1181 (Acacia mearnsii)
C. cacaofunesta C2031 (Theobroma cacao)
C. fimbriata C2042 (Acacia mearnsii)
C. fimbriata LPF1489 (Caryocar brasiliense)
C. fimbriata C1889 (Mangifera indica)
C. fimbriata LPF2199 (Tectona grandis)
C. fimbriata LPF1394 (Hevea brasiliensis)
C. fimbriata LPF1323 (Gmelina arborea)
.../1.0
C. fimbriata T1S8 (Mangifera indica)
C. fimbriata C2759 (Mangifera indica)
C. fimbriata LPF1322 (Gmelina arborea)
C. fimbriata LPF1331 (Annona squamosa)
93/1.0
C. fimbriata LPF1682 (Actinidia sp.)
C. fimbriata LPF1465 (Actinidia sp.)
.../1.0
C. fimbriata LPF1443 (Actinidia sp.)
C. cacaofunesta LPF1332 (Theobroma cacao)
C. fimbriata f. sp. carapa LPF1560 (Carapa guianensis)
C. fimbriata LPF1912 (Eucalyptus sp.)
C. fimbriata LPF1156 (Mangifera indica)
C. fimbriata LPF1336 (Ficus carica)
C. cacaofunesta C1004 (Theobroma cacao)
C. destructans C1963 (Prunus serotina)
0.005

Supplementary Figure S4. Maximum Likelihood (ML) phylogenetic tree based on portions of the TEF-1α mating type genes of isolates of the Latin American Clade of the *Ceratocystis fimbriata* complex. The tree was rooted to *C. destructans*, of the North American clade. Bootstrap values greater than 70% are indicated on appropriate branches and PPs > 0.70 for BI are indicated along branches. Bold text indicates the 14 Brazilian isolates analyzed in this study. Fungal species are shown before the isolate name. Host sources of the isolates are shown in parenthesis.

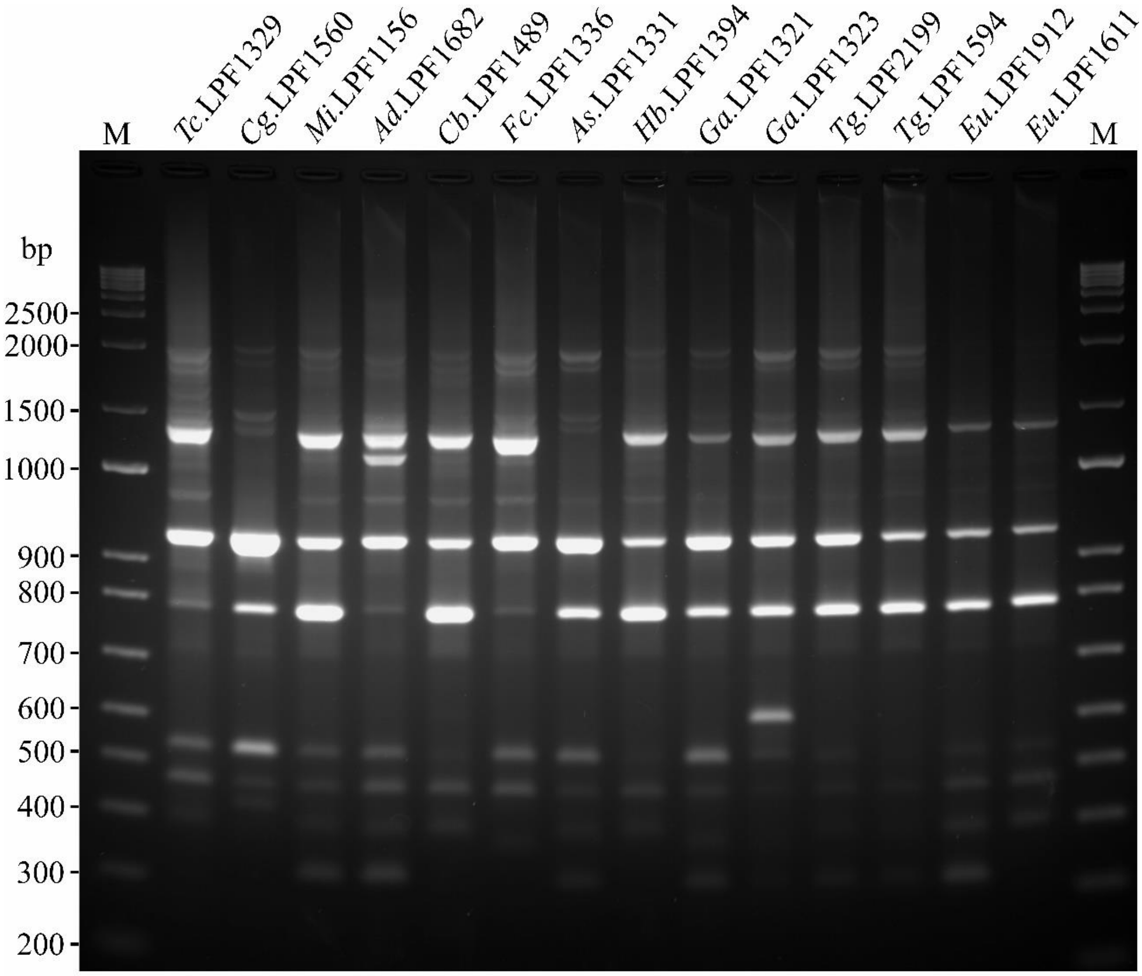

Supplementary Figure S5. Electrophoretic profile of amplicons from *Ceratocystis* sp. generated by retrotransposon-microsatellite amplified polymorphism (REMAP). The two letters before isolate names indicate their host source (*Tc* = *Theobroma cacao*; *Cg* = *Carapa guianensis*; *Mi* = *Mangifera indica*; *Ad* = *Actinidia deliciosa*; *Cb* = *Caryocar brasiliense*; *Fc* = *Ficus carica*; *As* = *Annona squamosa*; *Hb* = *Hevea brasiliensis*; *Ga* = *Gmelina arborea*; *Tg* = *Tectona grandis*; *Eu* = *Eucalyptus* sp.). M represents the molecular weight marker (1Kb DNA ladder).